CONFIDENTIAL

Copy
RM L57L18a

NACA RM L57L18a

NACA

RESEARCH MEMORANDUM

AN INVESTIGATION AT MACH NUMBERS 1.94 AND 2.41 OF JET EFFECTS UPON THE LONGITUDINAL AND DIRECTIONAL STABILITY OF A GENERAL AIRCRAFT CONFIGURATION EMPLOYING WING-TIP-MOUNTED NACELLES

By Frank L. Clark and Clyde L. W. Edwards

Langley Aeronautical Laboratory
Langley Field, Va.

CLASSIFIED DOCUMENT

NATIONAL ADVISORY COMMITTEE
FOR AERONAUTICS

WASHINGTON

March 4, 1958

CONFIDENTIAL

NATIONAL ADVISORY COMMITTEE FOR AERONAUTICS

RESEARCH MEMORANDUM

AN INVESTIGATION AT MACH NUMBERS 1.94 AND 2.41 OF JET EFFECTS UPON THE LONGITUDINAL AND DIRECTIONAL STABILITY OF A GENERAL AIRCRAFT CONFIGURATION EMPLOYING WING-TIP-MOUNTED NACELLES

By Frank L. Clark and Clyde L. W. Edwards

SUMMARY

An investigation has been conducted in the Langley 9-inch supersonic tunnel to determine the effects that jet interference has upon the longitudinal and directional stability of a general aircraft configuration employing wing-tip-mounted nacelles. Tests were conducted using a cold jet in which the free-stream Mach number, jet static-pressure ratio, tail configurations, angle of attack, and angle of sideslip were varied. The jet-interference studies were conducted at free-stream Mach numbers of 1.94 and 2.41, and boundary-layer transition was artificially induced.

The results indicated that an increase in the jet static-pressure ratio and the vertical displacement of the horizontal tail produced no significant changes in the directional stability. Jet interference increased the values of normal force at both angles of attack and angles of sideslip and produced nonlinearities in the pitching-moment curves for all complete tail configurations. In general, the effects of jet interference became more pronounced as the height of the horizontal tail was increased.

An increase in the free-stream Mach number decreased the directional stability of the model. This reduction was caused by the decrease in the vertical-tail effectiveness rather than by jet interference. Increasing Mach number caused the jet-interference effects upon the values of normal force and pitching moment to be reduced in intensity for the same jet static-pressure ratios.

When the jets were operated at unequal jet static-pressure ratios, jet interference had little effect upon the normal force and pitching moment at the test values of angle of sideslip but it produced significant changes in these quantities at an angle of attack of 4°. The values of side force and yawing moment were affected by the jet interference both at angles of attack and at angles of sideslip.

INTRODUCTION

In the past decade increased attention has been accorded to the study of flow characteristics associated with subsonic and supersonic jets exhausting both hot and cold gases into still, subsonic, and supersonic airstreams. (See refs. 1 to 3.) It has been shown in reference 1 that at supersonic speeds a jet exhausting cold gases can be used to simulate hot-jet conditions.

Investigations have been conducted at supersonic speeds to determine the jet-interference effects upon the aerodynamic characteristics of isolated geometric surfaces when the surfaces were introduced into the interference flow field. (See refs. 4 to 8.) Numerous studies have been conducted to determine the effects that jet interference has upon the boattail and base pressures of various afterbody configurations. (See refs. 9 to 12.) In general, there have been very few jet-interference studies conducted in which a complete airplane configuration was involved. (See ref. 13.) In view of this lack of experimental information, the present investigation was initiated to determine the jet-interference effects upon the static longitudinal and directional stability of a general aircraft configuration.

Two models featuring wing-tip-mounted nacelles were employed in the investigation. The jet-interference studies were conducted for a cold-jet condition at free-stream Mach numbers of 1.94 and 2.41 and covered a range of jet static-pressure ratios from the jet-off condition to 15 at a Mach number of 1.94 and from the jet-off condition to 25 at a Mach number of 2.41. In addition to varying the jet static-pressure ratio and the free-stream Mach number, the models were also tested over an angle-of-attack range from -2° to 8° and over an angle-of-sideslip range from -8° to 2° for each of the following tail configurations: (a) no horizontal or vertical tail, (b) with vertical tail only, (c) with no vertical tail but with horizontal tail located on the body center line, and (d) with both horizontal and vertical tail and with the horizontal tail positioned in three different vertical locations.

SYMBOLS

b	wing span (nacelles not included)
$\bar{c}$	wing mean aerodynamic chord
C_m	pitching-moment coefficient, $\frac{\text{Pitching moment}}{qS\bar{c}}$

C_N normal-force coefficient, $\frac{\text{Normal force}}{qS}$

C_n yawing-moment coefficient, $\frac{\text{Yawing moment}}{qSb}$

C_Y side-force coefficient, $\frac{\text{Side force}}{qS}$

$C_{m_\alpha} = \frac{\partial C_m}{\partial \alpha}$

$C_{N_\alpha} = \frac{\partial C_N}{\partial \alpha}$

$C_{n_\beta} = \frac{\partial C_n}{\partial \beta}$

$C_{Y_\beta} = \frac{\partial C_Y}{\partial \beta}$

M free-stream Mach number

p static pressure

q free-stream dynamic pressure

S total wing area

α angle of attack

β angle of sideslip

Subscripts:

j jet exit

∞ free stream

APPARATUS AND TESTS

Wind Tunnel

The Langley 9-inch supersonic tunnel is a closed-circuit, direct-drive tunnel in which the pressure, temperature, and humidity of the enclosed air may be controlled. Throughout the tests the quantity of

water vapor in the tunnel was kept at a minimum so that condensation would have no appreciable effect on the flow in the supersonic nozzle. The test Mach number was varied by means of interchangeable nozzle blocks forming a test section approximately 9 inches square. A schlieren optical system provided qualitative visual flow observations.

Models

The present investigation employed two models identical in geometric features. Each model featured wing-tip-mounted nacelles. The nacelles on one model were inoperative and the nacelles on the other contained a jet with a jet-exit Mach number of 1.96. Henceforth, the model having the inoperative nacelles will be referred to as the no-jet model and the model having the operative nacelles will be referred to as the jet model.

A drawing of the model illustrating the construction details and giving pertinent design dimensions is presented in figure 1. The sting consisted of seven 0.1875-inch-diameter copper tubes and two 0.040-inch-diameter monel tubes, soft-soldered together to form one unit approximately 0.5625 inch in diameter. This sting extended into the body to approximately $0.5\bar{c}$ of the wing. At this point the tubes were separated into two sets and led to each nacelle. The three copper tubes located in each wing served as supply lines through which high-pressure dry air was conducted to each jet while the seventh copper tube served as a conduit for strain-gage wires. The 0.040-inch-diameter monel tubes served as pressure taps to indicate the stagnation pressure in each nacelle. A 0.1-inch gap was maintained between the sting and the inside diameter of the body and approximately 0.020-inch gap was maintained between the wing and body of the model.

Except for the air supply lines located in each wing, the jet model was constructed entirely of mild steel. The sting and wing formed a rigid support and the body and its various tail arrangements were joined to the wing through a four-component internally mounted strain-gage balance. This was done in a manner that permitted the forces and moments on only the body and tail assemblies to be measured in the presence of the wing and nacelles.

The no-jet model was also constructed entirely of mild steel, and a two-component internally mounted strain-gage balance connected the model to the sting. Since a two-component strain-gage balance was employed for this model, it was necessary to roll the model about the balance from one plane to the other before measurement of the forces and moments in that plane could be made. The forces and moments were measured on the entire model.

In order to facilitate the changing of model configurations, all tail assemblies were constructed as individual units. Each unit was soft-soldered in place and faired to form a smooth contoured surface. A photograph showing the jet model with the low horizontal tail in place, the no-jet model with the high horizontal tail in place, and the mid-horizontal-tail—vertical-tail configuration is presented in figure 2(a). A photograph of the jet model illustrating the jet exit is presented in figure 2(b).

Tests and Procedure

Jet-interference studies were conducted at a tunnel stagnation pressure of approximately 1 atmosphere and therefore the Reynolds numbers based on wing chord were about 0.49×10^6 and 0.39×10^6 for Mach numbers 1.94 and 2.41, respectively. During the tests a turbulent boundary layer was artificially induced by an approximately 0.006-inch-thick roughness strip located on the model as shown in figure 1.

The models were tested over a maximum angle-of-attack range of -2° to 8° for an angle of sideslip of 0°, and over a maximum angle-of-sideslip range of -8° to 2° for an angle of attack of 0°. The angle of attack or angle of sideslip of the model was determined optically by reflecting a point source light from a 0.0625-inch-diameter mirror, which was flush-mounted in the model, onto a calibrated scale.

The Mach number distributions across the exit of each jet nacelle were determined by a total-pressure survey in a manner similar to that reported in reference 12, with the exception that the jet stagnation pressure was measured instead of the static pressure at the lip of the nacelle.

The high-pressure air supply for each jet emanated from a common source thereby insuring that equal pressure was maintained in the stagnation chamber of each jet at all times. The pressure within each jet stagnation chamber was recorded on precision high-pressure gages and was varied by means of manually controlled valves located outside the tunnel. This system was later modified for additional tests to permit the stagnation pressure in each jet to be regulated independently of the other.

Accuracies

The estimated accumulative errors in the aerodynamic characteristics and test variables are presented in the following table:

	Accuracies for Mach number -	
	1.94	2.41
M	±0.010	±0.015
α, deg	±0.1	±0.1
β, deg	±0.1	±0.1
C_N	±0.0058	±0.0078
C_m	±0.0026	±0.0032
C_Y	±0.0060	±0.0077
C_n	±0.0013	±0.0017
p_j/p_∞	±0.25	±0.25

PRELIMINARY CONSIDERATIONS

Reference 3 presents a large number of calculated jet boundaries for supersonic jets exhausting into still air. The boundaries were calculated using the method of characteristics for various jet Mach numbers, specific heat ratios, nozzle divergence angles, and jet static-pressure ratios. It is shown in this reference that increasing the jet static-pressure ratio increases the initial inclination of the jet boundary and the diameter of the jet boundary, and shifts the maximum diameter of the jet boundary downstream. Even though these conditions were computed for a jet exhausting into still air, the trends are directly applicable to a supersonic jet exhausting into a supersonic stream. The major difference is that a jet exhausting into a supersonic stream undergoes less expansion than does a jet exhausting into still air. (See ref. 1.) The fact that the same trends exist for the two cases is readily apparent in figure 3 in which photographs of the jet-interference flow field are presented for various jet static-pressure ratios at free-stream Mach numbers of 1.94 and 2.41. The photographs show that an increase in the jet static-pressure ratio increases the initial inclination of the jet-exit shock. This factor produces the three following major consequences: First, it increases the pressure rise across the jet-exit shock which, in turn, greatly increases the effect that the jet interference has upon neighboring surfaces. Second, it causes the jet-exit shock to advance farther forward while, simultaneously, the shock within the jet moves rearward. This increases the possibility for the jet-exit shock to impinge and reflect from neighboring surfaces and reduces the possibility of the shock within the jet affecting the neighboring surfaces. Third, it increases the diameter of the jet boundary which, in turn, increases

the flow angularity within the expansion region between the jet-exit shock and the mixing boundary. The significance of these effects is governed primarily by the location of a surface in the interference flow field.

Sketches illustrating the horizontal-tail, vertical-tail, and body areas that were influenced by the jet-exit shock and shock from within the jet for the three complete tail configurations are presented in figure 4 for various jet static-pressure ratios at free-stream Mach numbers of 1.94 and 2.41. These diagrams were constructed from schlieren photographs on the assumption that the shock waves were conical in structure and emanated from a point source. The patterns are meant only to serve as a visual aid in understanding the flow phenomena that normally accompany an increase in the jet static-pressure ratio and do not accurately represent the true condition.

It will be noted that as the jet static-pressure ratio was increased the jet-exit shock moved forward, thereby influencing a greater portion of the body and tail assembly. At the same time the shock from within the jet shifted rearward and eventually moved off the horizontal tail. The amount of horizontal-tail area influenced by the jet-exit shock and the jet shock was lessened as the height of the horizontal tail was increased above the center line of the body.

A comparison of figure 4(a) with figure 4(b) shows that less overall area of the body and tail assembly is affected by the jet-exit shock and jet shock at a Mach number of 2.41 than at a Mach number of 1.94. This can be attributed to the fact that the exhausting jet had to undergo less expansion than the jet at a Mach number of 1.94. This characteristic is qualitatively analogous to the previously mentioned effect of a jet exhausting into a supersonic stream as contrasted to a jet exhausting into still air.

RESULTS

The basic data for the jet model are presented in figures 5 and 6. The jet-interference effects upon the aerodynamic characteristics of the same model are presented in incremental form in figures 7 and 8. The incremental values were determined by subtracting the values obtained for the jet-off condition from the corresponding values obtained for the jet-on condition for a specific configuration and angular attitude of the model. The basic data for the no-jet model are presented in figure 9, and the combined aerodynamic characteristics of the no-jet model plus the jet-interference effects of the jet model are presented in figures 10 and 11. The combined data of configurations 4, 5, and 6

simulate the actual characteristics of a complete airplane configuration. The static longitudinal- and directional-stability derivatives resulting from these combined effects are presented in figure 12.

By referring to figures 1 and 2, it can be seen that the airplane configuration employed has much too short a nose to simulate current types of configurations. This condition evolved during the model design from testing considerations, space limitations in the tunnel, and attempting to maintain a realistic distance between the jet exits and the tail surfaces. Because of the short nose on the model, the moment results which have been referenced to the $0.5\bar{c}$ of the wing provide an unrealistic static margin. Therefore, when the incremental jet-interference data are added to the no-jet data, the smallness of the jet-interference effects is entirely misleading with regard to its relative importance on the moments of the complete airplane configuration. Also, this unrealistic static margin may mask important nonlinearities existing in the curves presented in figures 10 and 11. Figure 13 shows the effect of transferring the center of gravity of the model upon the pitching moment and the yawing moment of the no-jet model for configurations 4, 5, and 6 at Mach numbers 1.94 and 2.41. The relative importance of the jet-interference effects is shown more realistically in figure 14 wherein the combined moment data (no-jet plus jet interference) are presented for the model center of gravity located at the wing trailing edge.

Presented in figure 15 are the aerodynamic characteristics for configuration 4 of the jet model for the condition wherein the jet nacelles were operated at different jet static-pressure ratios. The pressure ratio of the right nacelle was held at a constant value while the pressure ratio of the left nacelle was varied.

DISCUSSION

Effect of Varying Jet Static-Pressure Ratio

Jet model.- With few exceptions, an increase in the jet static-pressure ratio caused the jet interference to increase the value of normal force at angles of attack and angles of sideslip for configurations 5 and 6. (See figs. 7 and 8.) These increases are associated with an increase in the inclination of the jet-exit shock, an increase in the pressure rise across the jet-exit shock, and an increased flow angularity within the jet-interference flow field.

Pitching-moment curves exhibited nonlinear trends for $p_j/p_\infty > 5$ with angle of attack and angle of sideslip. (See figs. 7 and 8.) Jet

interference produced a stabilizing pitching-moment increment which increased in magnitude as p_j/p_∞ increased.

It will be noted that for a given value of p_j/p_∞, the normal force for all configurations changed very little with an increase in angle of attack at $M_\infty = 1.94$ (fig. 7) or with a decrease in angle of sideslip at $M_\infty = 1.94$ and 2.41 (figs. 7 and 8). Therefore, it is believed that the nonlinear variations in the pitching-moment curves of configurations 4, 5, and 6 for these conditions resulted principally from shifts in the center of pressure of the jet-interference flow field. However, at $M_\infty = 2.41$ (fig. 8) it is shown that for configurations 5 and 6 at a given value of p_j/p_∞, an increase in angle of attack produced significant variations in the value of normal force. For these configurations at a specific value of p_j/p_∞ the nonlinear behavior of the pitching-moment curves is attributed to a combination of shifts in center of pressure of the jet-interference flow field plus a variation in the value of normal force.

Combined effects.- The general effects of increasing p_j/p_∞ from 5 to 15 upon the values and trends of the pitching moment may be most easily seen by comparing figures 13 and 14 for equivalent model configurations, model center of gravity, and Mach number. At both Mach numbers all configurations experienced reductions in the values of pitching moment, with the reduction in value being greater for $M_\infty = 1.94$ than for $M_\infty = 2.41$.

Effect of Increasing the Vertical Displacement of the Horizontal Tail

Jet-interference effects upon the values of normal force and pitching moment at both α and β become more pronounced as the vertical displacement of the horizontal tail was increased above the center line of the body. (See figs. 7 and 8.) This fact seems contrary to what would be expected in view of the diagrams presented in figure 4. These diagrams indicated that configuration 6 would have less tail area influenced by the jet-interference flow field than would either configuration 4 or 5. However, due to the relative location of the horizontal tail of configuration 6 to the jet-exit shock and within the interference flow field, it was influenced to a greater extent by flow

angularity than was either configuration 4 or 5. In general, the farther from the jet-exit shock the horizontal tail is positioned in the jet-interference flow field, the less it would be influenced by flow angularity. This fact is illustrated by comparing configurations 5 and 6 in figure 7 or 8.

Jet interference had little effect upon the values of side force or yawing moment as the height of the horizontal tail was increased. (See figs. 7 and 8.) This result would be expected since all horizontal tails were maintained at zero incidence and the model was maintained at an angle of attack of 0°.

Effect of Increasing Free-Stream Mach Number

An increase in M_∞ from 1.94 to 2.41 reduced the static directional stability for all complete tail configurations. (See fig. 12.) This reduction is associated with the well-known decrease in vertical-tail effectiveness that normally accompanies a Mach number increase rather than by jet interference. An increase in free-stream Mach number caused jet interference to have less effect upon the values of pitching moment at angles of attack as p_j/p_∞ was increased. (See fig. 14.)

Effects of Operating the Jets at Unequal Jet Static-Pressure Ratios

The effects of operating the jets at unequal jet static-pressure ratios are shown for configuration 4 in figure 15. In assessing the data of this figure it should be remembered that the body and tail were connected to the strain-gage beams, which were in turn connected to the rigid wing and nacelles. Therefore, the balances did not measure the thrust of the jets and the results represent purely the jet-interference effects. Figure 15 shows that jet interference had little effect upon the normal force and pitching moment at the test values of angle of sideslip but that it produced significant changes in these quantities at an angle of attack of 4° at $M_\infty = 1.94$. The values of side force and yawing moment were affected by the jet interference of the unequally operated jets both at angles of sideslip of 0° and 4° and angles of attack of 0° and 4°. The yawing moment produced by the jet interference from the differentially operated jets opposed in direction the moment that would be produced by the direct action of the jet thrust and, based on the calculated values of the jet thrust, with a difference in pressure ratio of 15, amounted to about 11.5 percent of the yawing moment which would be produced by the jet thrust at a Mach number of 1.94. At a Mach number of 2.41 and

a difference in jet static-pressure ratios between the jets of 15, the jet-interference yawing moment would be opposite to and about 7.8 percent of the yawing moment which would be produced by the jet thrust force.

CONCLUSIONS

An investigation to determine the jet-interference effects upon the longitudinal and directional stability of a general aircraft configuration employing wing-tip-mounted nacelles resulted in the following conclusions:

1. Jet interference had no significant effect upon the directional stability at an angle of attack of 0° as the jet static-pressure ratio and vertical displacement of the horizontal tail were increased.

2. Addition of the jets to the free-stream flow field generally increased the values of normal force both at angles of attack and angles of sideslip and produced nonlinearities in the pitching-moment curves for all complete tail configurations. The extent of the jet-interference effects depended primarily upon the relative location of the horizontal tail in the jet-interference flow field and on the jet static-pressure ratio.

3. An increase in free-stream Mach number reduced the directional stability of the model; this decrease was associated with the well-known decrease in vertical-tail effectiveness that normally accompanies a Mach number increase rather than by jet interference. A Mach number increase did cause a reduction in the jet-interference effects upon the values of normal force and pitching moment, however.

4. For the particular configuration tested when the jets were operated at unequal jet static-pressure ratios, jet interference had little effect upon the normal force and pitching moment at the test values of angle of sideslip, but it produced significant changes in these quantities at an angle of attack of 4°. The values of side force and yawing moment were affected by the jet interference both at angles of attack and at angles of sideslip.

5. A reduction in the static margin of the model to a more realistic value amplified the nonlinearities that existed in the pitching-moment

curves and showed that jet interference produced important effects upon the values of pitching moment for an airplane configuration of this type.

Langley Aeronautical Laboratory,
National Advisory Committee for Aeronautics,
Langley Field, Va., December 5, 1957.

REFERENCES

1. Love, Eugene S., and Grigsby, Carl E.: Some Studies of Axisymmetric Free Jets Exhausting from Sonic and Supersonic Nozzles Into Still Air and Into Supersonic Stream. NACA RM L54L31, 1955.

2. Love, Eugene S.: Initial Inclination of the Mixing Boundary Separating An Exhausting Supersonic Jet From a Supersonic Ambient Stream. NACA RM L55J14, 1956.

3. Love, Eugene S., Woodling, Mildred J., and Lee, Louise P.: Boundaries of Supersonic Axisymmetric Free Jets. NACA RM L56G18, 1956.

4. Englert, Gerald W., Wasserbauer, Joseph F., and Whalen, Paul: Interaction of a Jet and Flat Plate Located in an Airstream. NACA RM E55G19, 1955.

5. Salmi, Reino J., and Klann, John L.: Interference Effects at Mach 1.9 on a Horizontal Tail Due to Trailing Shock Waves From an Axisymmetric Body with an Exiting Jet. NACA RM E55J13a, 1956.

6. Valerino, Alfred S.: Jet Effects on Pressure Loading of All-Movable Horizontal Stabilizer. NACA RM E54C24, 1954.

7. Wasserbauer, Joseph F., and Englert, Gerald W.: Interaction of an Exhaust Jet and Elementary Contoured Surfaces Located in a Supersonic Air Stream. NACA RM E56A16, 1956.

8. Bressette, Walter E., and Leiss, Abraham: Investigation of Jet Effects on a Flat Surface Downstream of the Exit of a Simulated Turbojet Nacelle at a Free-Stream Mach Number of 1.39. NACA RM L55L13, 1956.

9. O'Donnell, Robert M., and McDearmon, Russell W.: Experimental Investigation of Effects of Primary Jet Flow and Secondary Flow Through a Zero-Length Ejector on Base and Boattail Pressures of a Body of Revolution at Free-Stream Mach Numbers of 1.62, 1.93, and 2.41. NACA RM L54I22, 1954.

10. Bromm, August F., Jr., and O'Donnell, Robert M.: Investigation at Supersonic Speeds of the Effect of Jet Mach Number and Divergence Angle of the Nozzle Upon the Pressure of the Base Annulus of a Body of Revolution. NACA RM L54I16, 1954.

11. Cortright, Edgar M., Jr., and Schroeder, Albert H.: Investigation at Mach Number 1.91 of Side and Base Pressure Distributions Over Conical Boattails Without and With Jet Flow Issuing From Base. NACA RM E51F26, 1951.

12. Love, Eugene S.: Aerodynamic Investigation of a Parabolic Body of Revolution at Mach Number of 1.92 and Some Effects of an Annular Supersonic Jet Exhausting From the Base. NACA TN 3709, 1956. (Supersedes NACA RM L9K09.)

13. Peck, Robert F.: Jet Effects on Longitudinal Trim of an Airplane Configuration Measured at Mach Numbers Between 1.2 and 1.8. NACA RM L54J29a, 1955.

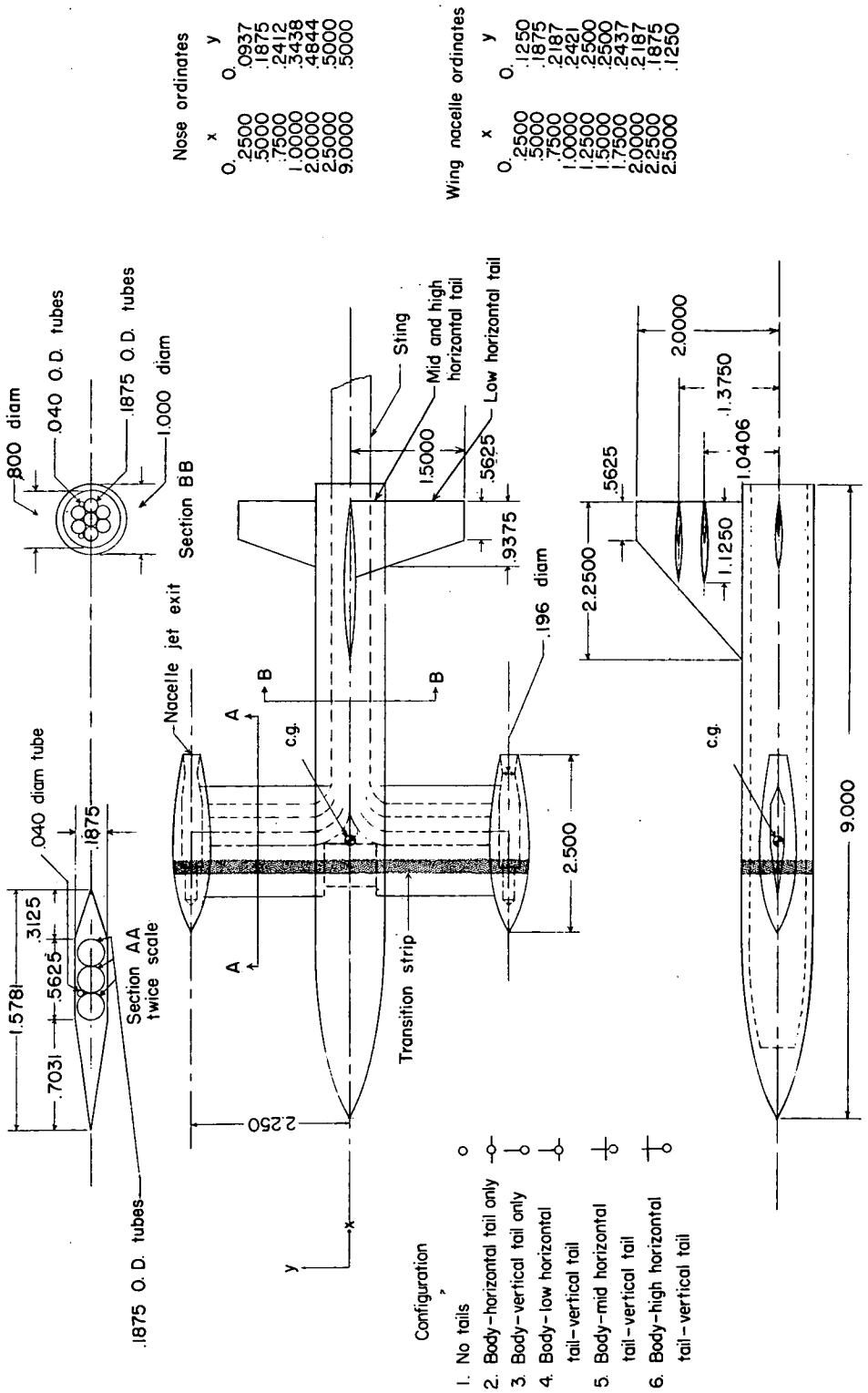

Figure 1.- Drawing of jet model showing principal dimensions. (All dimensions are in inches.)

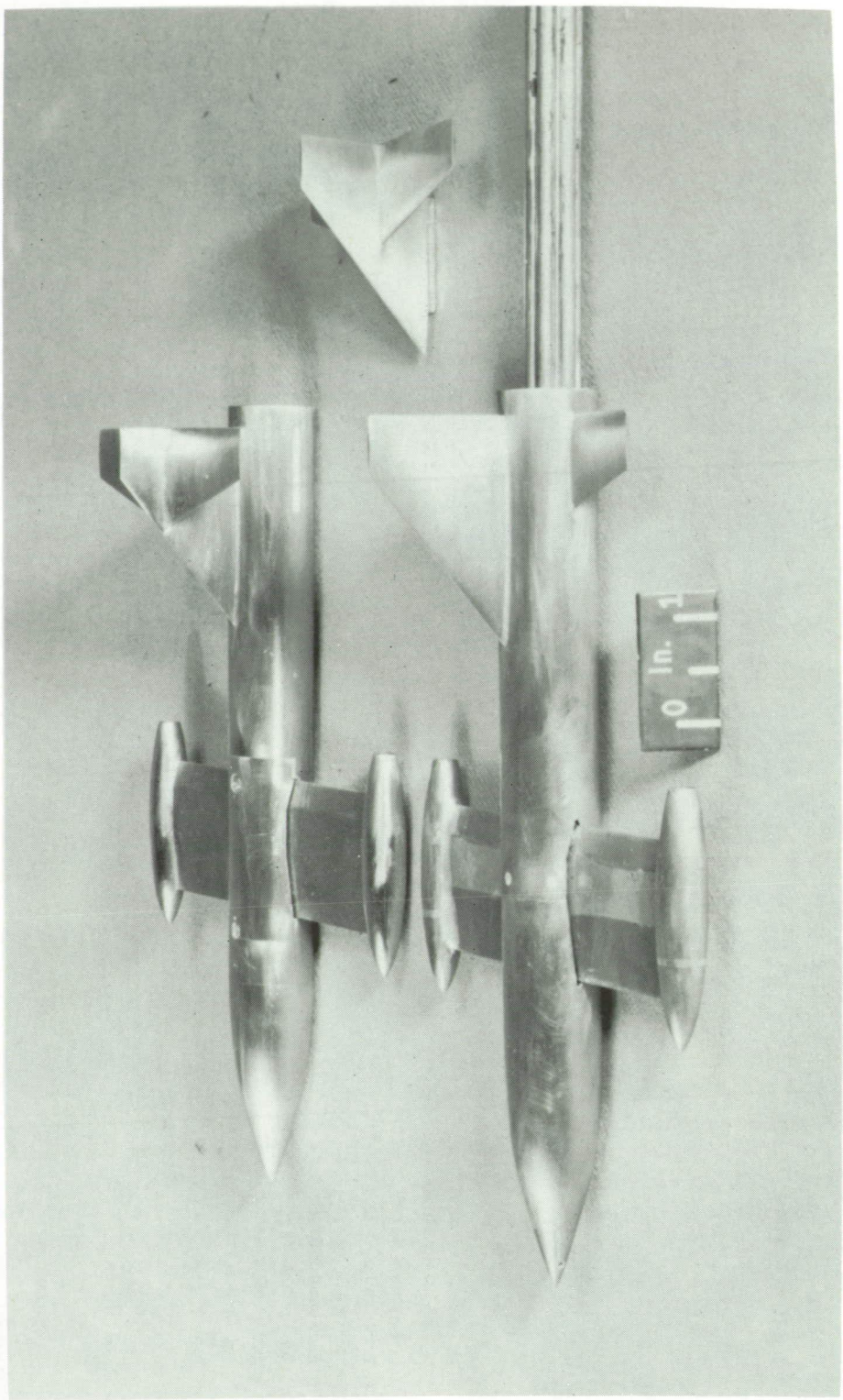

(a) Illustration of three complete tail configurations. L-94228

Figure 2.- Photographs of models tested.

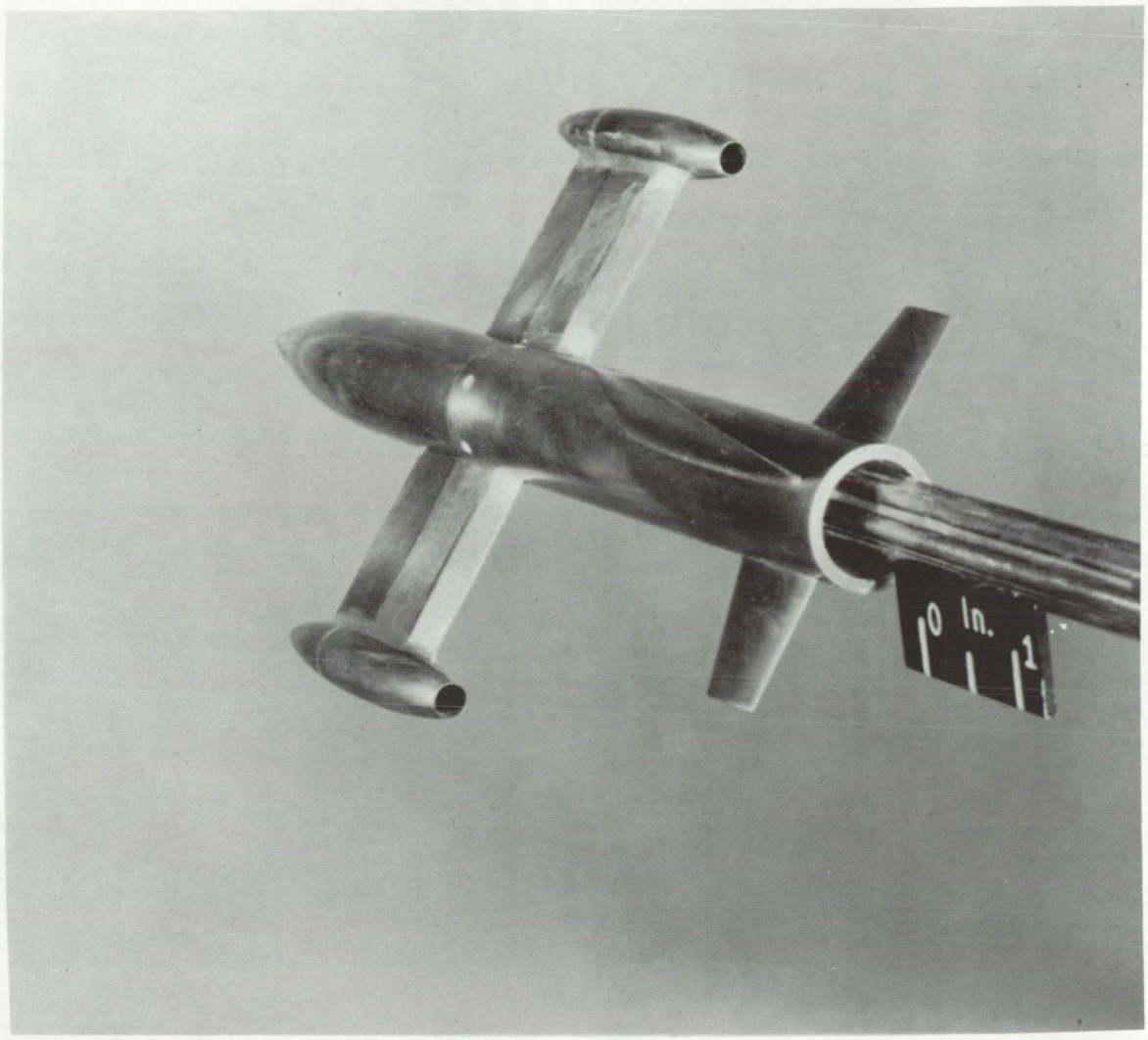

(b) Illustration of jet exits. L-94229

Figure 2.- Concluded.

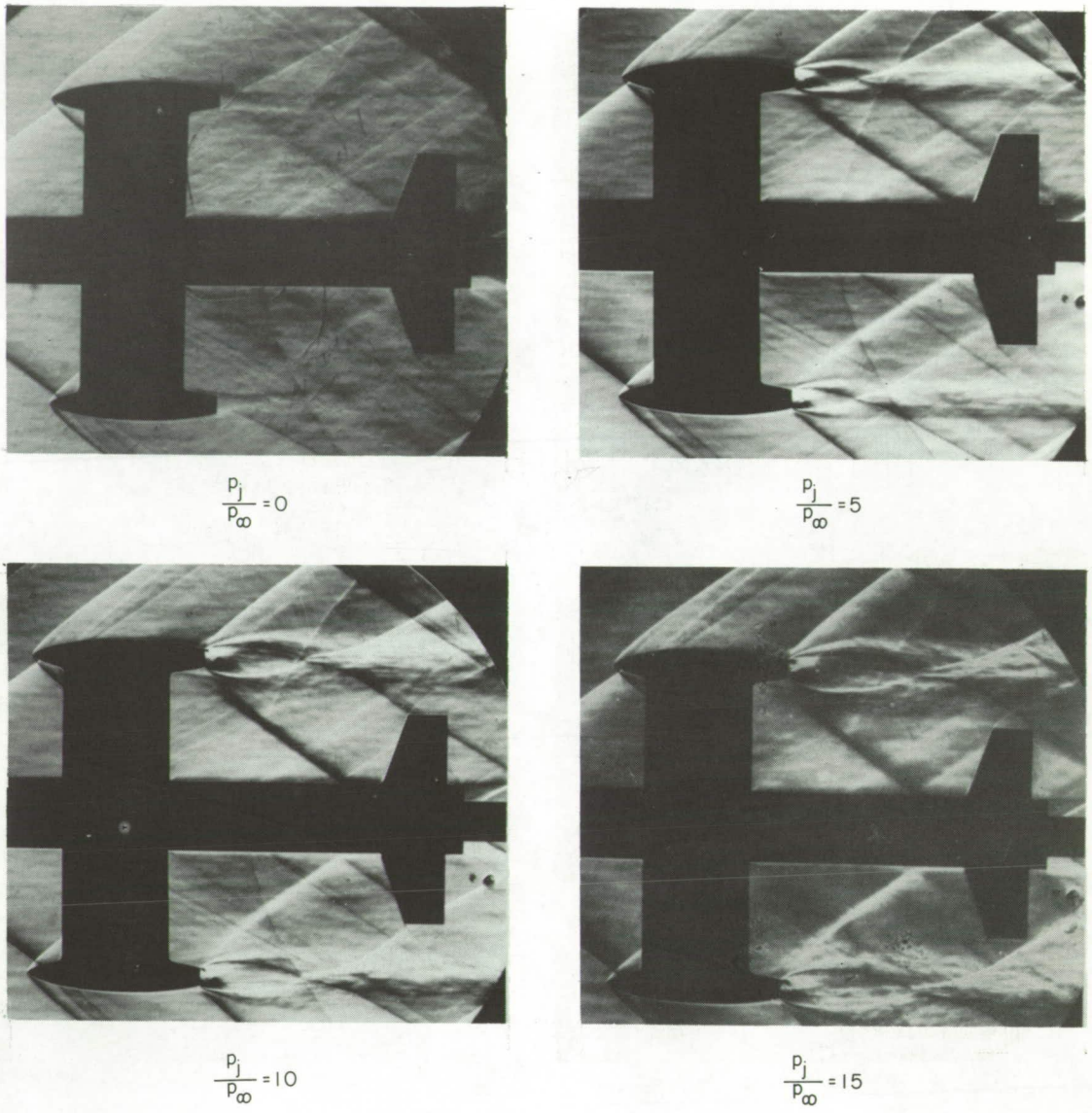

(a) $\alpha = 0^\circ$; $\beta = 0^\circ$; $M_\infty = 1.94$. L-57-4444

Figure 3.- Schlieren photographs illustrating the effect of increasing jet static-pressure ratio.

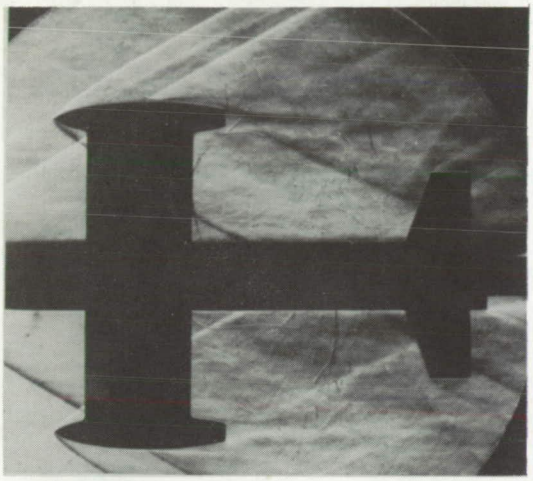

$\frac{p_j}{p_\infty} = 0$

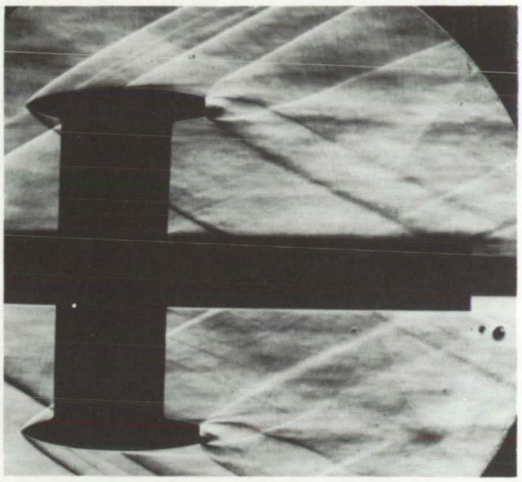

$\frac{p_j}{p_\infty} = 5$

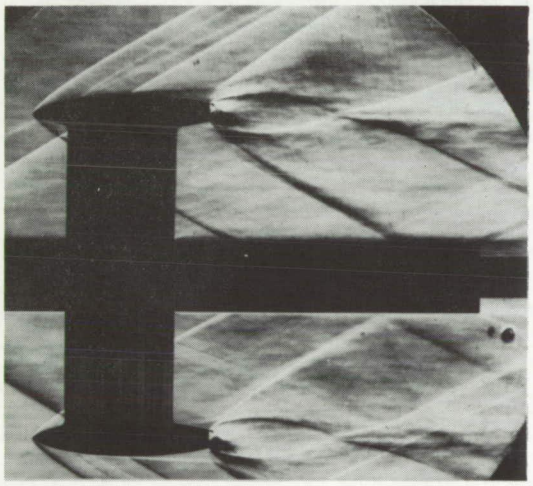

$\frac{p_j}{p_\infty} = 15$

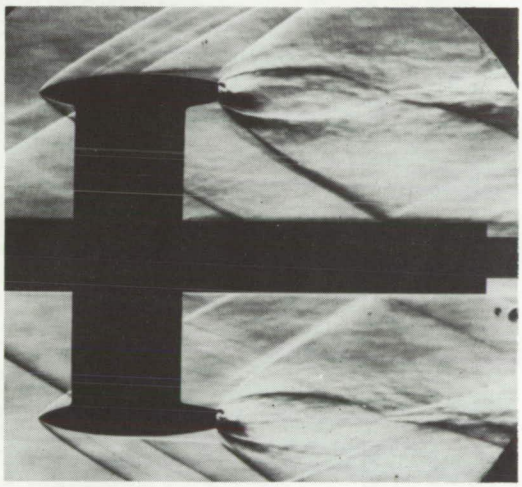

$\frac{p_j}{p_\infty} = 25$

(b) $\alpha = 0^\circ$; $\beta = 0^\circ$; $M_\infty = 2.41$. L-57-4445

Figure 3.- Concluded.

(Note: Shocks shown on horizontal tails are for configurations 4, 5, and 6, left to right, respectively.)

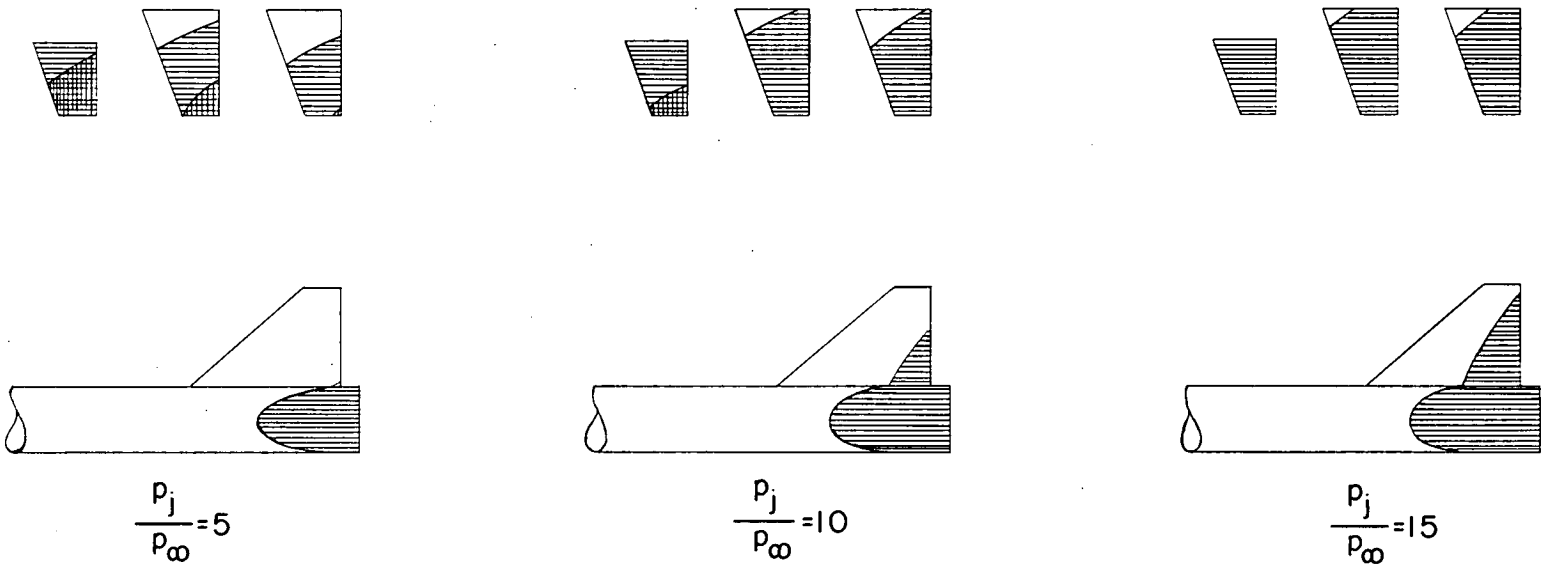

(a) $\alpha = 0^\circ$; $\beta = 0^\circ$; $M_\infty = 1.94$.

Figure 4.- Horizontal-tail, vertical-tail, and body areas influenced by jet-exit shock and shock from within the jet. Horizontal shading denotes jet-exit shock and vertical shading denotes shock from within jet.

(Note: Shocks shown on horizontal tails are for configurations 4, 5, and 6, left to right, respectively.)

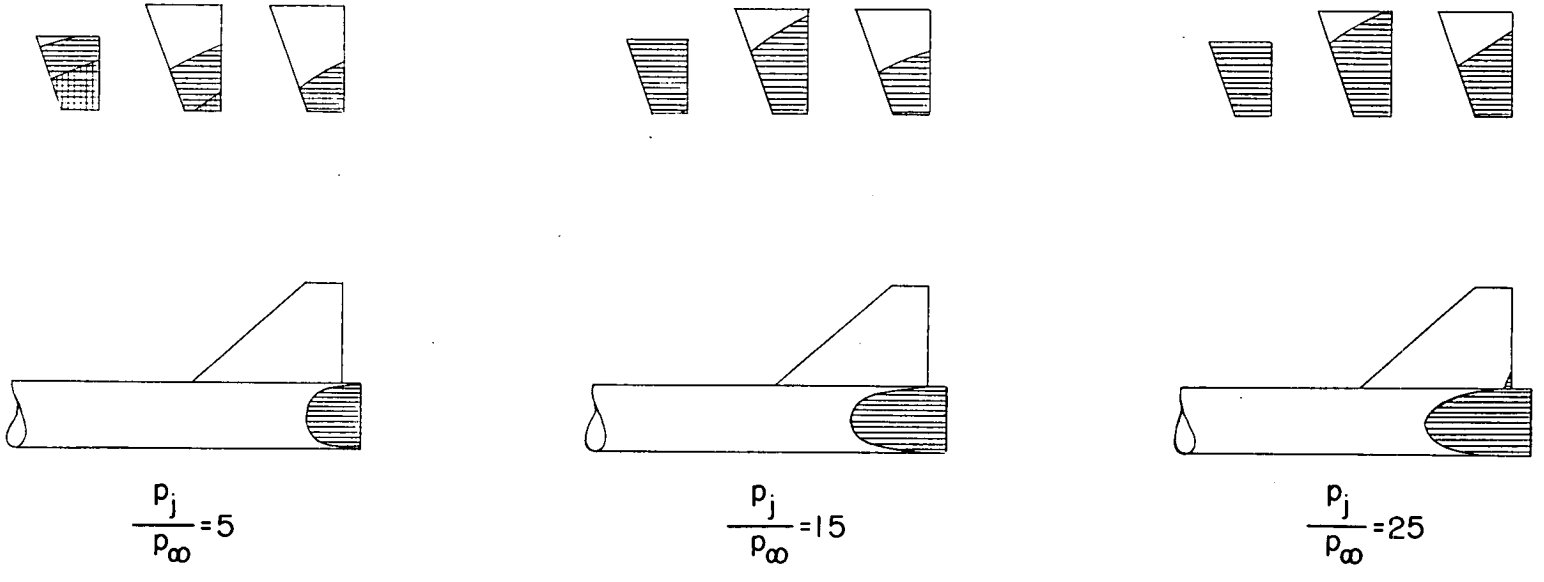

(b) $\alpha = 0^\circ$; $\beta = 0^\circ$; $M_\infty = 2.41$.

Figure 4.- Concluded.

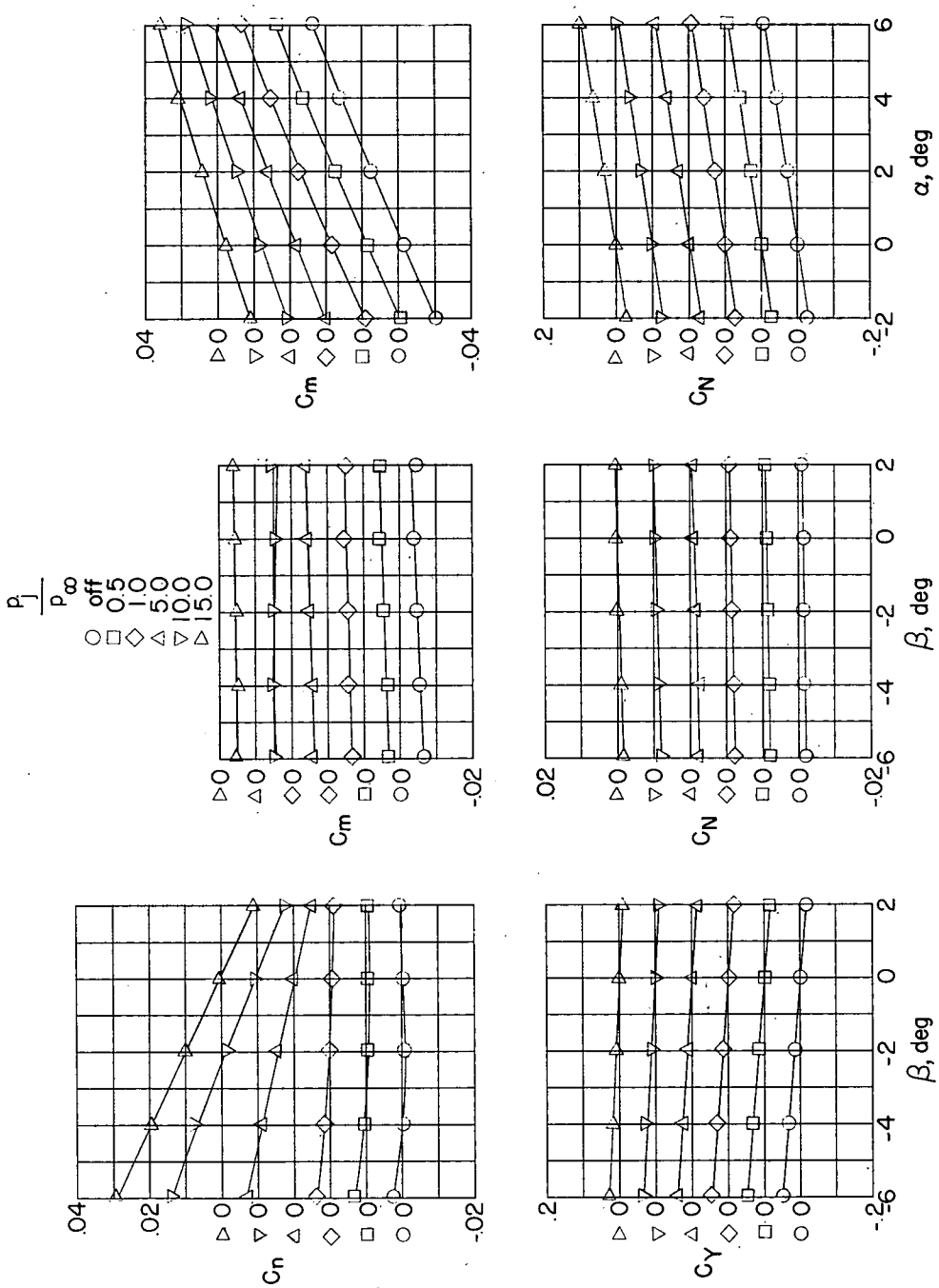

(a) Configuration 1.

Figure 5.- Aerodynamic characteristics of jet model. $M_\infty = 1.94$.

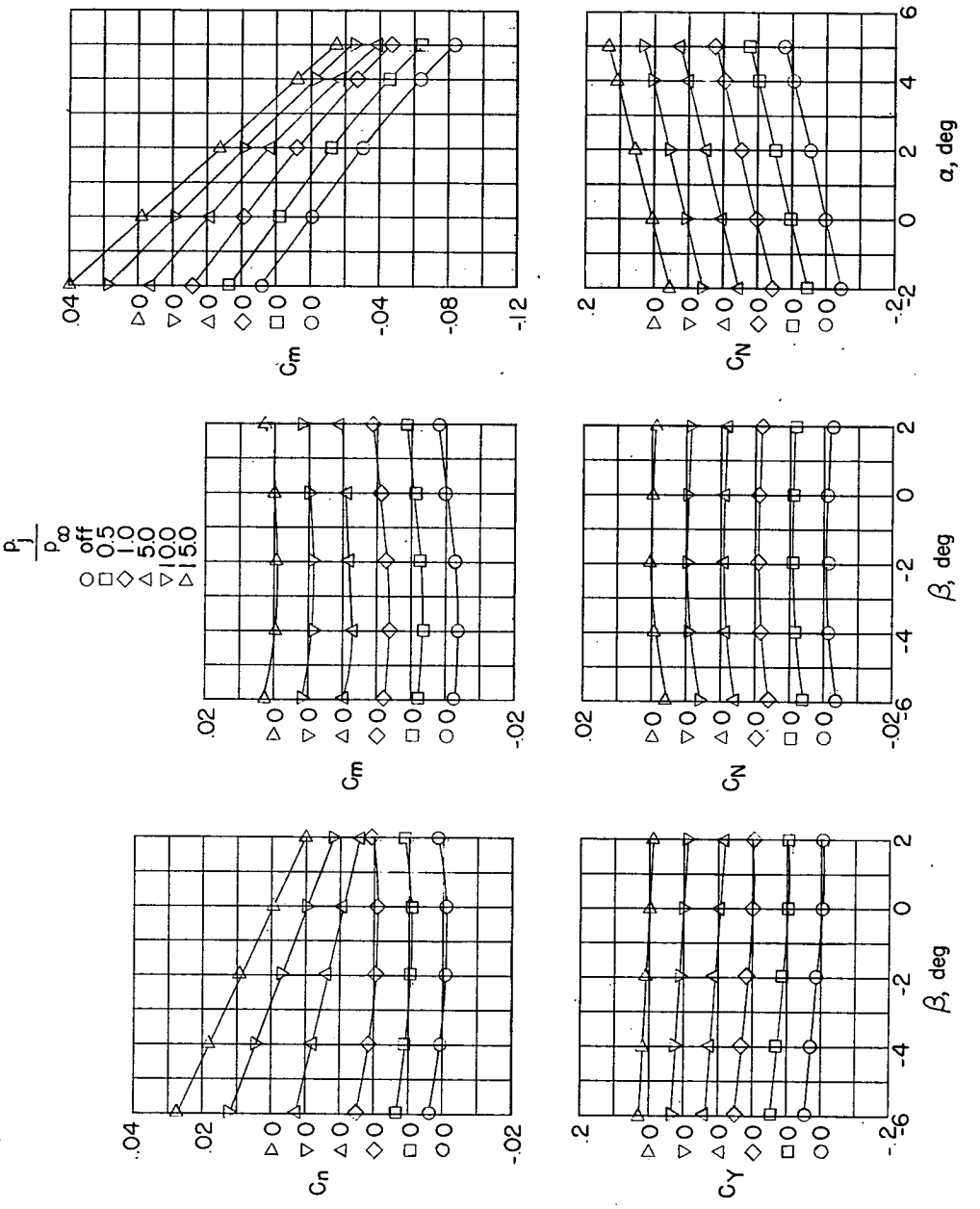

(b) Configuration 2.

Figure 5.- Continued.

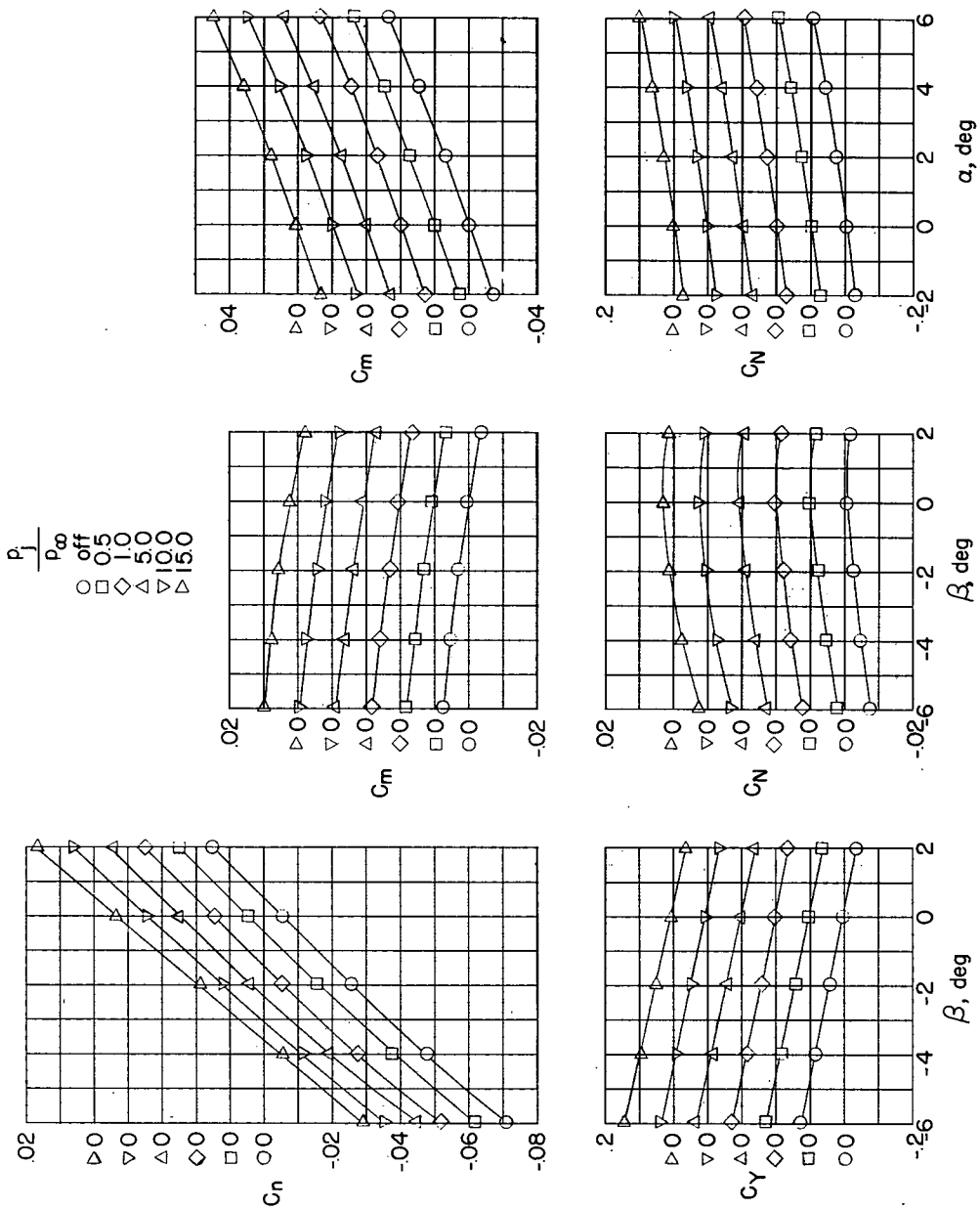

(c) Configuration 3.

Figure 5.- Continued.

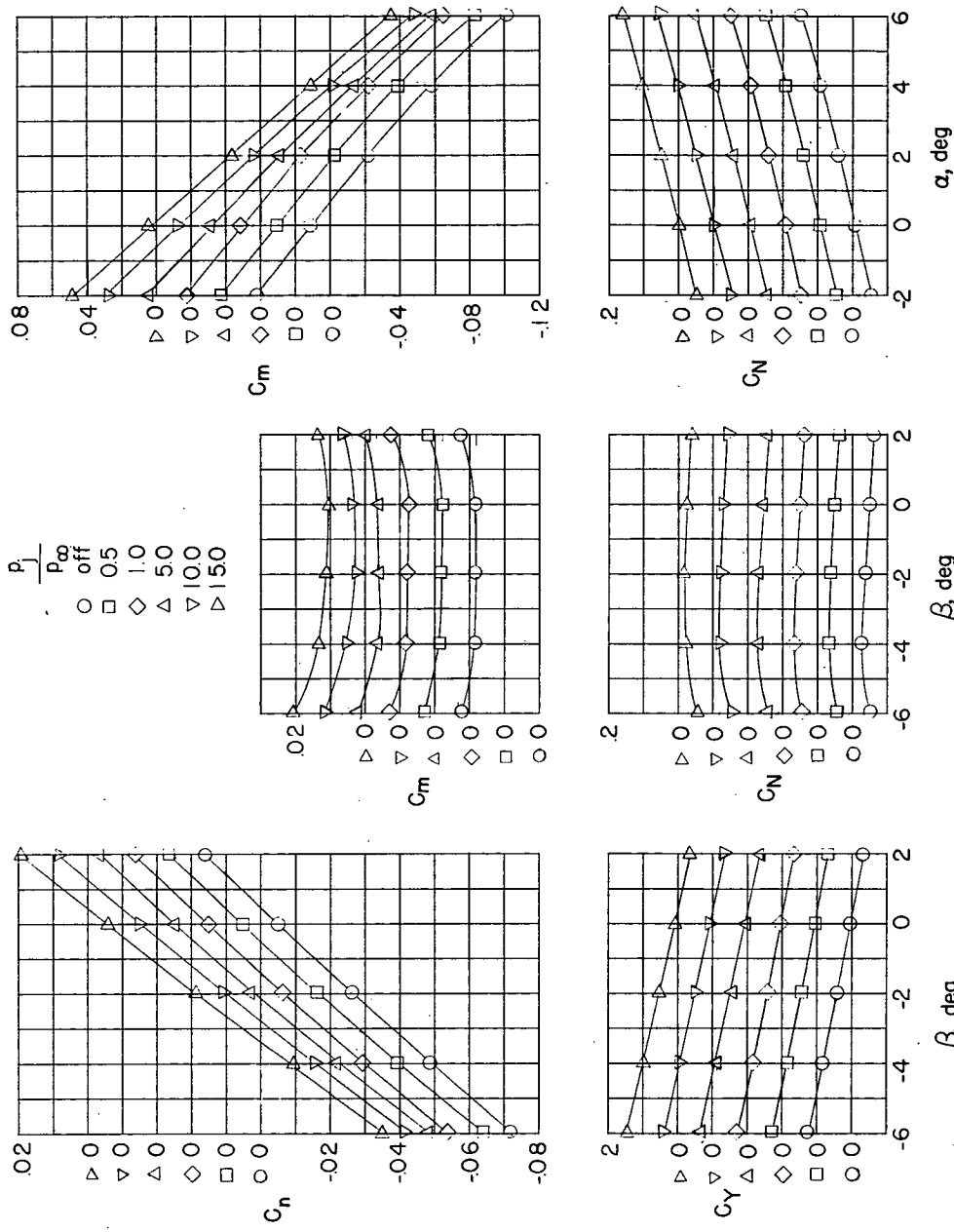

(d) Configuration 4.

Figure 5.- Continued.

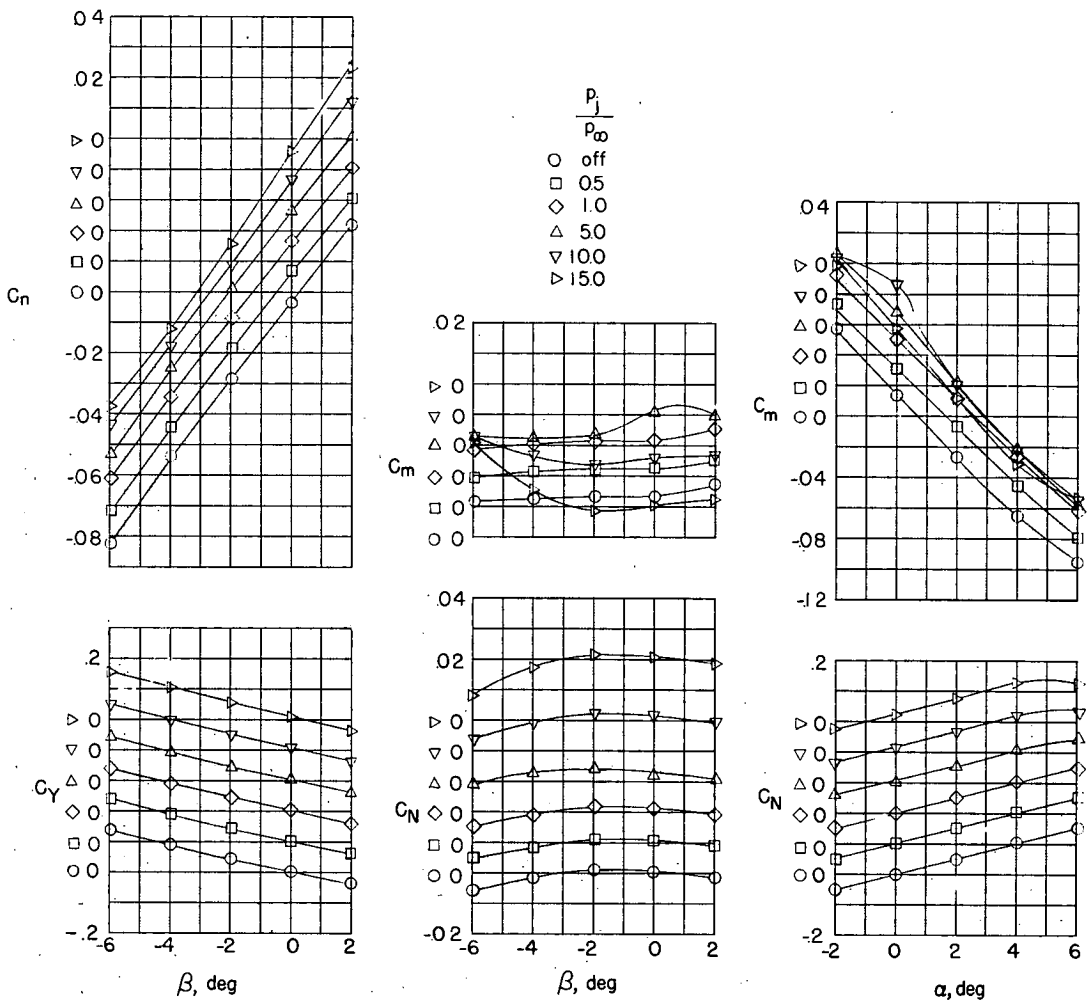

(e) Configuration 5.

Figure 5.- Continued.

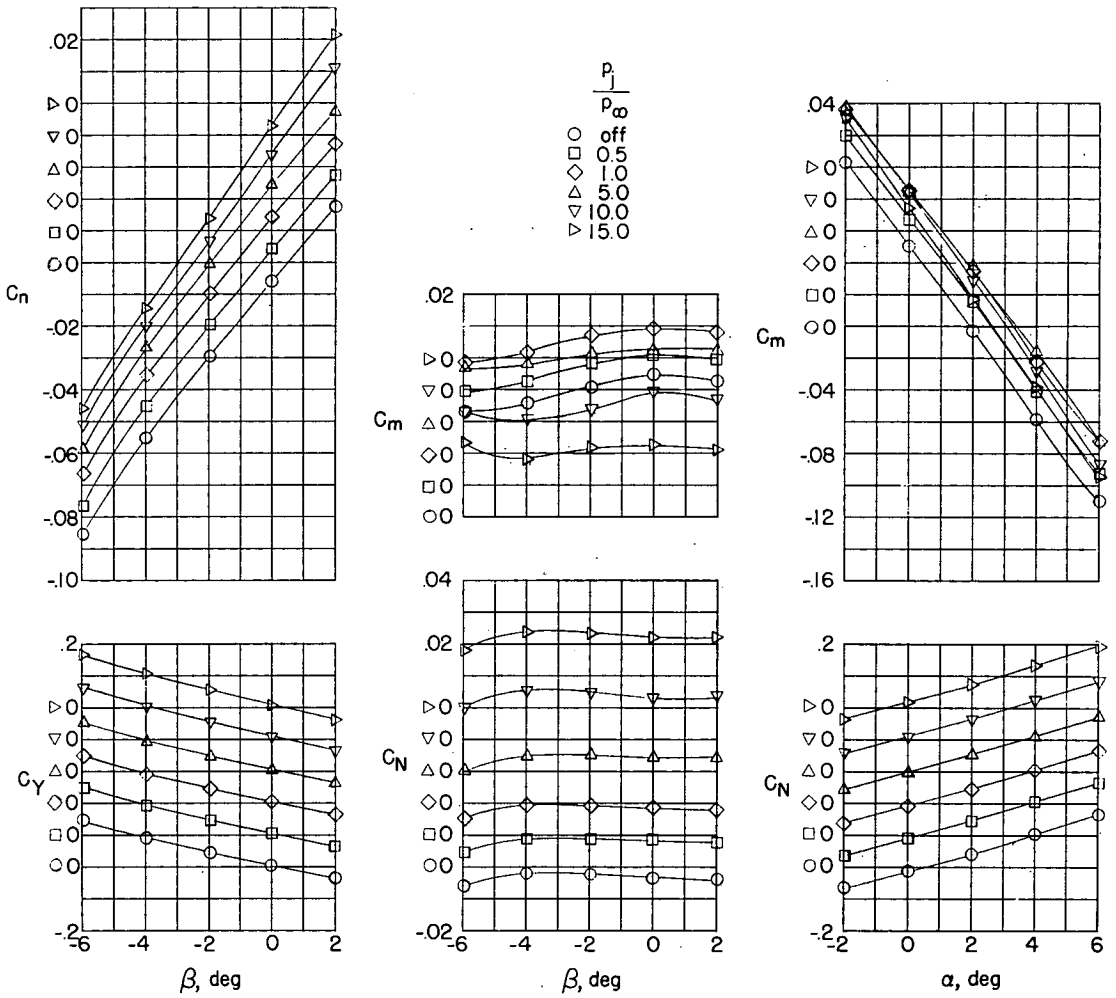

(f) Configuration 6.

Figure 5.- Concluded.

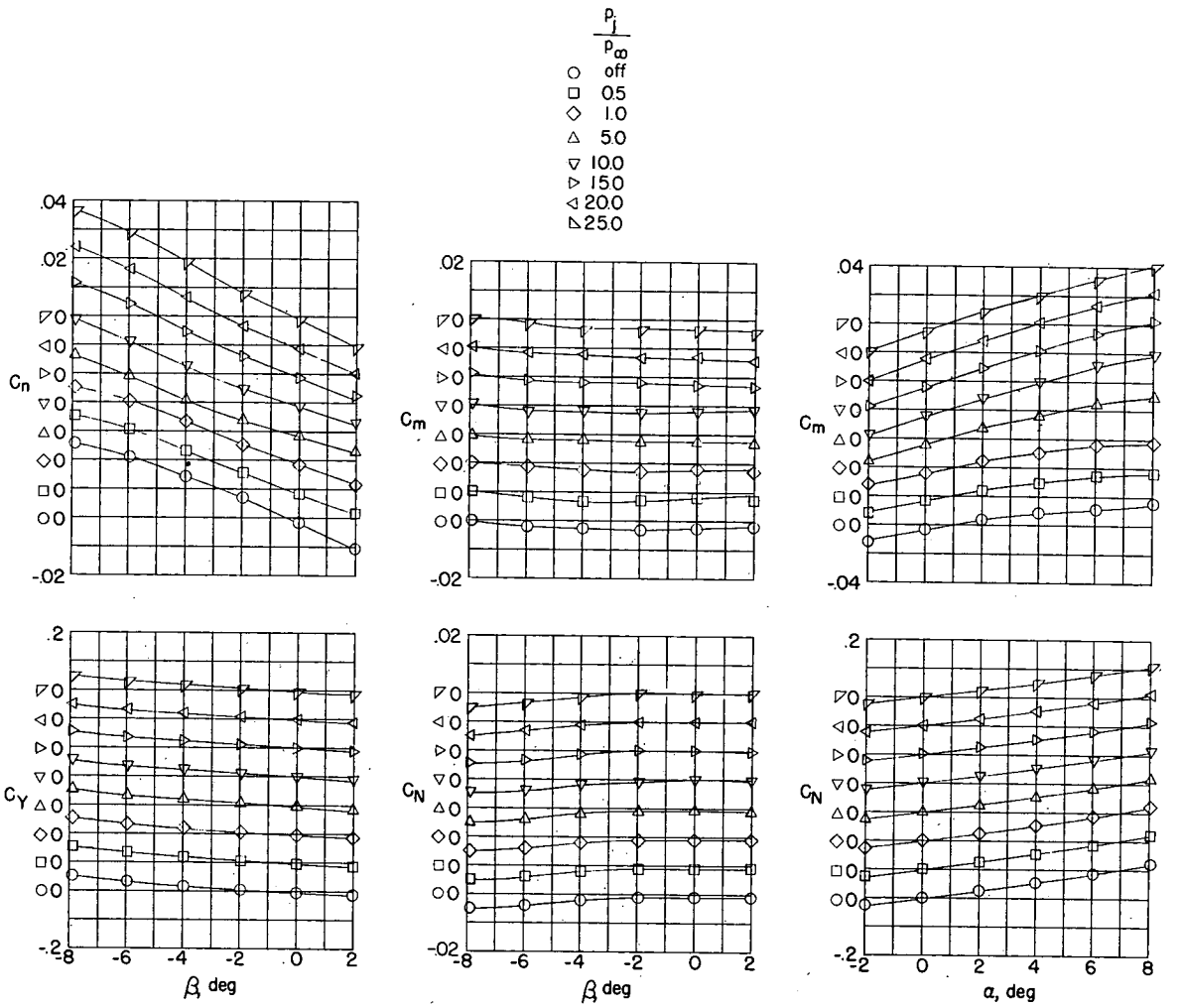

(a) Configuration 1.

Figure 6.- Aerodynamic charactersitics of jet model. $M_\infty = 2.41$.

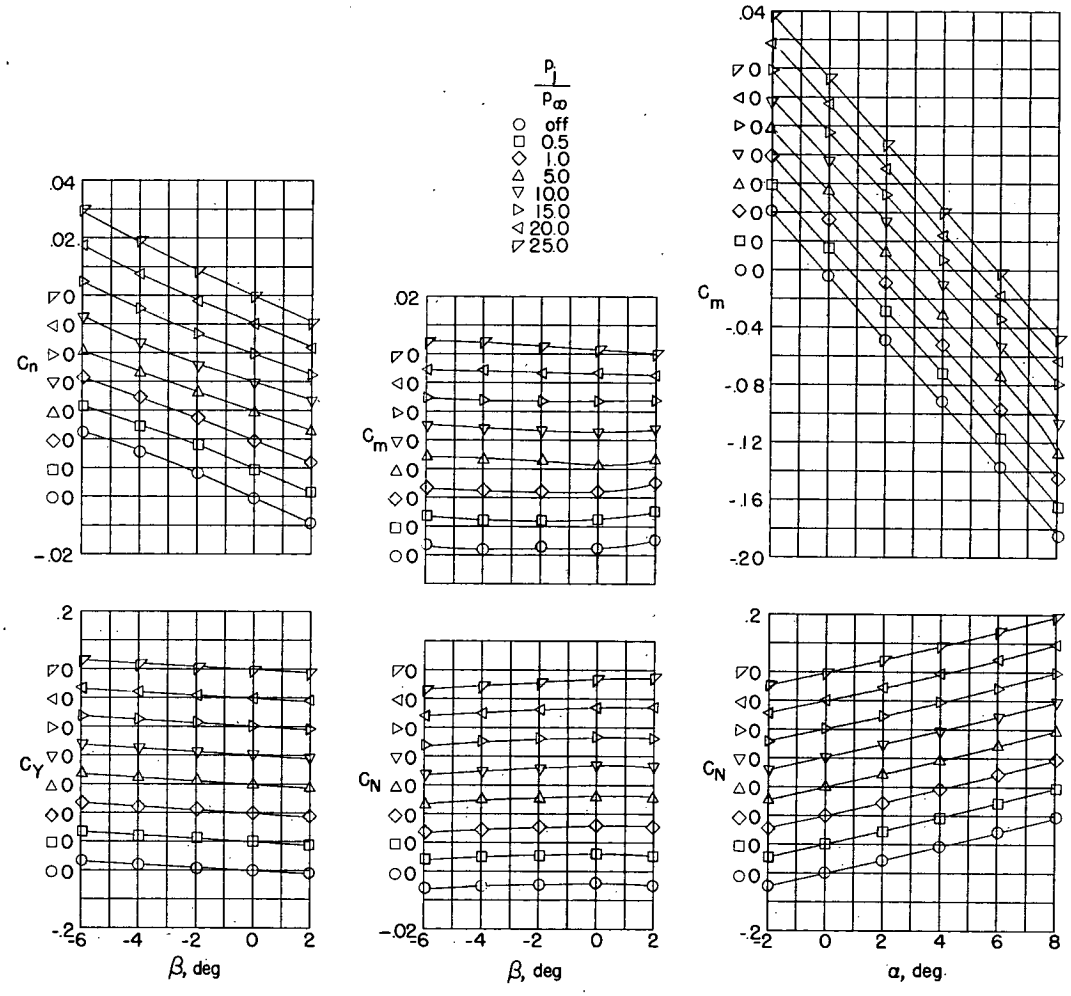

(b) Configuration 2.

Figure 6.- Continued.

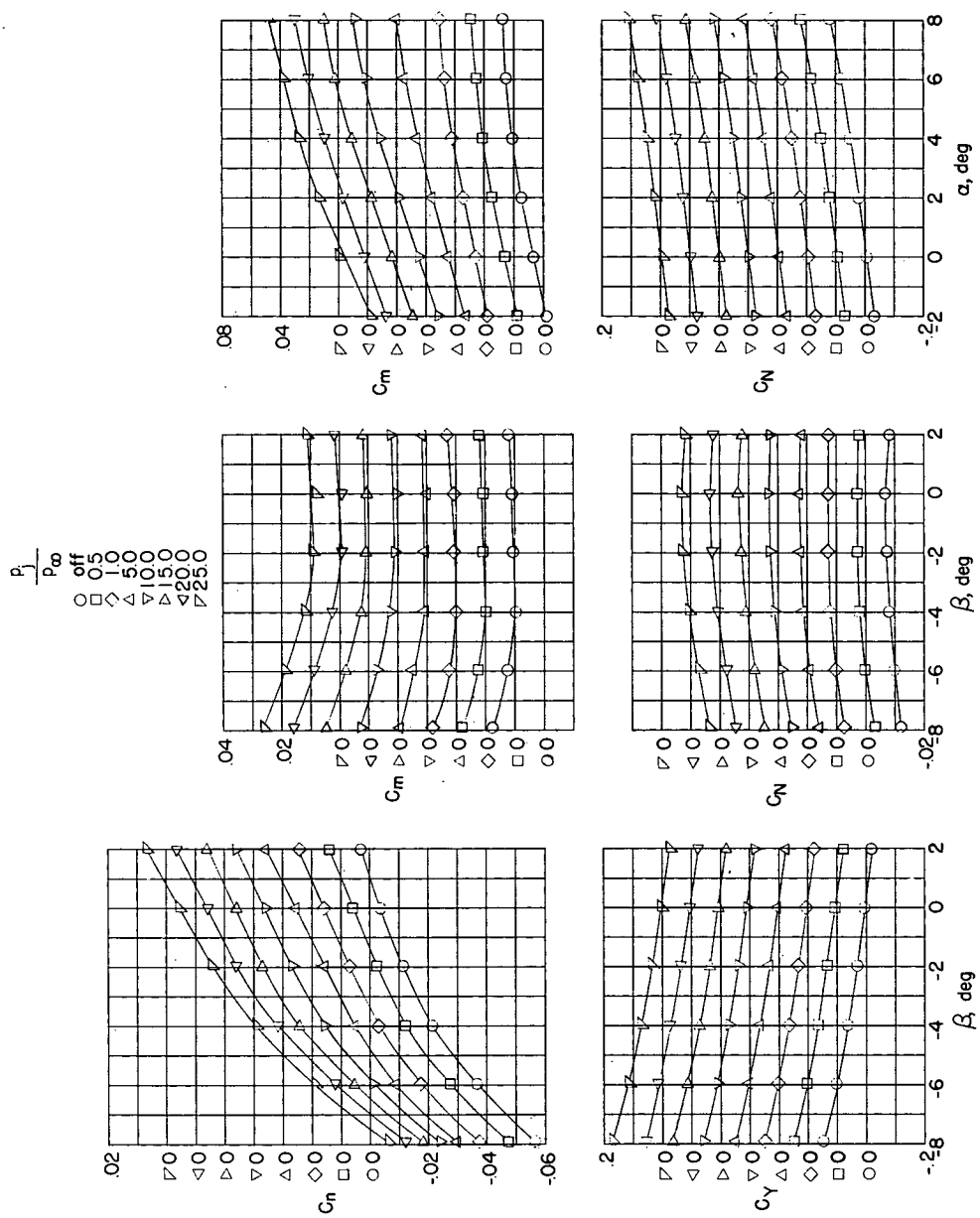

(c) Configuration 3.

Figure 6.- Continued.

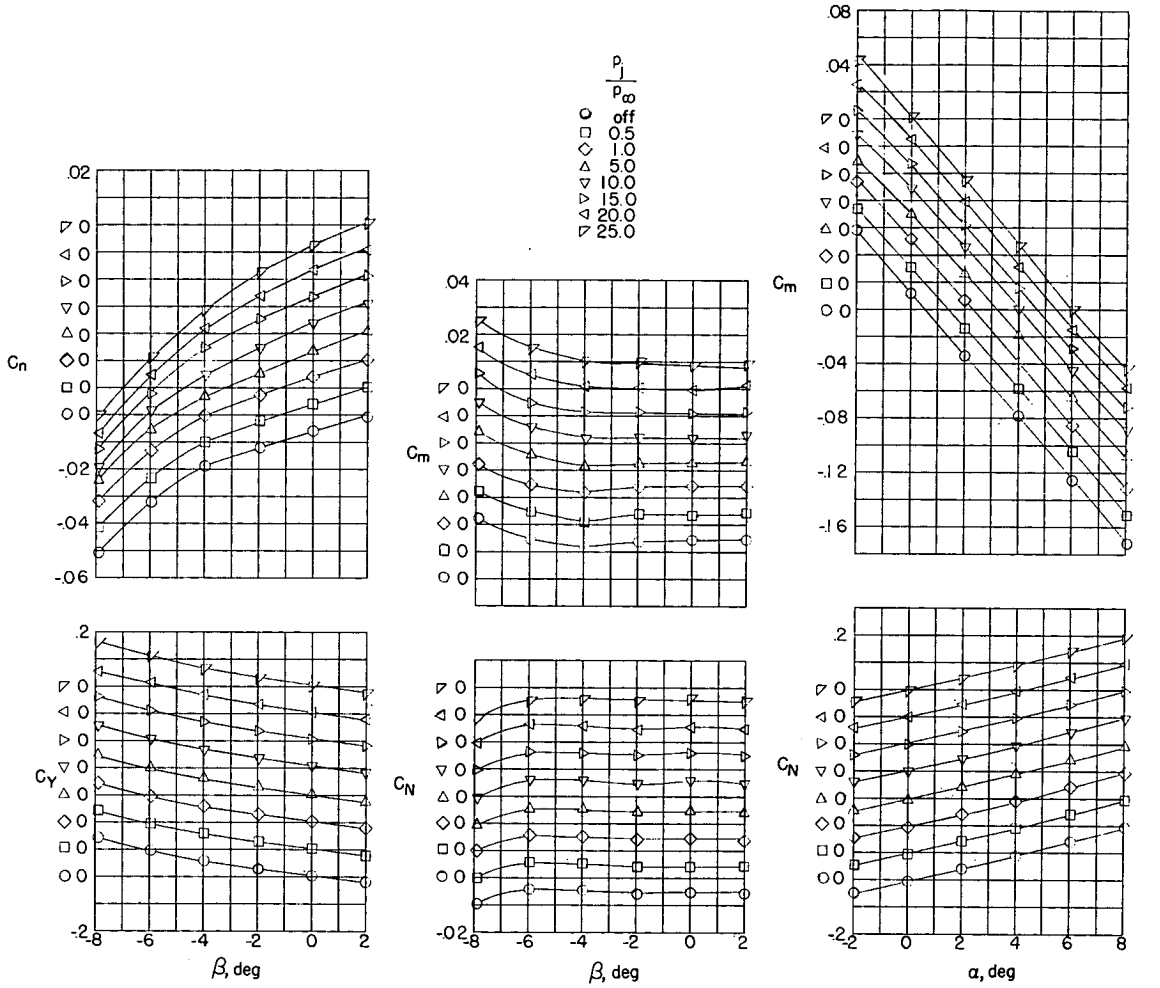

(d) Configuration 4.

Figure 6.- Continued.

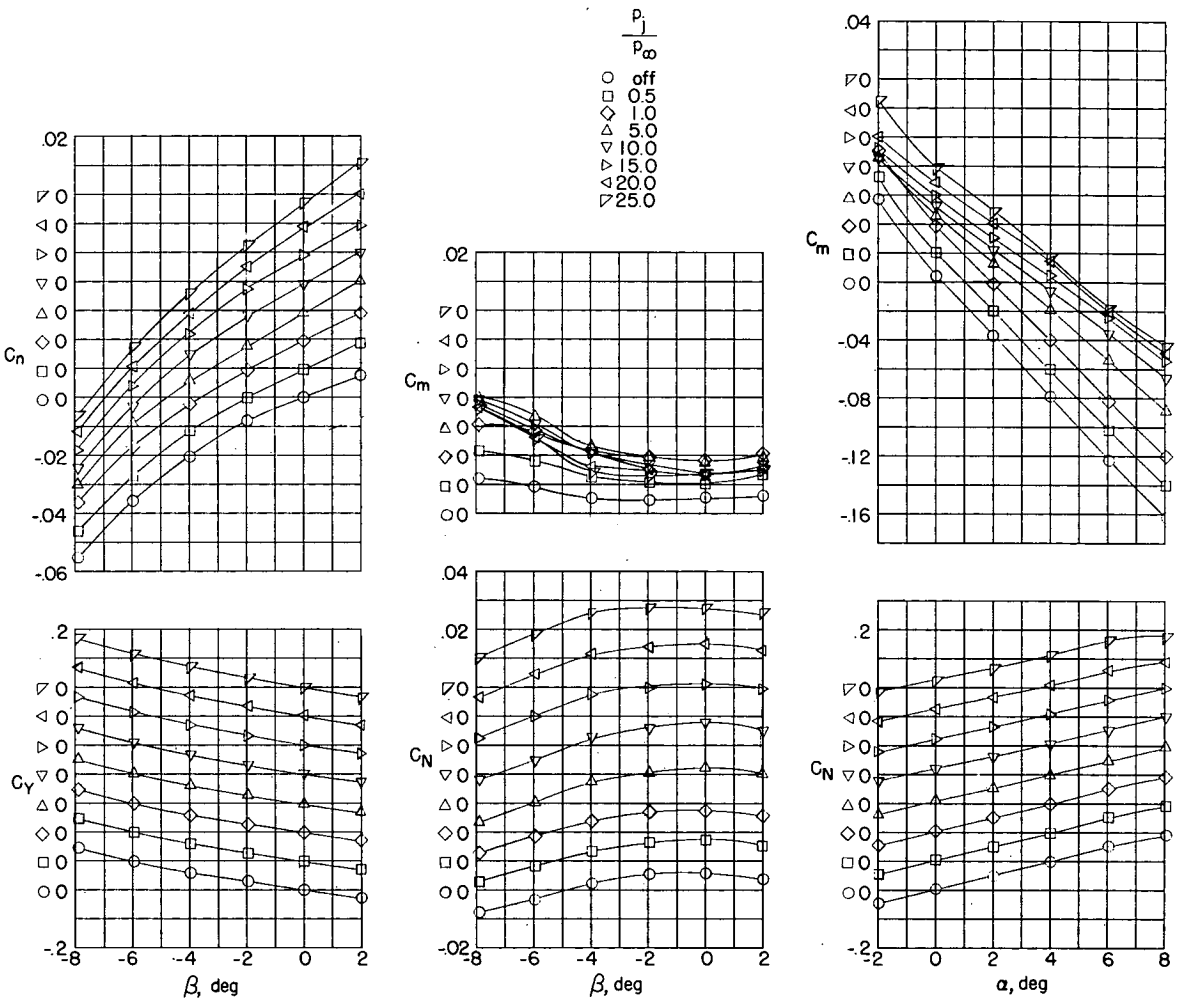

(e) Configuration 5.

Figure 6.- Continued.

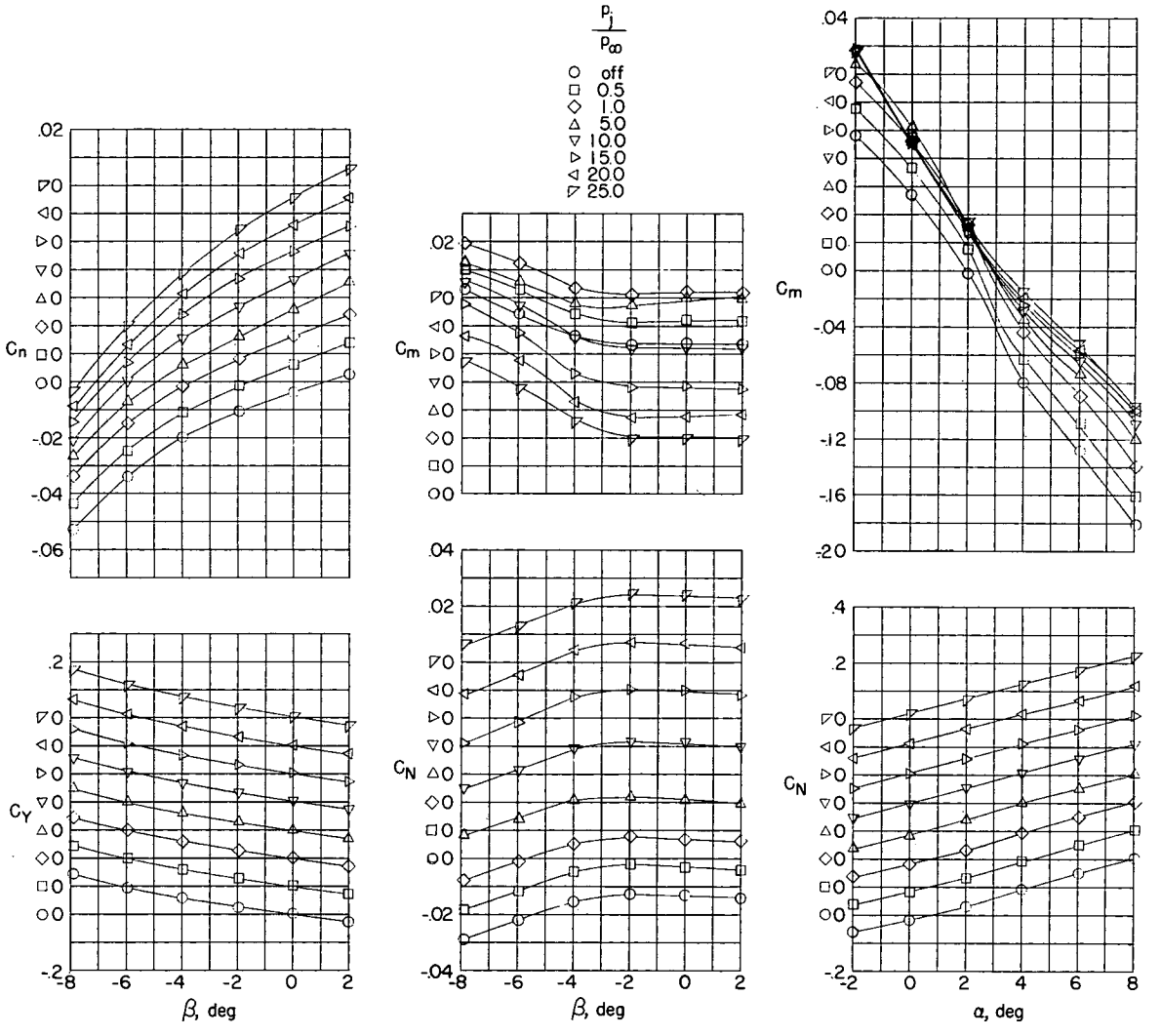

(f) Configuration 6.

Figure 6.- Concluded.

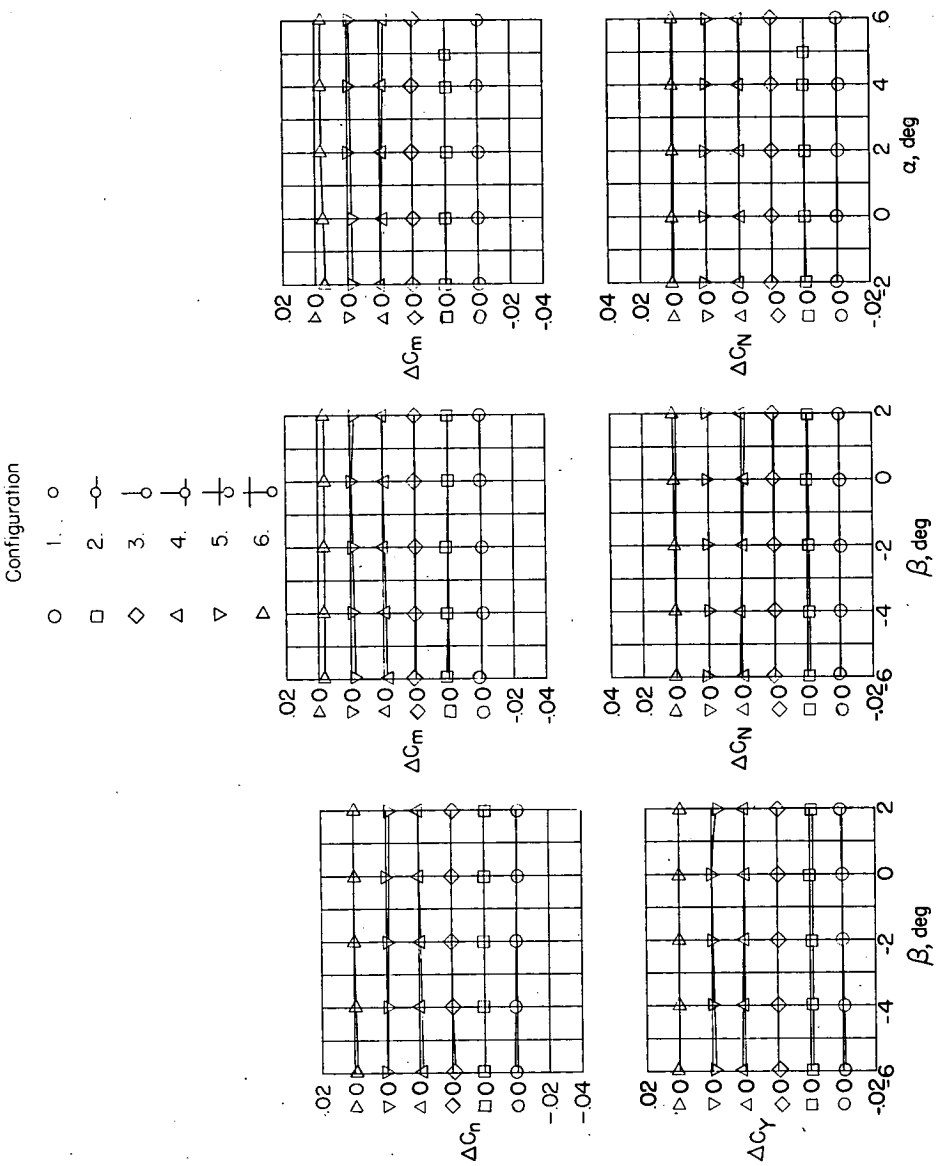

(a) $p_j/p_\infty = 0.5$.

Figure 7.- Incremental jet-interference effects (jet-on minus jet-off) upon the aerodynamic characteristics of the jet model. $M_\infty = 1.94$.

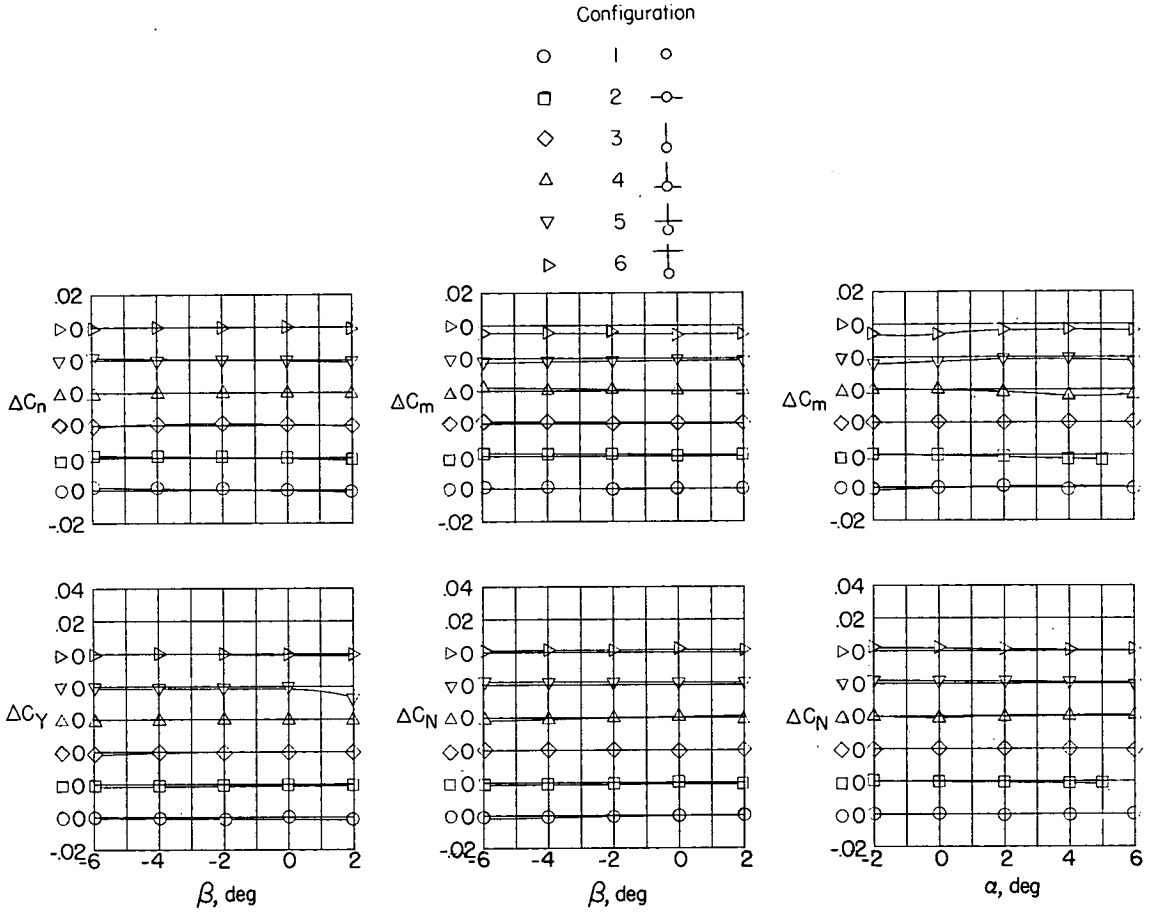

(b) $p_j/p_\infty = 1.0$.

Figure 7.- Continued.

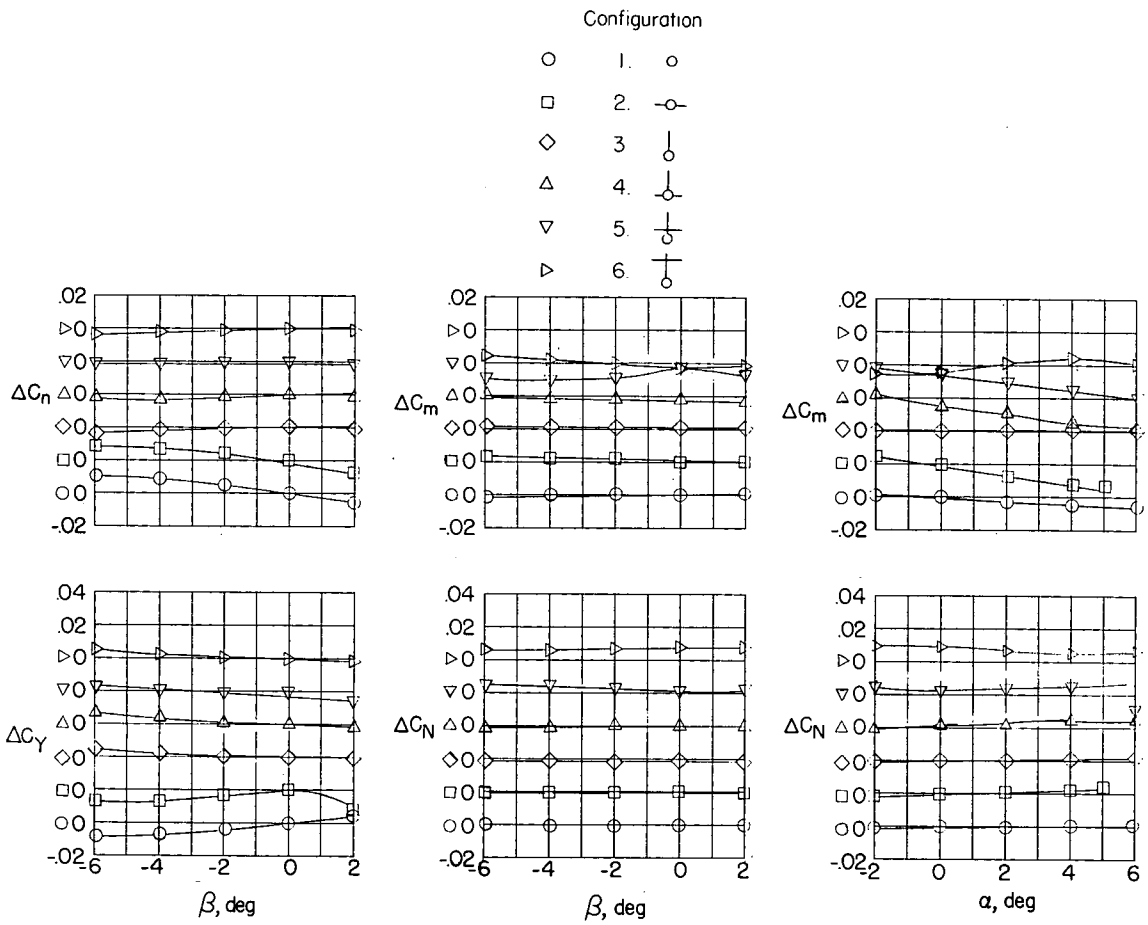

(c) $p_j/p_\infty = 5.0$.

Figure 7.- Continued.

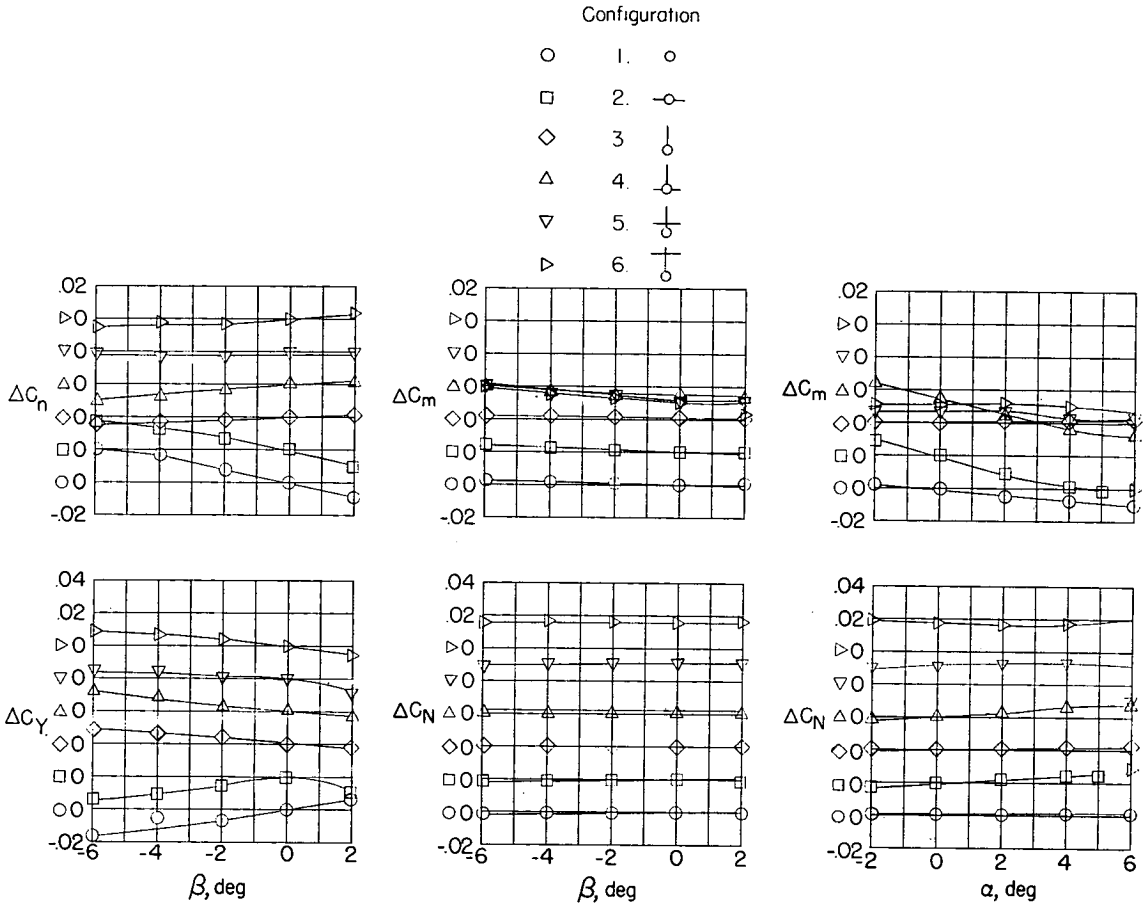

(d) $p_j/p_\infty = 10.0$.

Figure 7.- Continued.

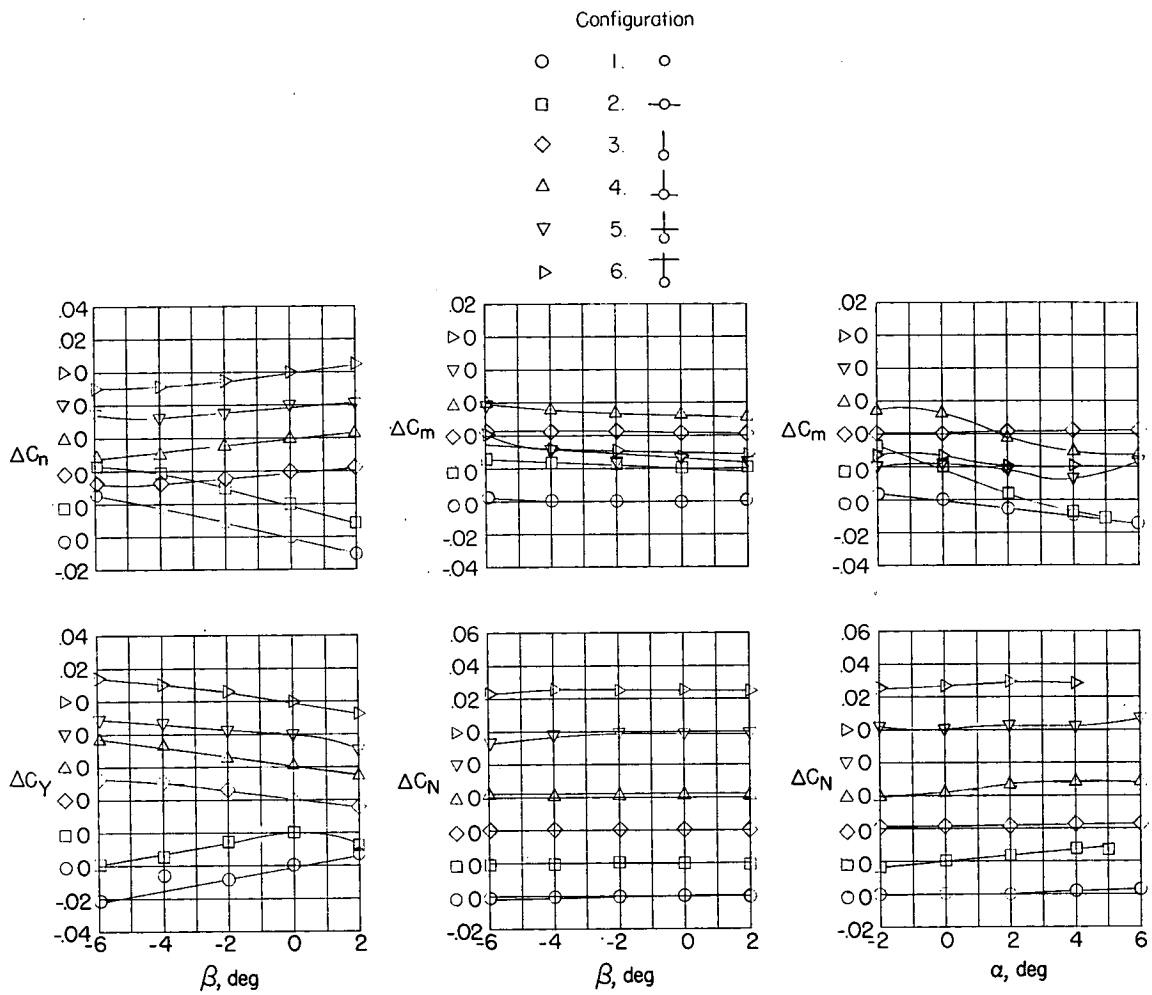

(e) $p_j/p_\infty = 15.0$.

Figure 7.- Concluded.

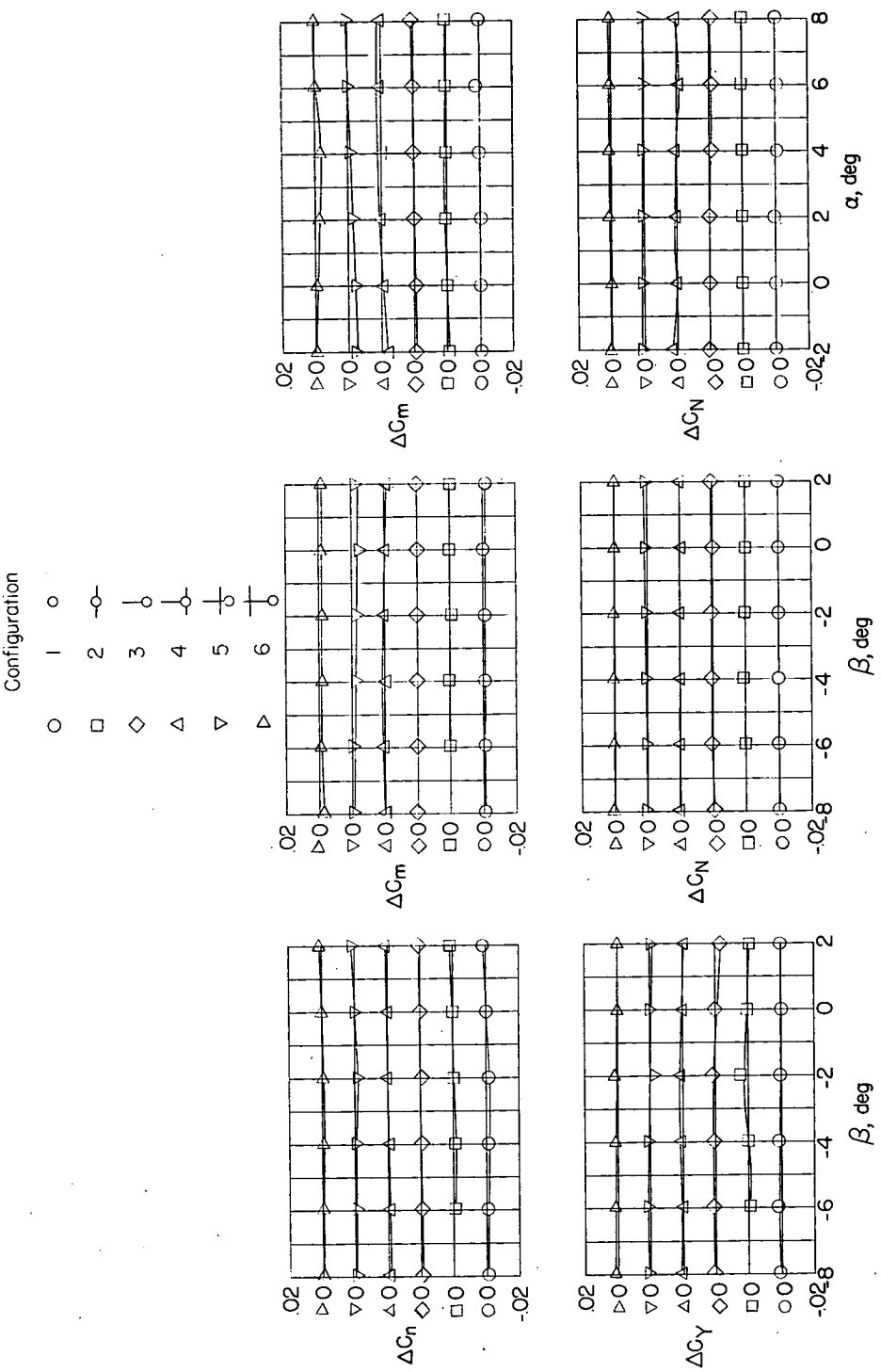

(a) $p_j/p_\infty = 0.5$.

Figure 8.- Incremental jet-interference effects (jet-on minus jet-off) upon the aerodynamic characteristics of the jet model. $M_\infty = 2.41$.

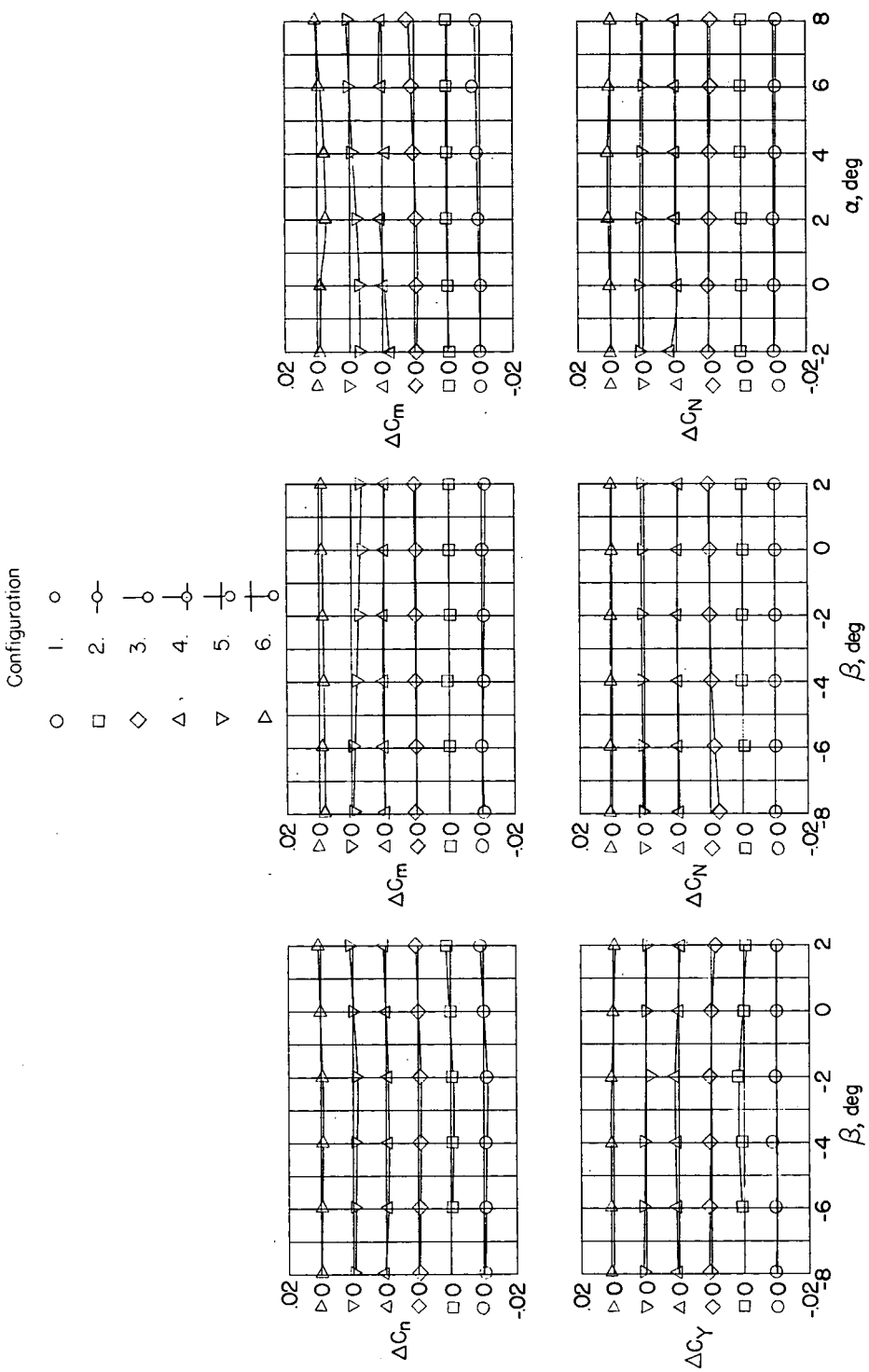

(b) $p_j/p_\infty = 1.0$.

Figure 8.- Continued.

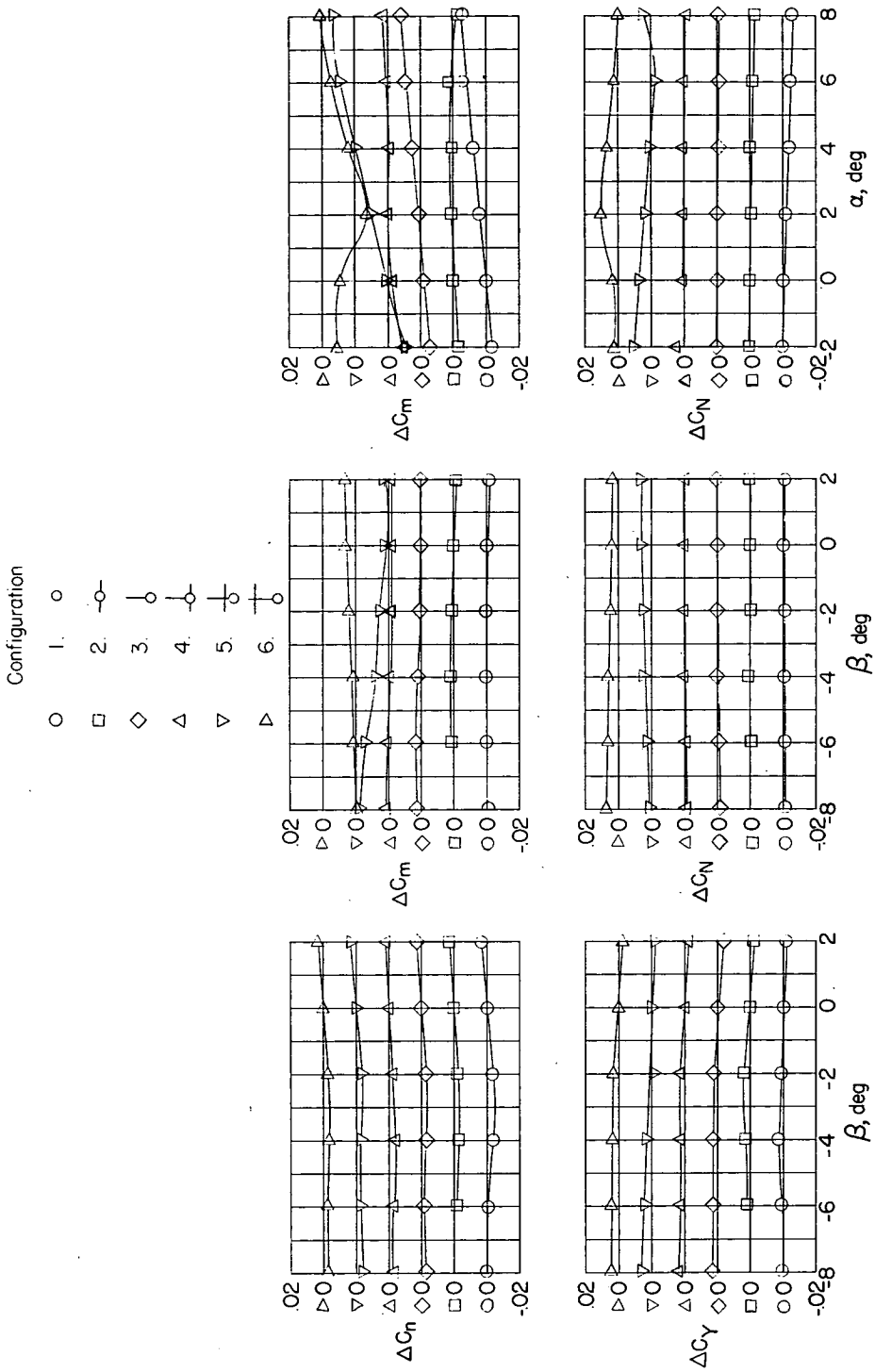

(c) $p_j/p_\infty = 5.0$.

Figure 8.- Continued.

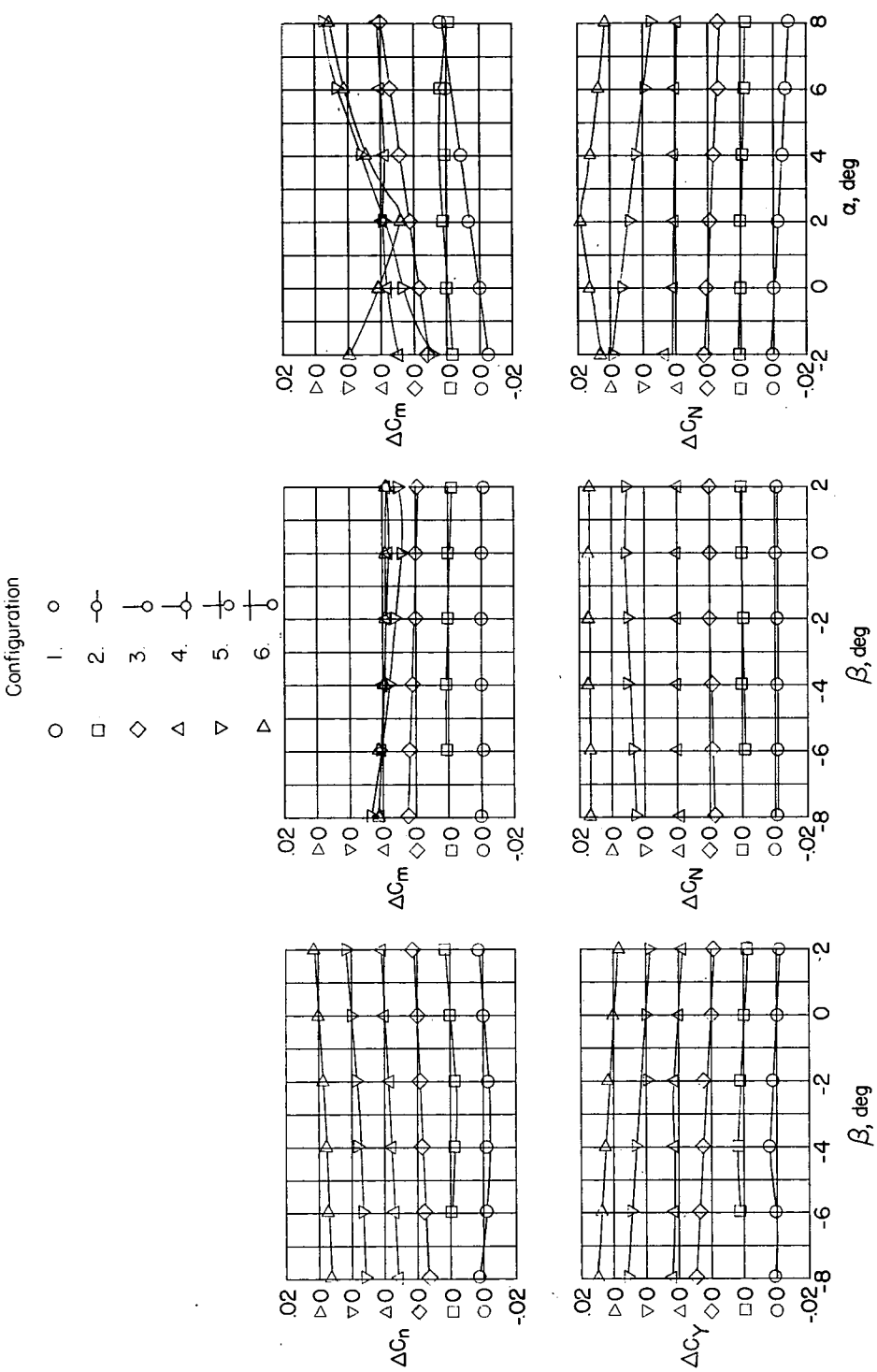

(d) p_j/p_∞ = 10.0.

Figure 8.- Continued.

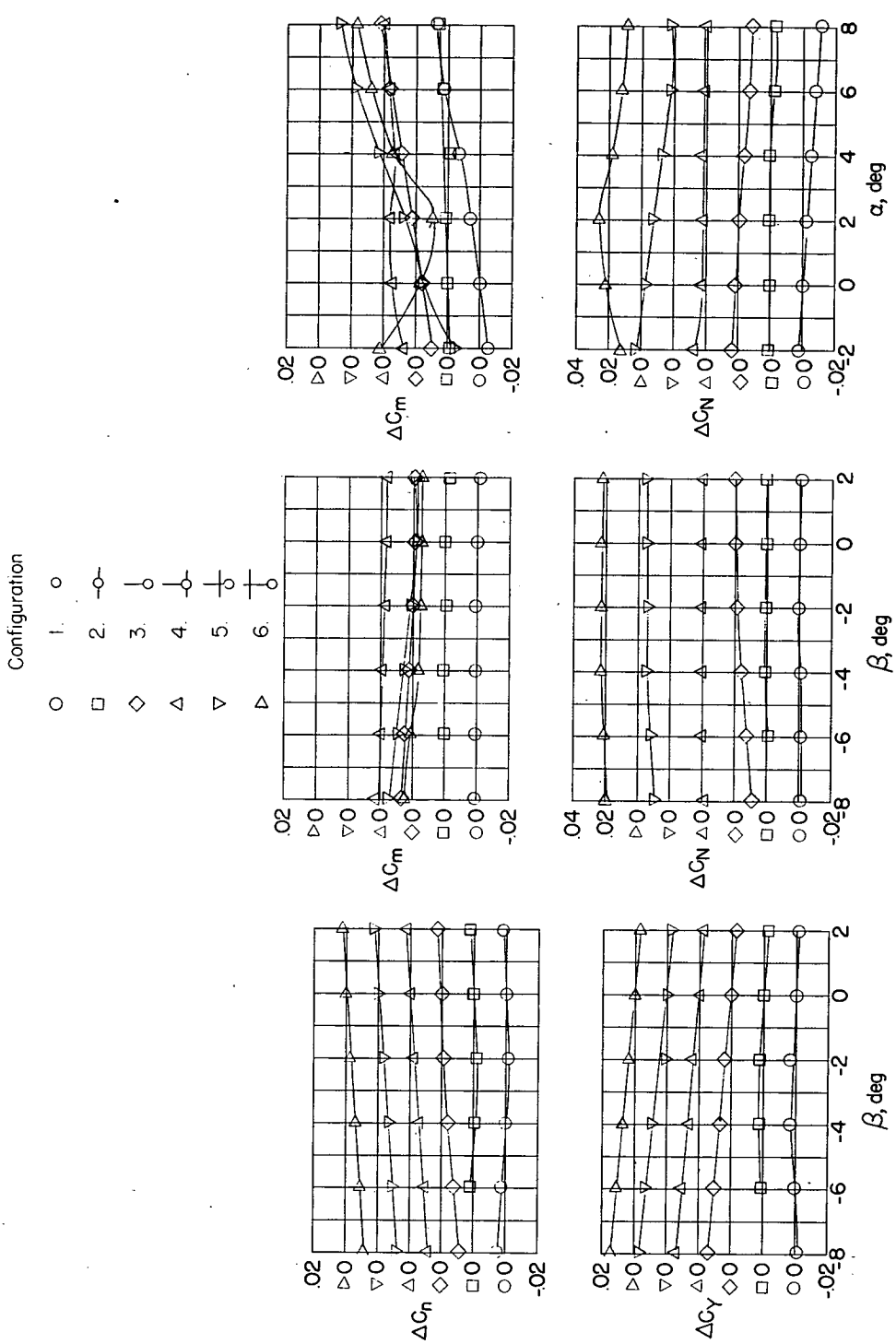

(e) $p_j/p_\infty = 15.0$.

Figure 8.- Continued.

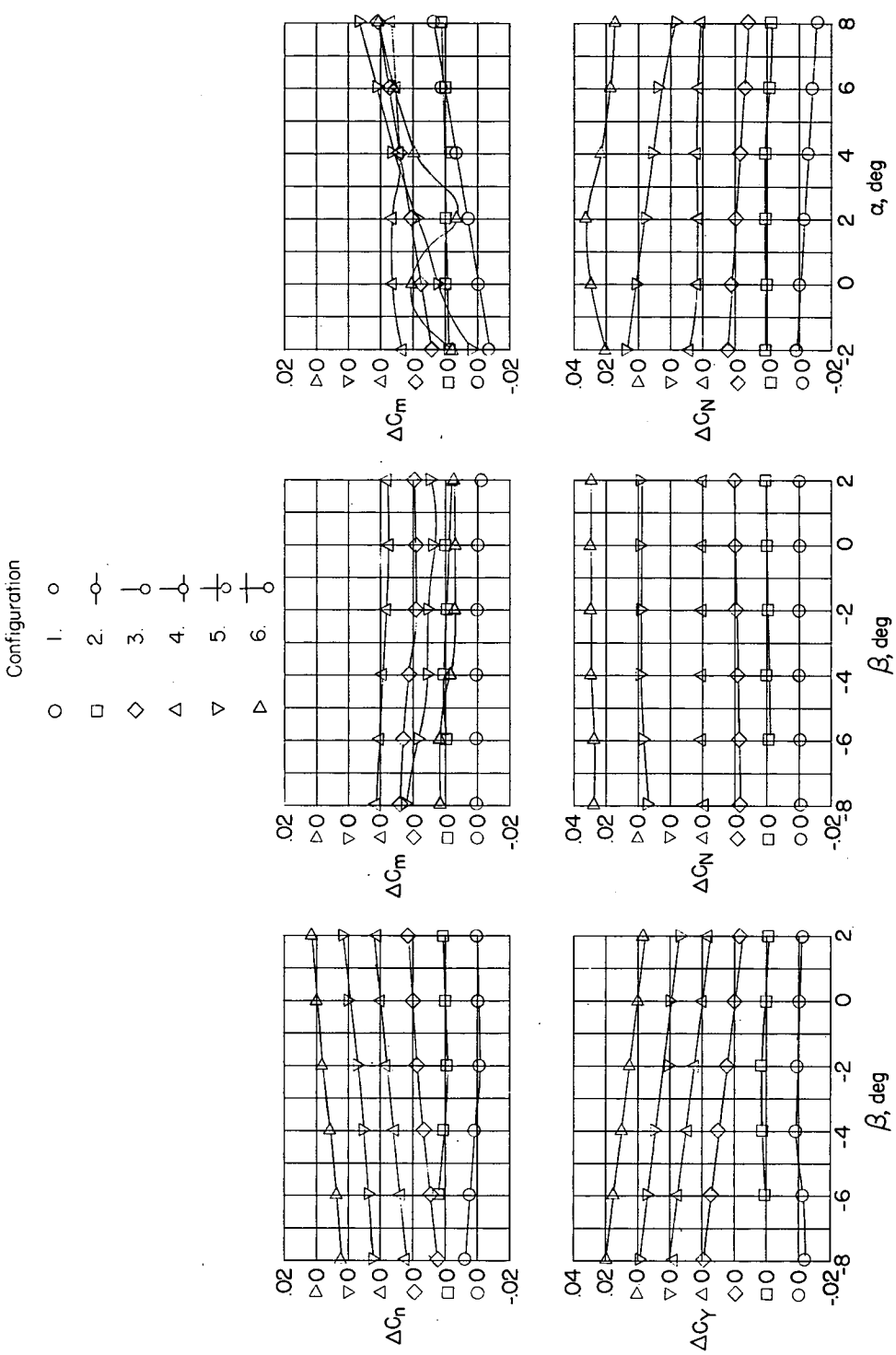

(f) $p_j/p_\infty = 20.0$.

Figure 8.- Continued.

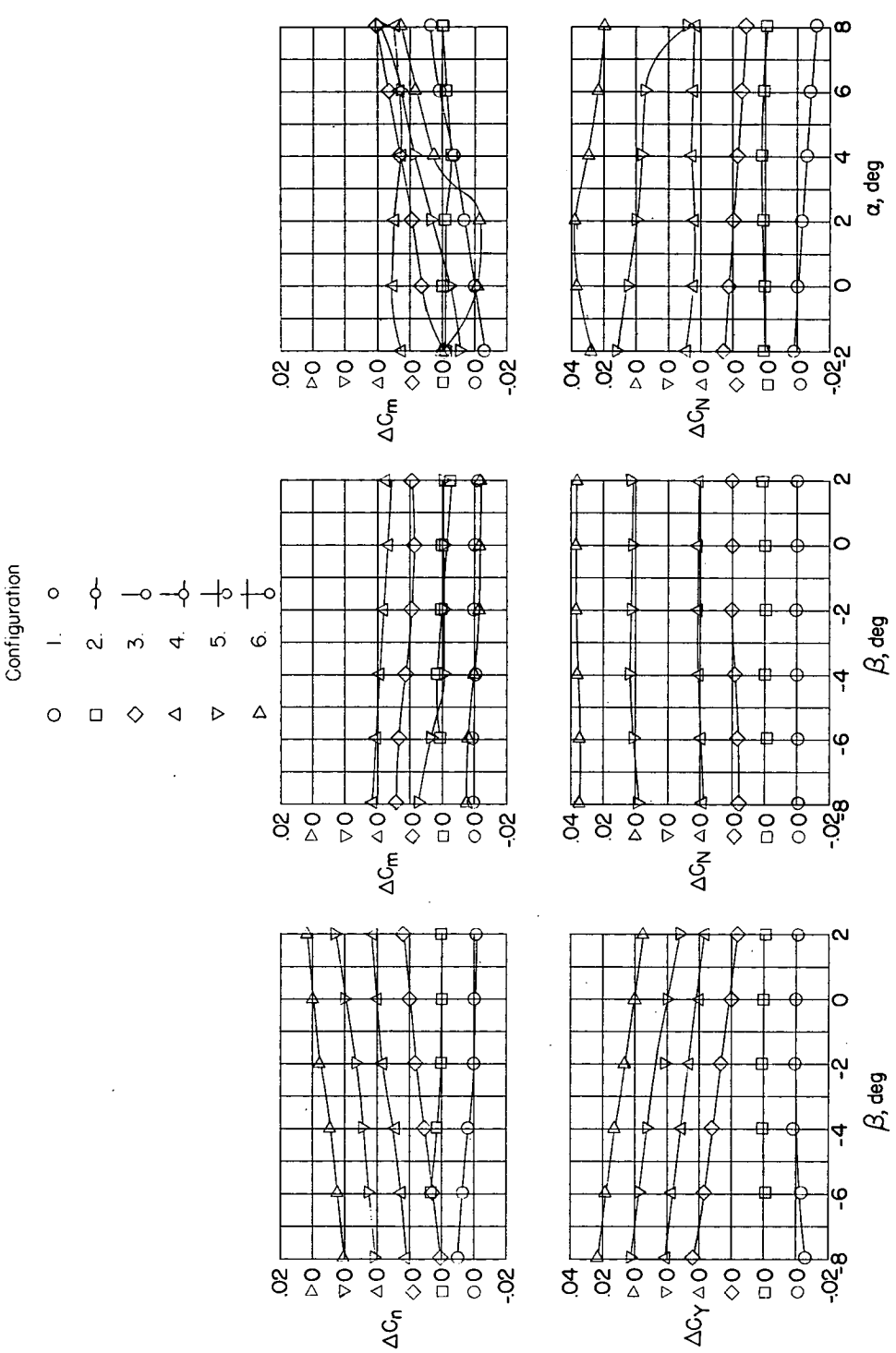

(g) $p_j/p_\infty = 25.0$.

Figure 8.- Concluded.

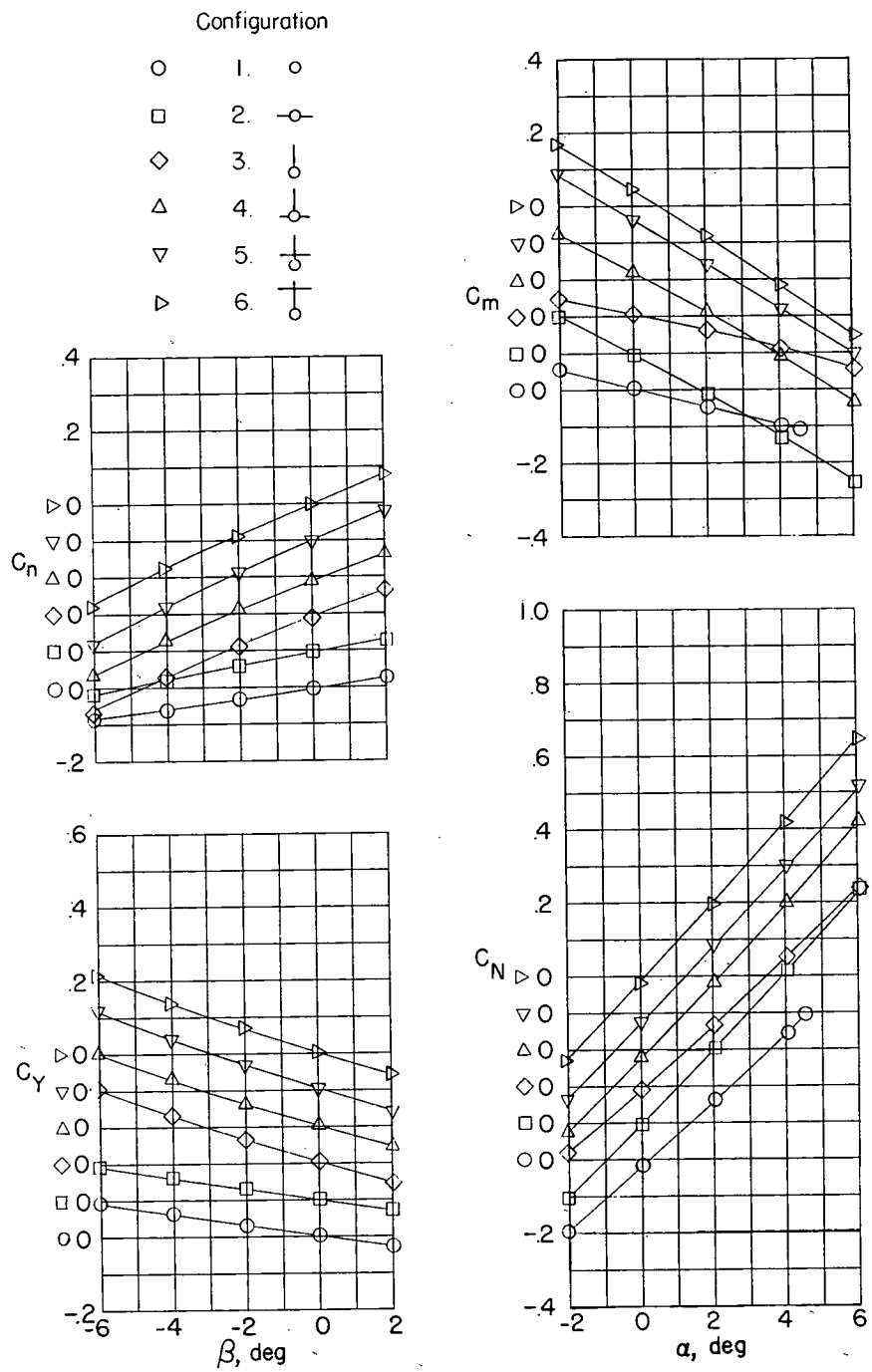

(a) $M_\infty = 1.94$.

Figure 9.- Aerodynamic charactersitics of the no-jet model.

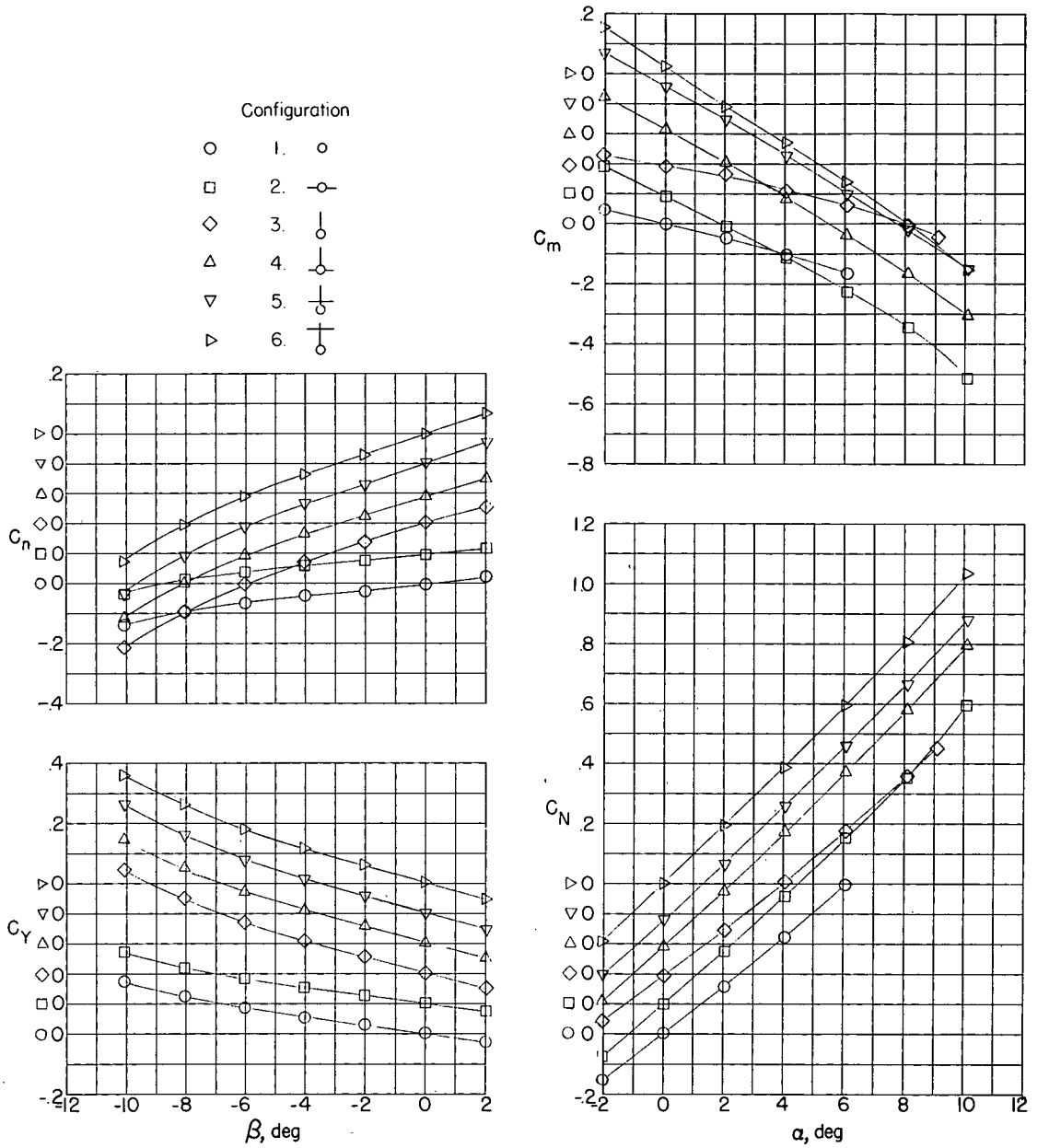

(b) $M_\infty = 2.22$.

Figure 9.- Continued.

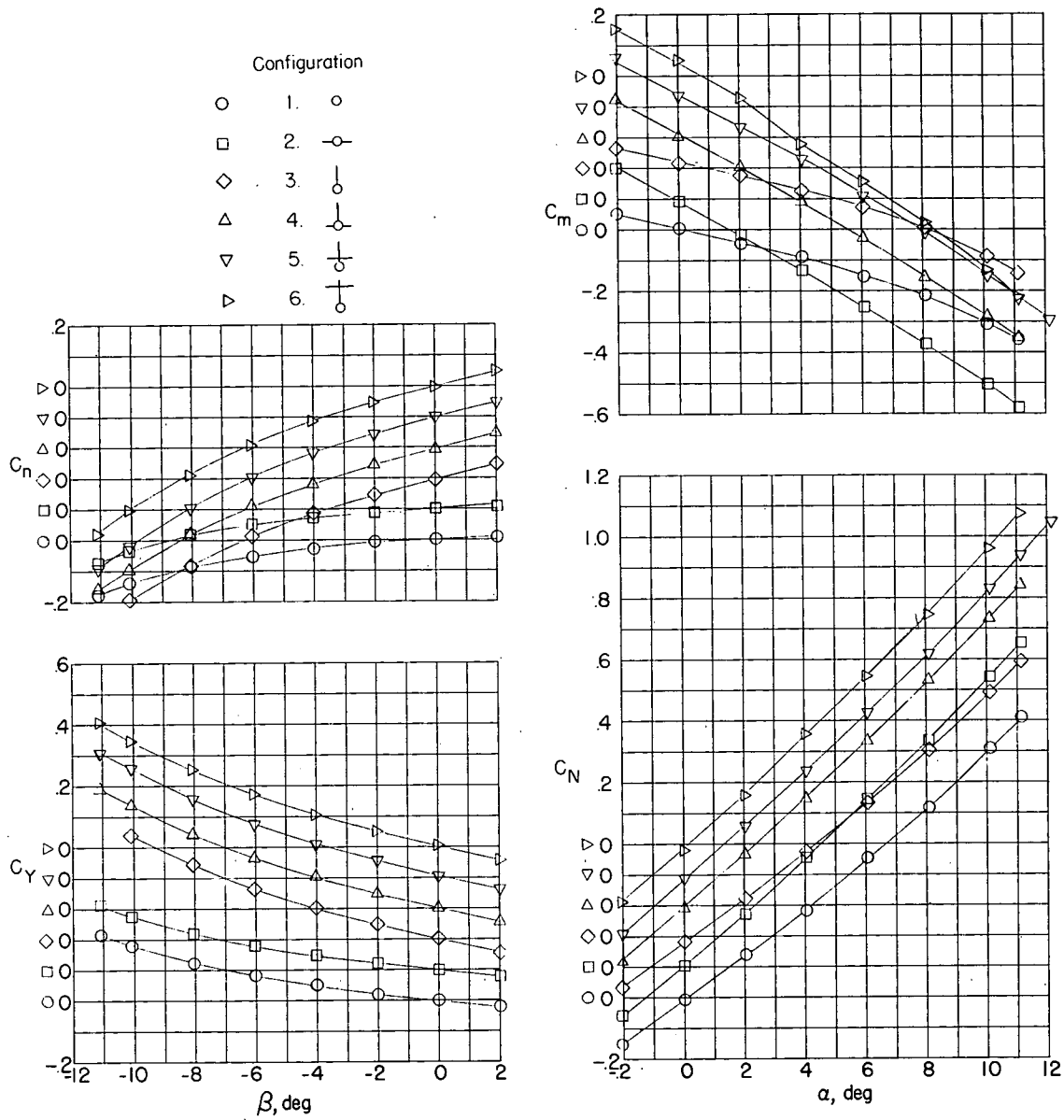

(c) $M_\infty = 2.41$.

Figure 9.- Continued.

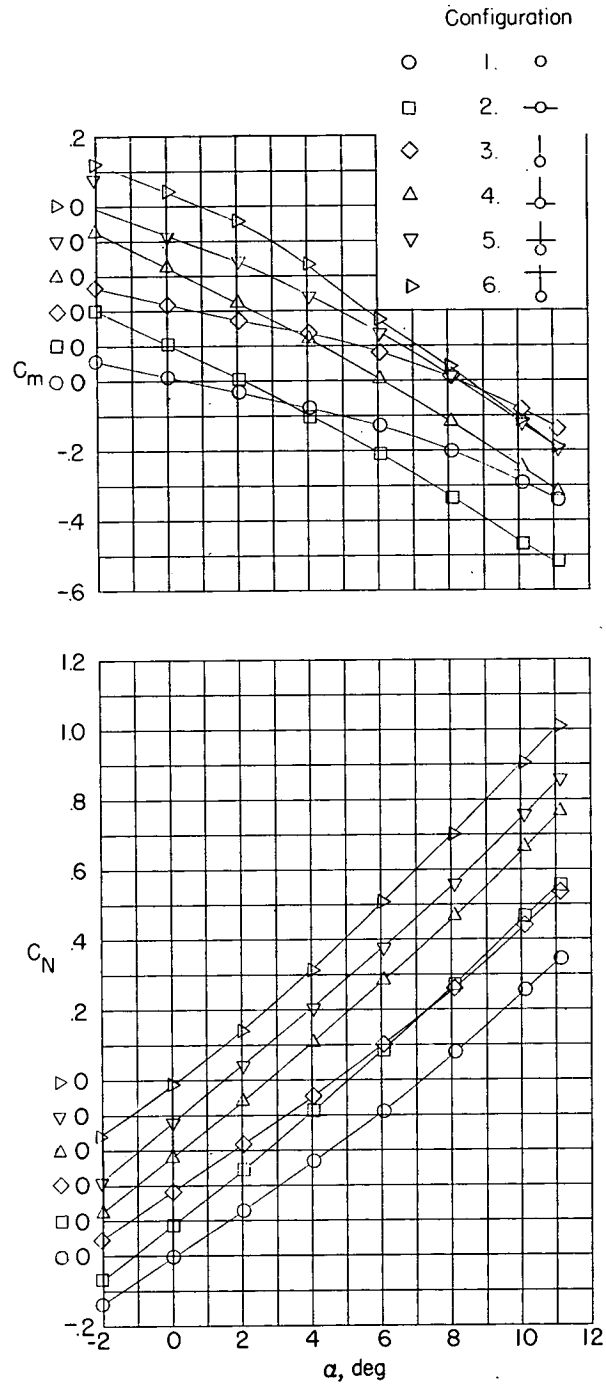

(d) $M_\infty = 2.62$.

Figure 9.- Concluded.

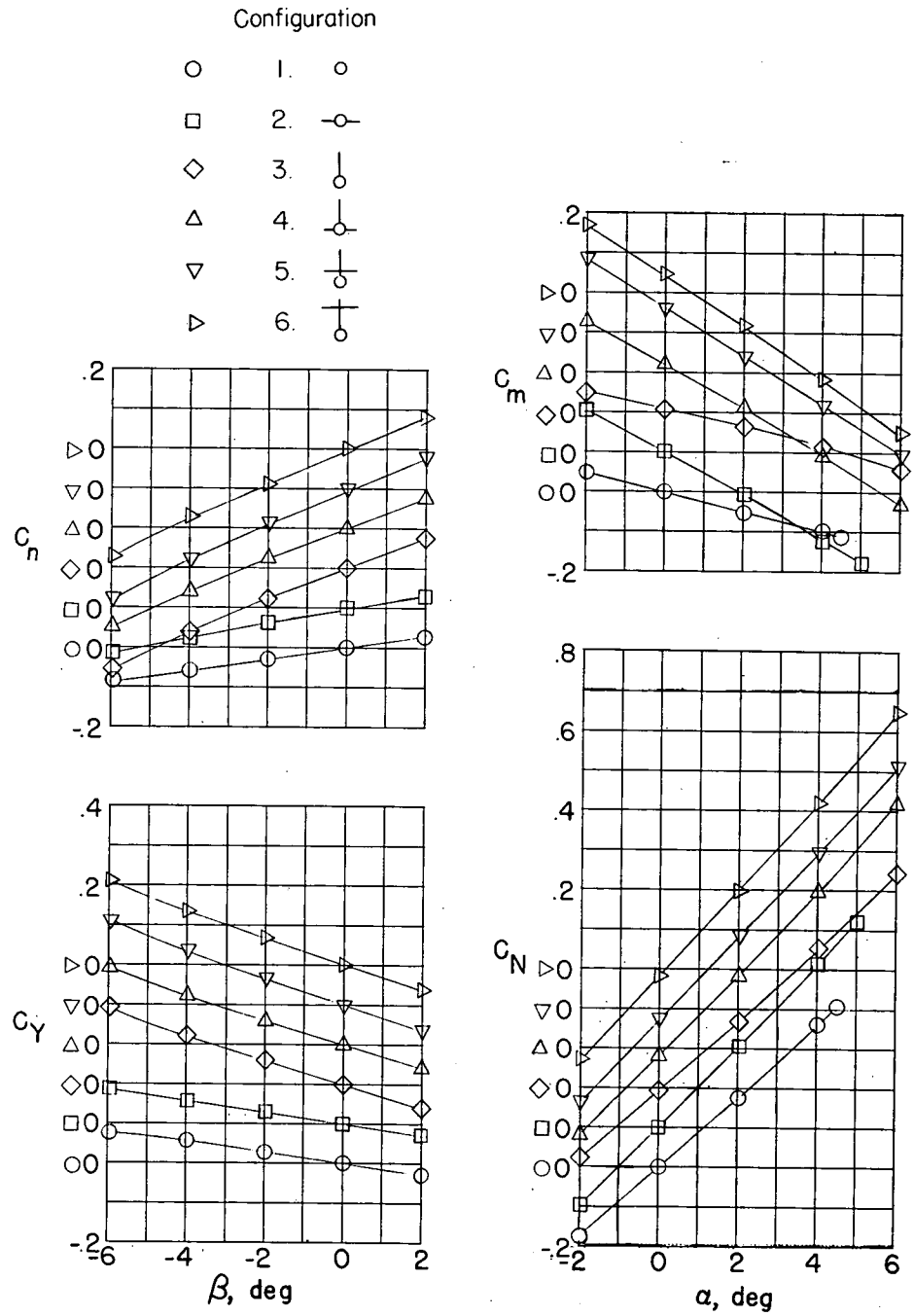

(a) $p_j/p_{\infty}' = 0$.

Figure 10.- Combined aerodynamic characteristics for no-jet model plus interference effects of jet model. $M_{\infty} = 1.94$.

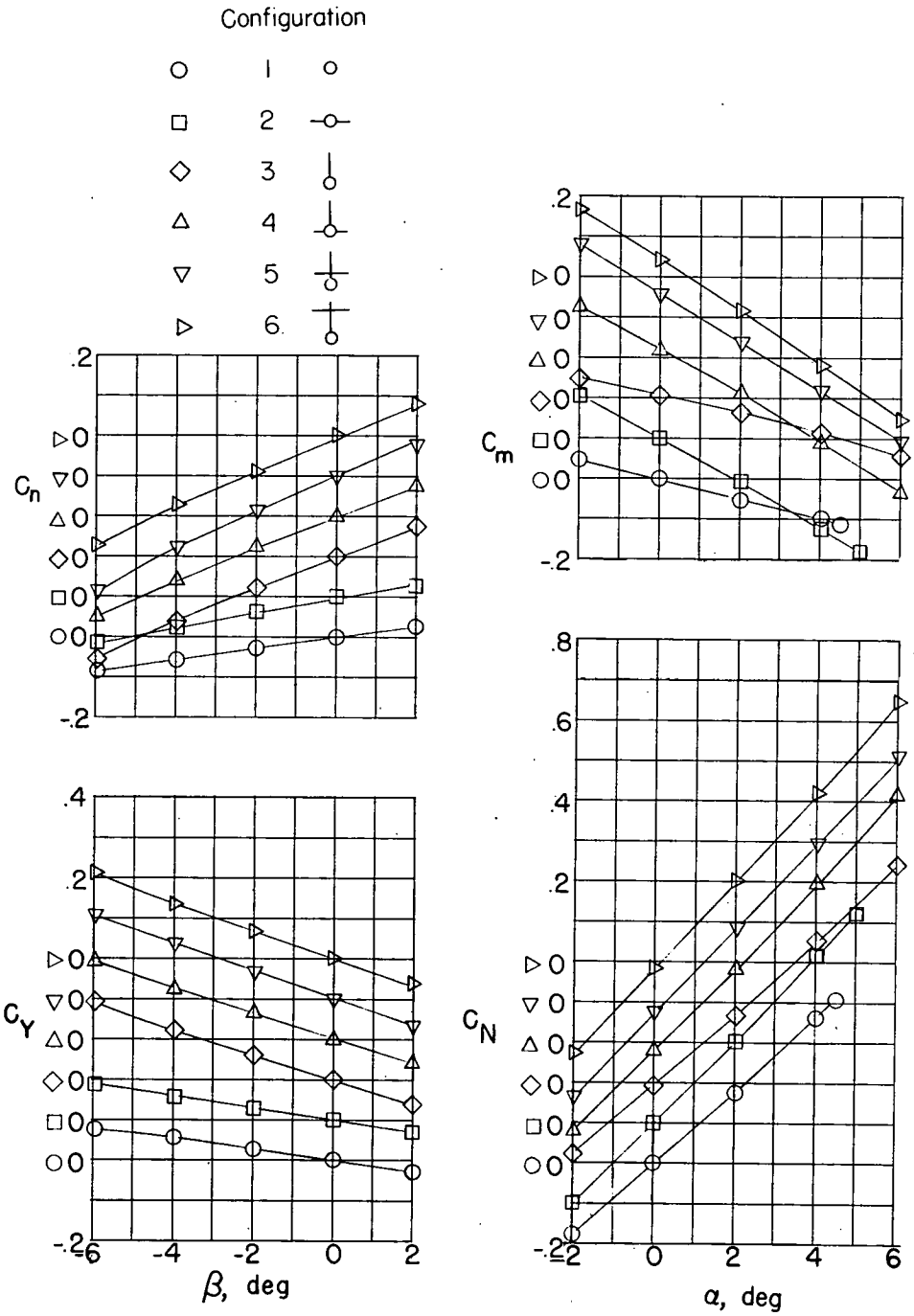

(b) $p_j/p_\infty = 0.5$.

Figure 10.- Continued.

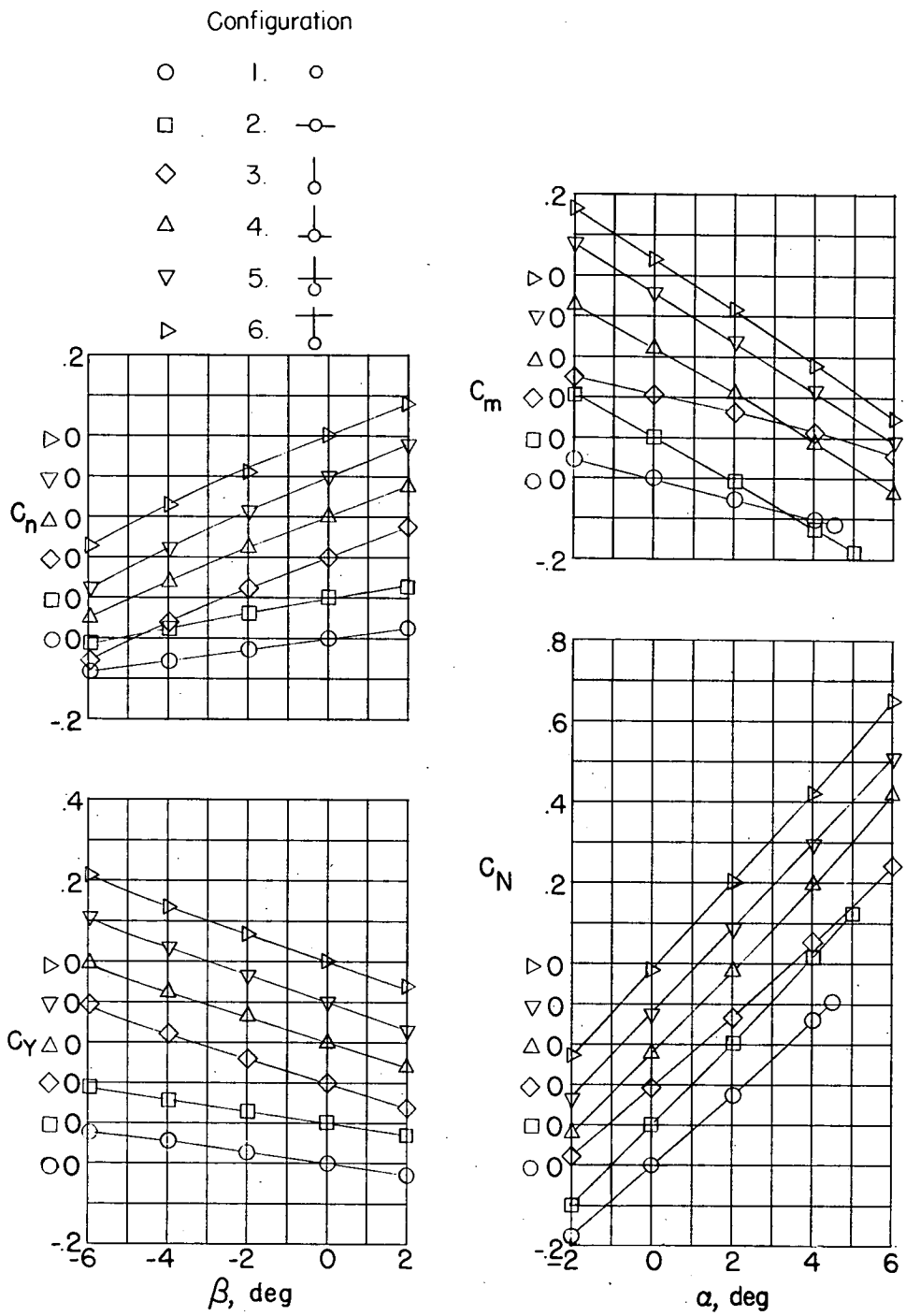

(c) $p_j/p_\infty = 1.0$.

Figure 10.- Continued.

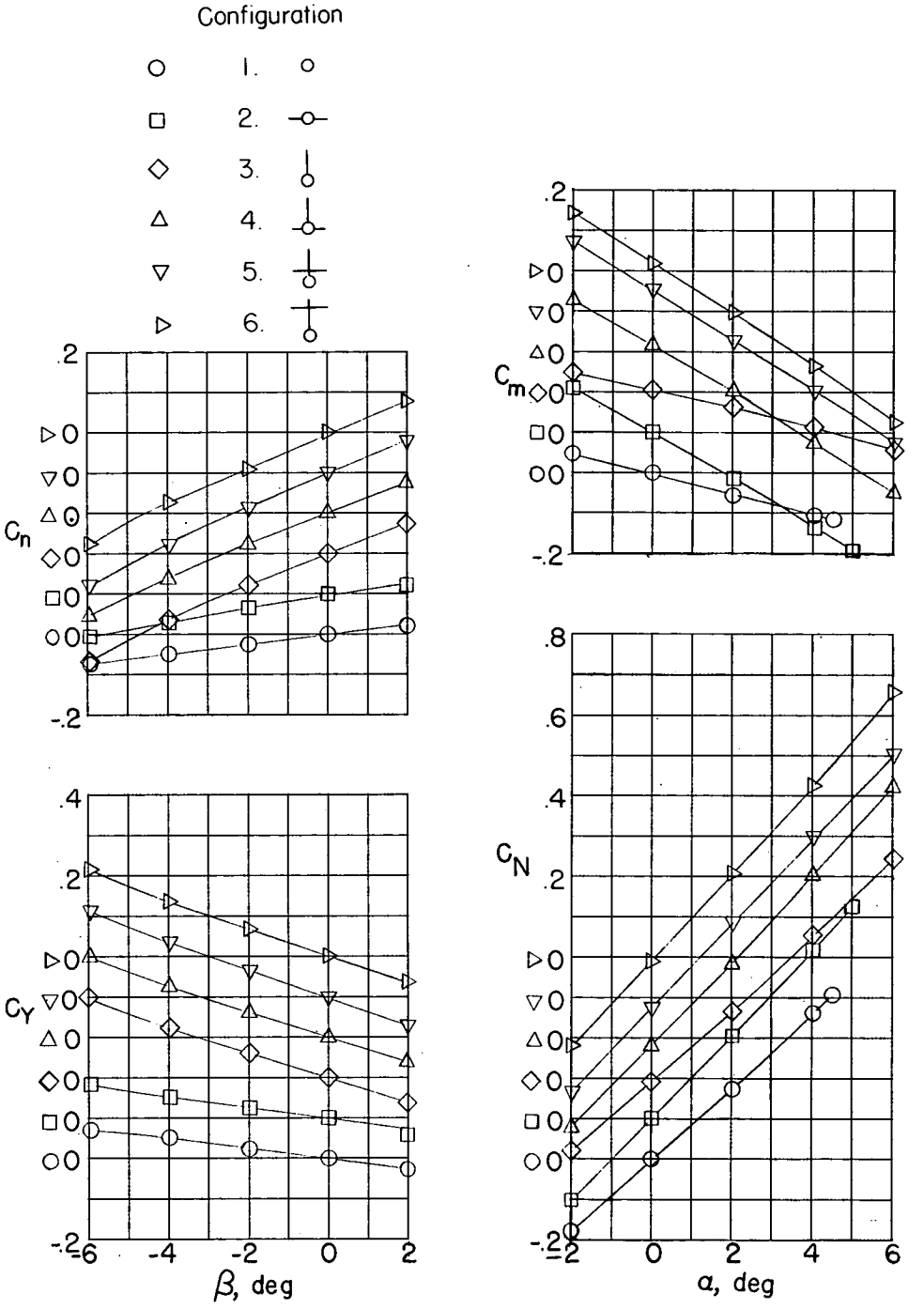

(d) $p_j/p_\infty = 5.0$.

Figure 10.- Continued.

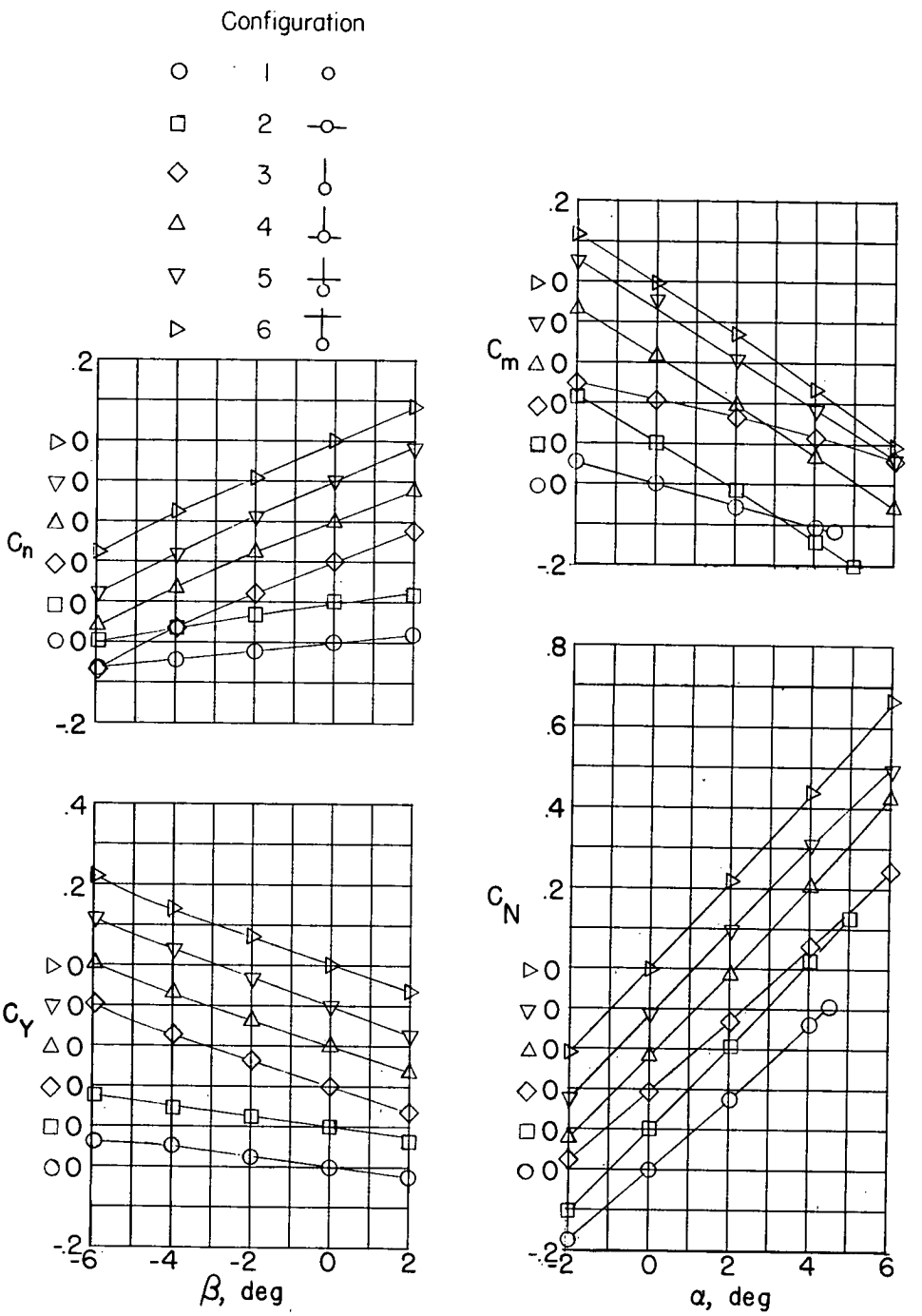

(e) $p_j/p_\infty = 10.0$.

Figure 10.- Continued.

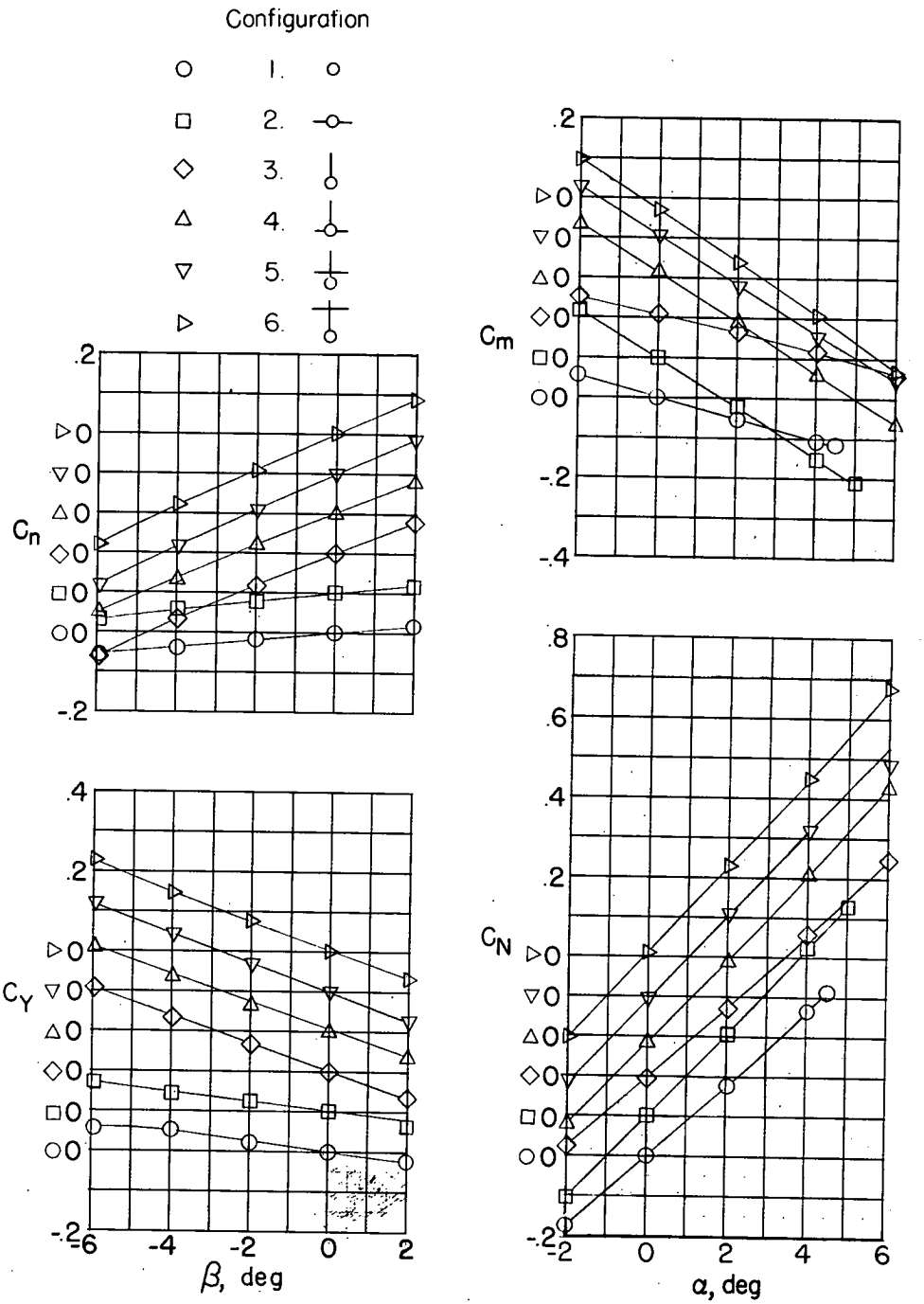

(f) $p_j/p_\infty = 15.0$.

Figure 10.- Concluded.

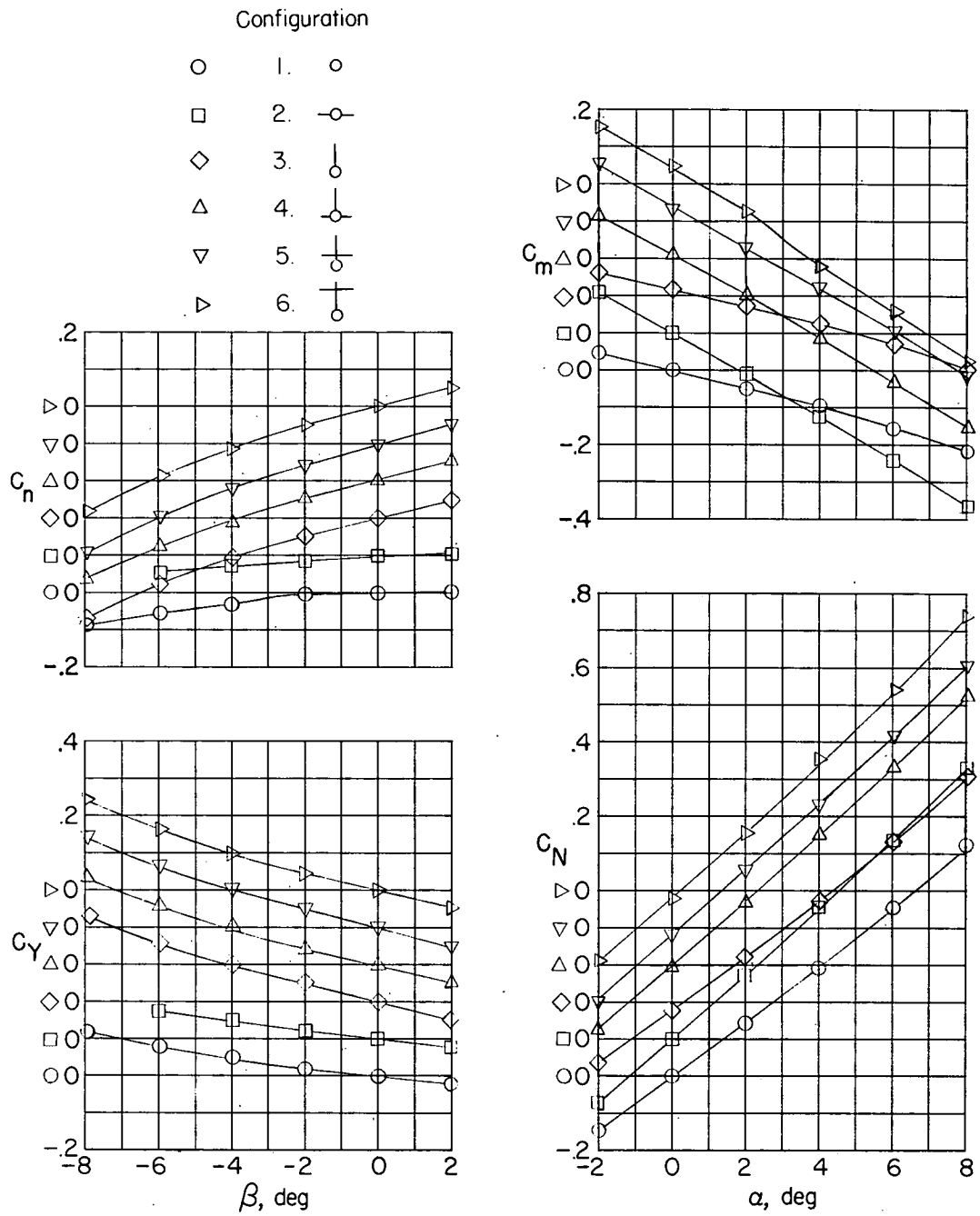

(a) $p_j/p_\infty = 0.$

Figure 11.- Combined aerodynamic characteristics for no-jet model plus interference effects of jet model. $M_\infty = 2.41.$

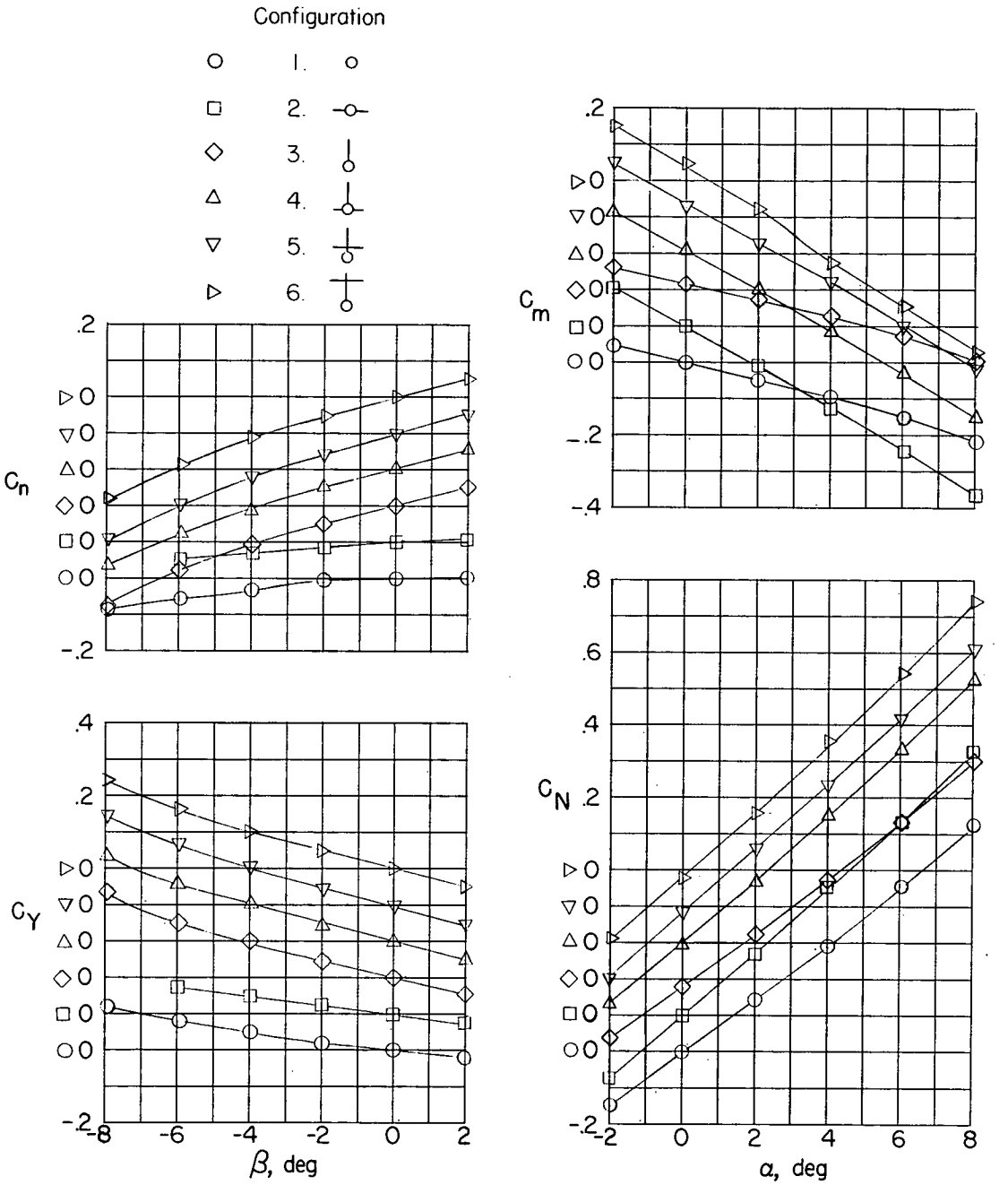

(b) $p_j/p_\infty = 0.5$.

Figure 11.- Continued.

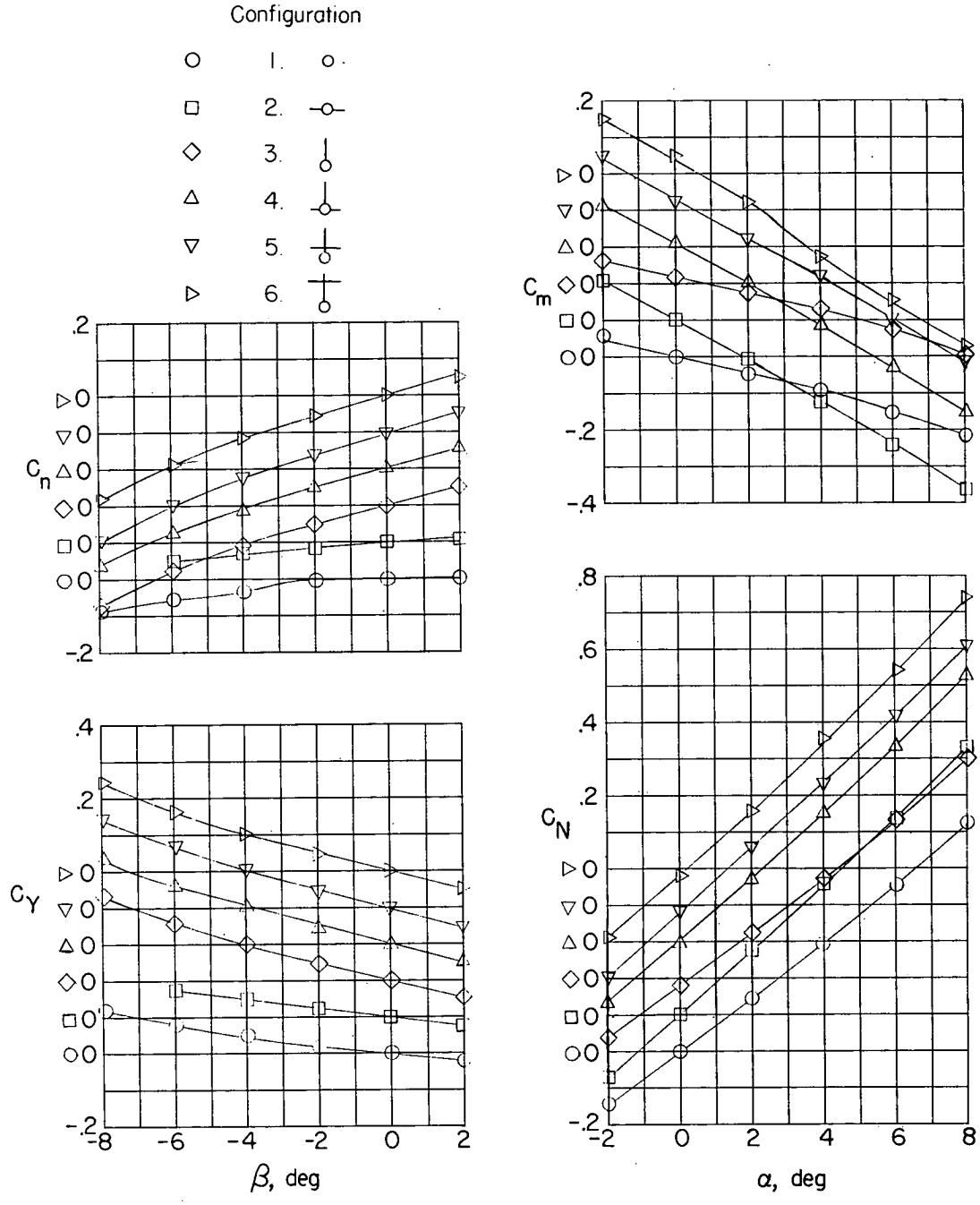

(c) $p_j/p_\infty = 1.0$.

Figure 11.- Continued.

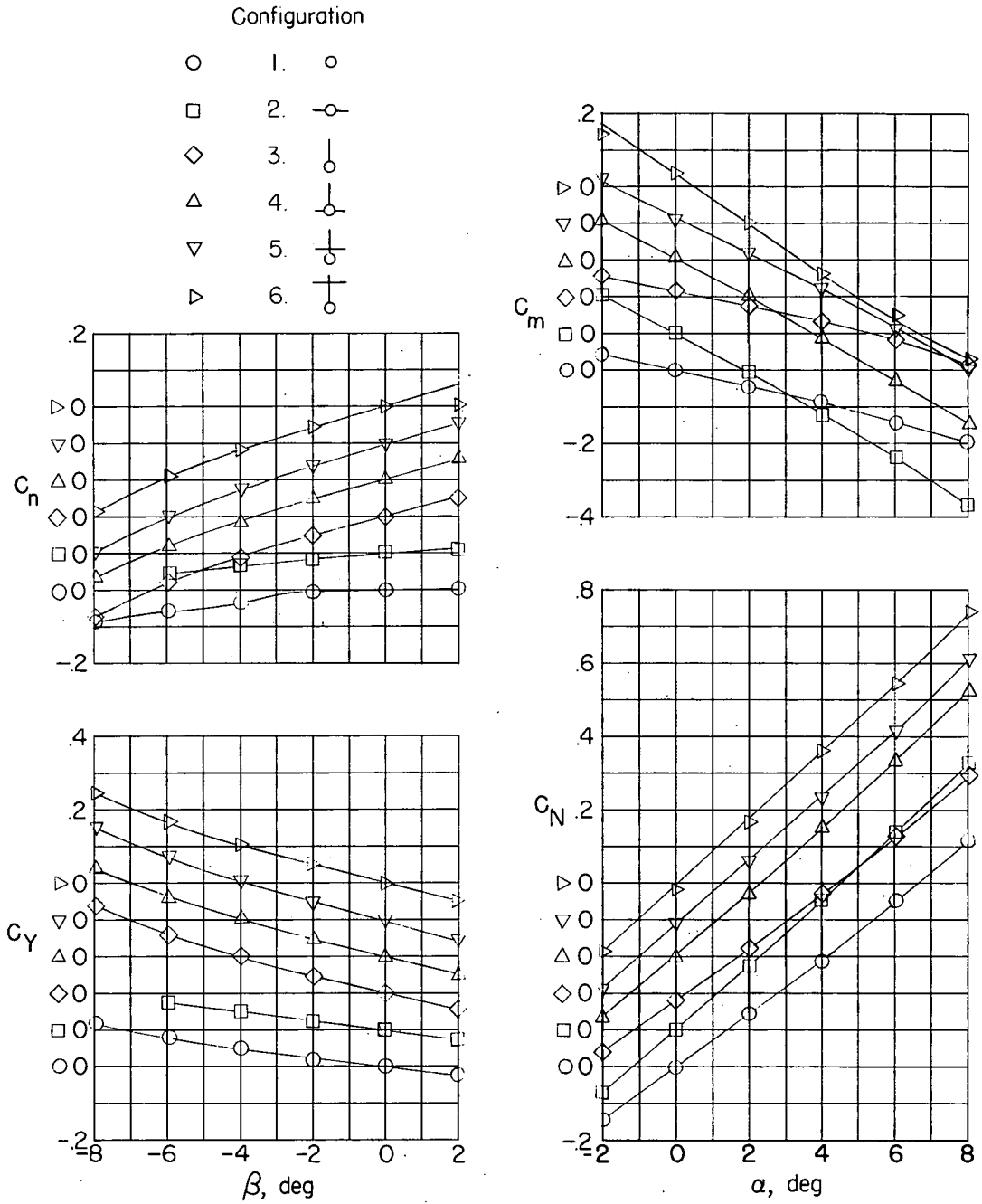

(d) $p_j/p_\infty = 5.0$.

Figure 11.- Continued.

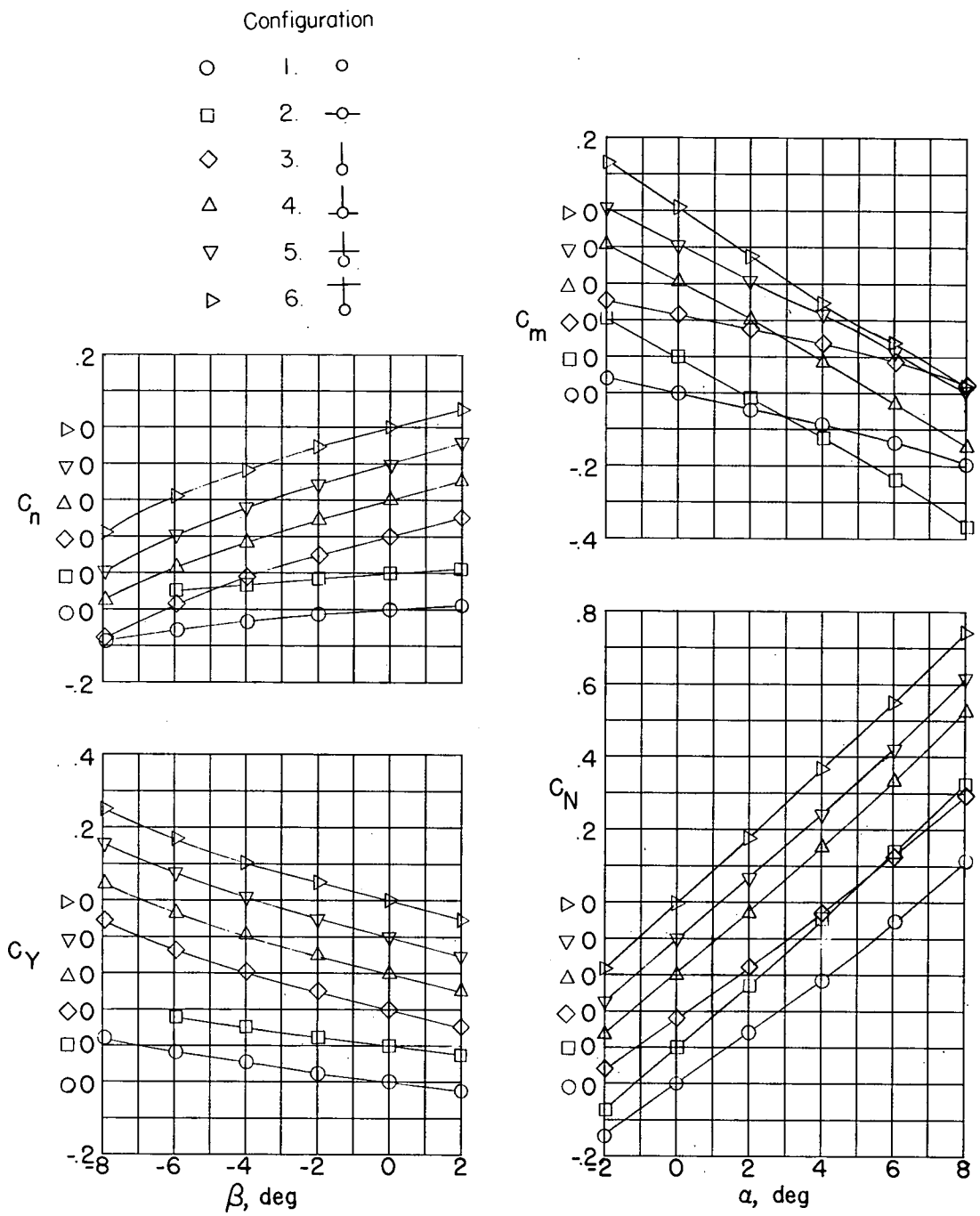

(e) $p_j/p_\infty = 10.0$.

Figure 11.- Continued.

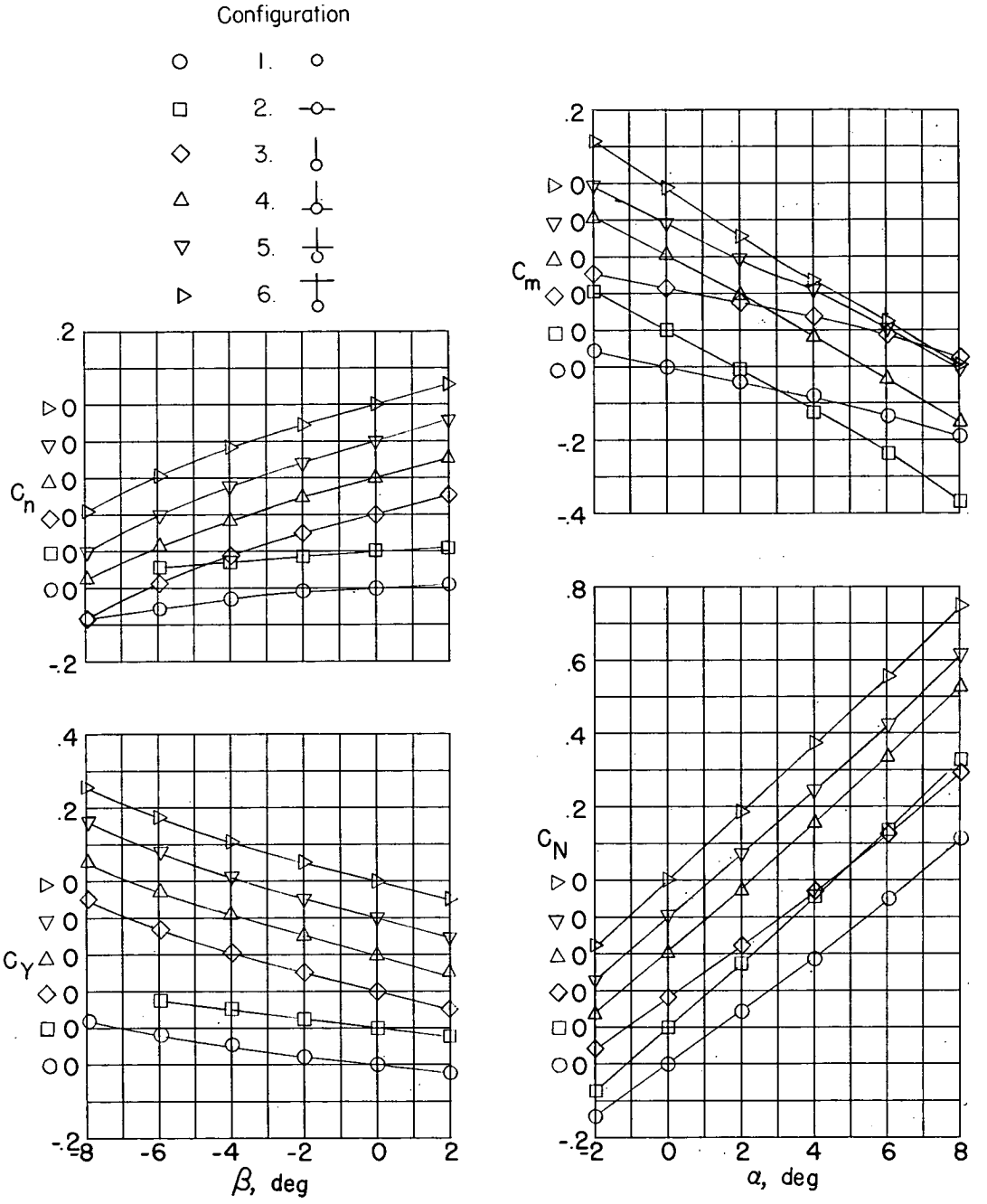

(f) $p_j/p_\infty = 15.0$.

Figure 11.- Continued.

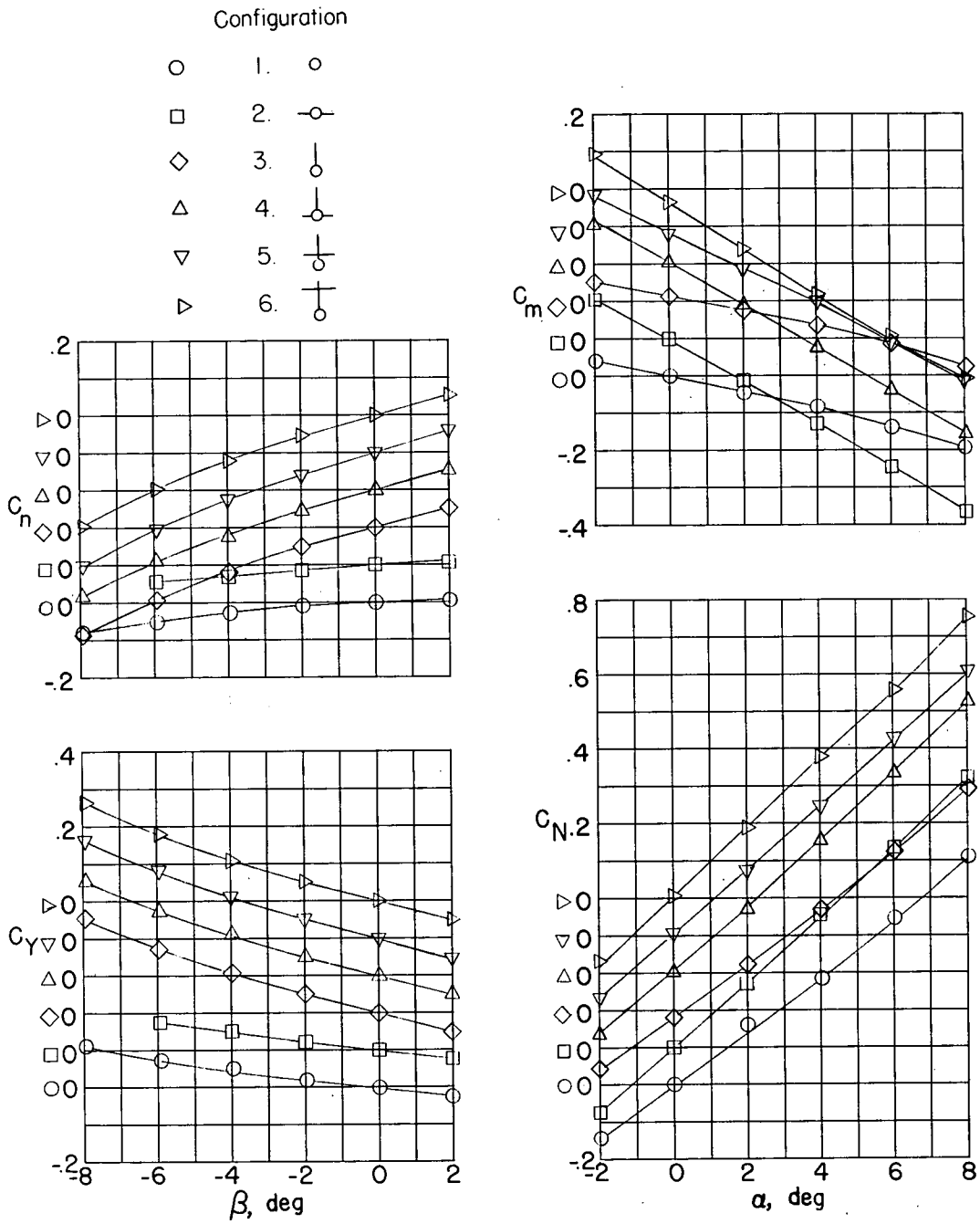

(g) $p_j/p_\infty = 20.0$.

Figure 11.- Continued.

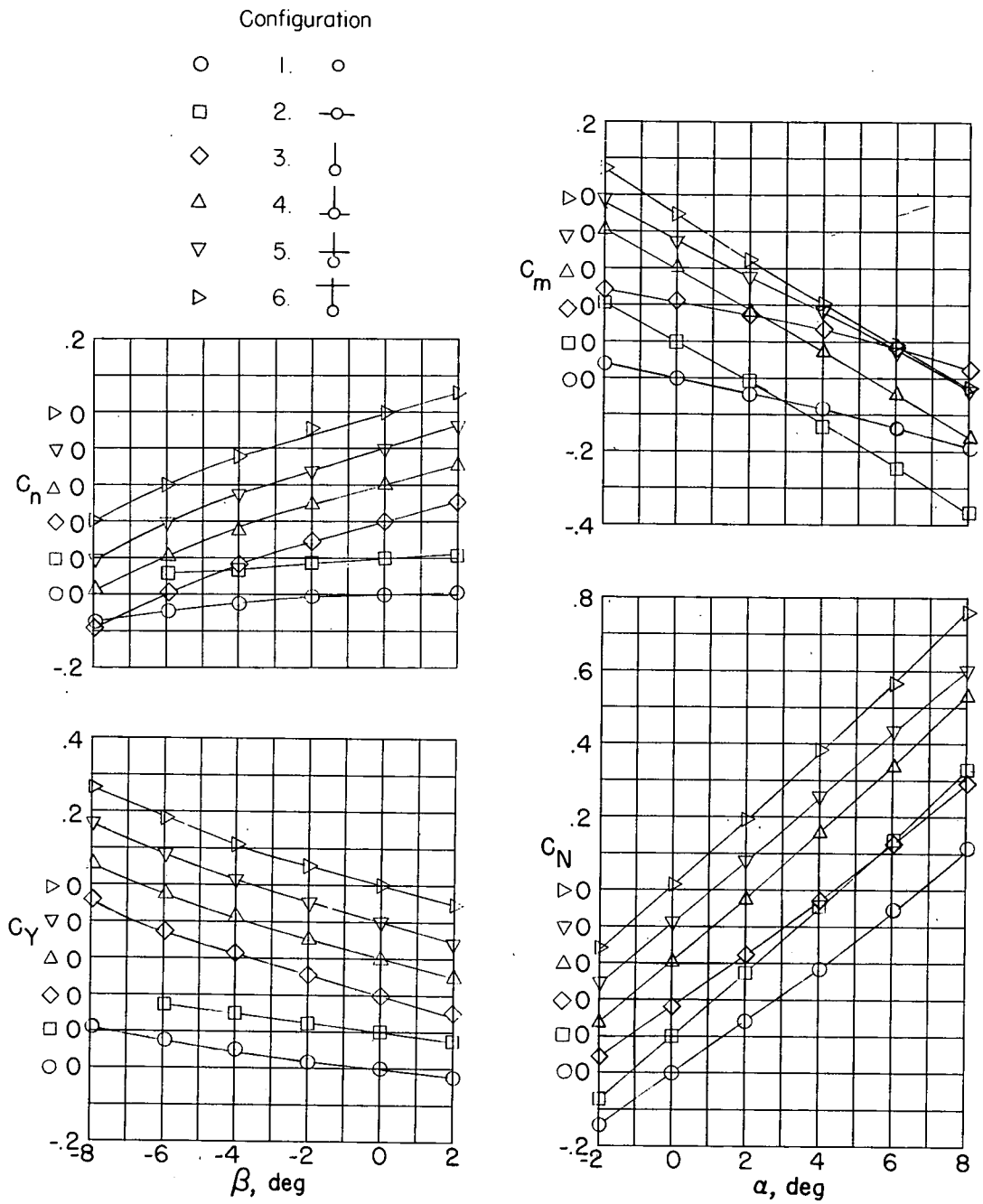

(h) $p_j/p_\infty = 25.0$.

Figure 11.- Concluded.

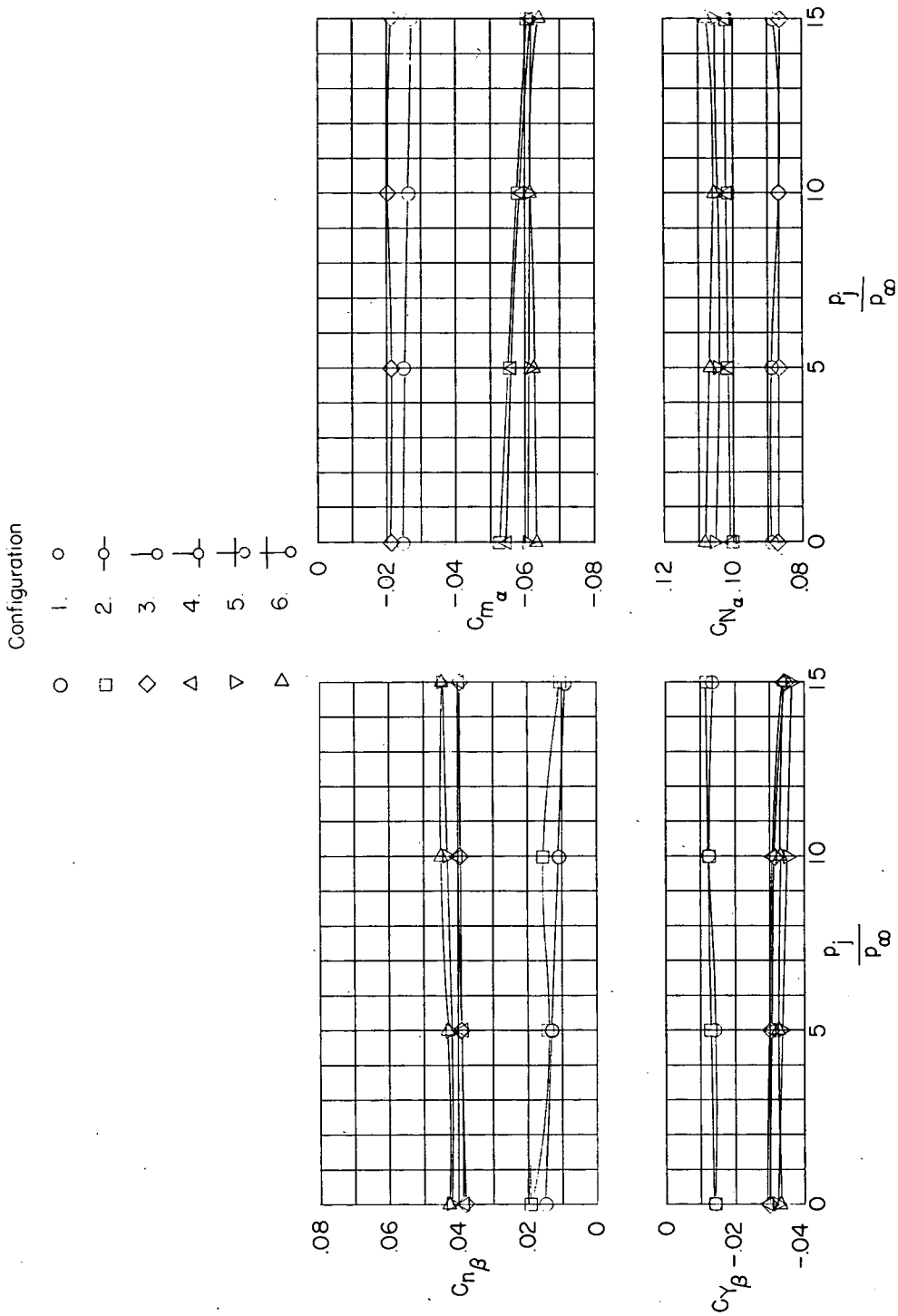

(a) $M_\infty = 1.94$.

Figure 12.- Variation of static-stability derivatives with jet static-pressure ratio.

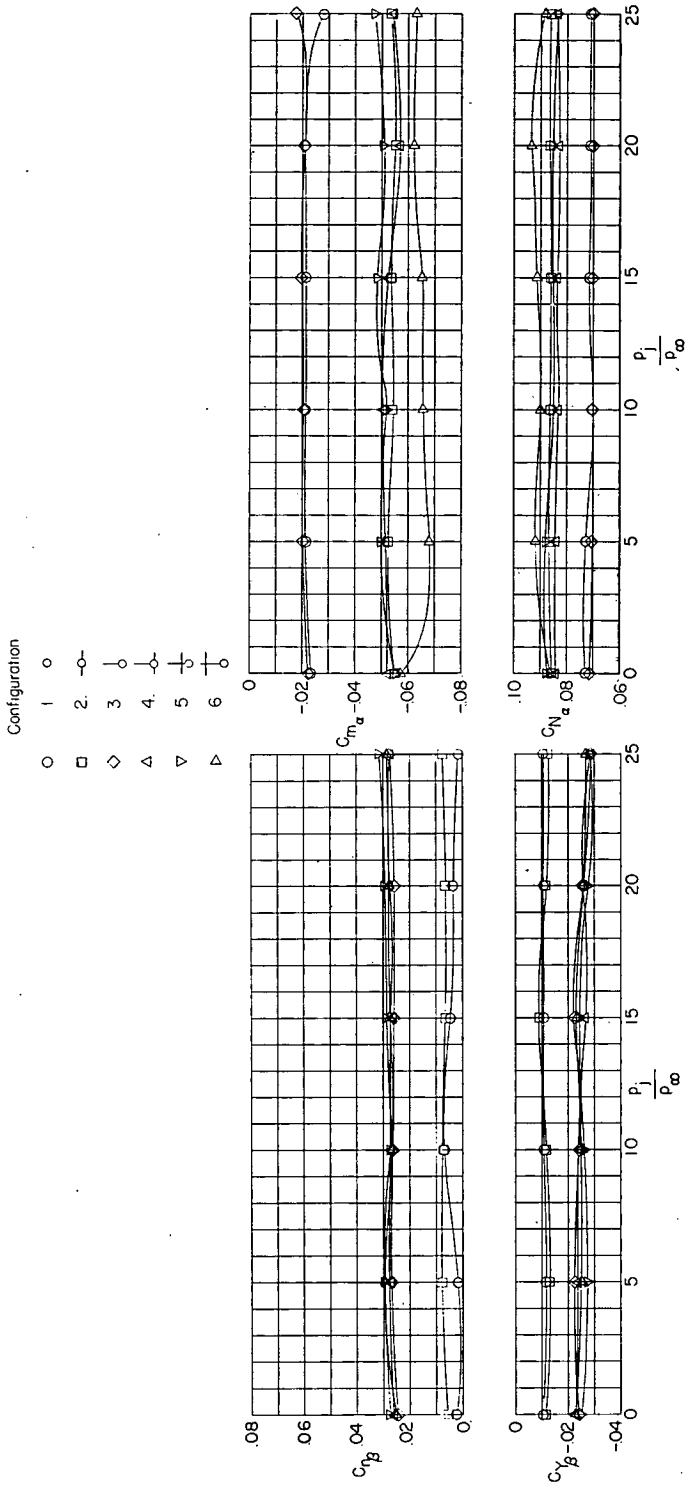

(b) $M_\infty = 2.41$.

Figure 12.- Concluded.

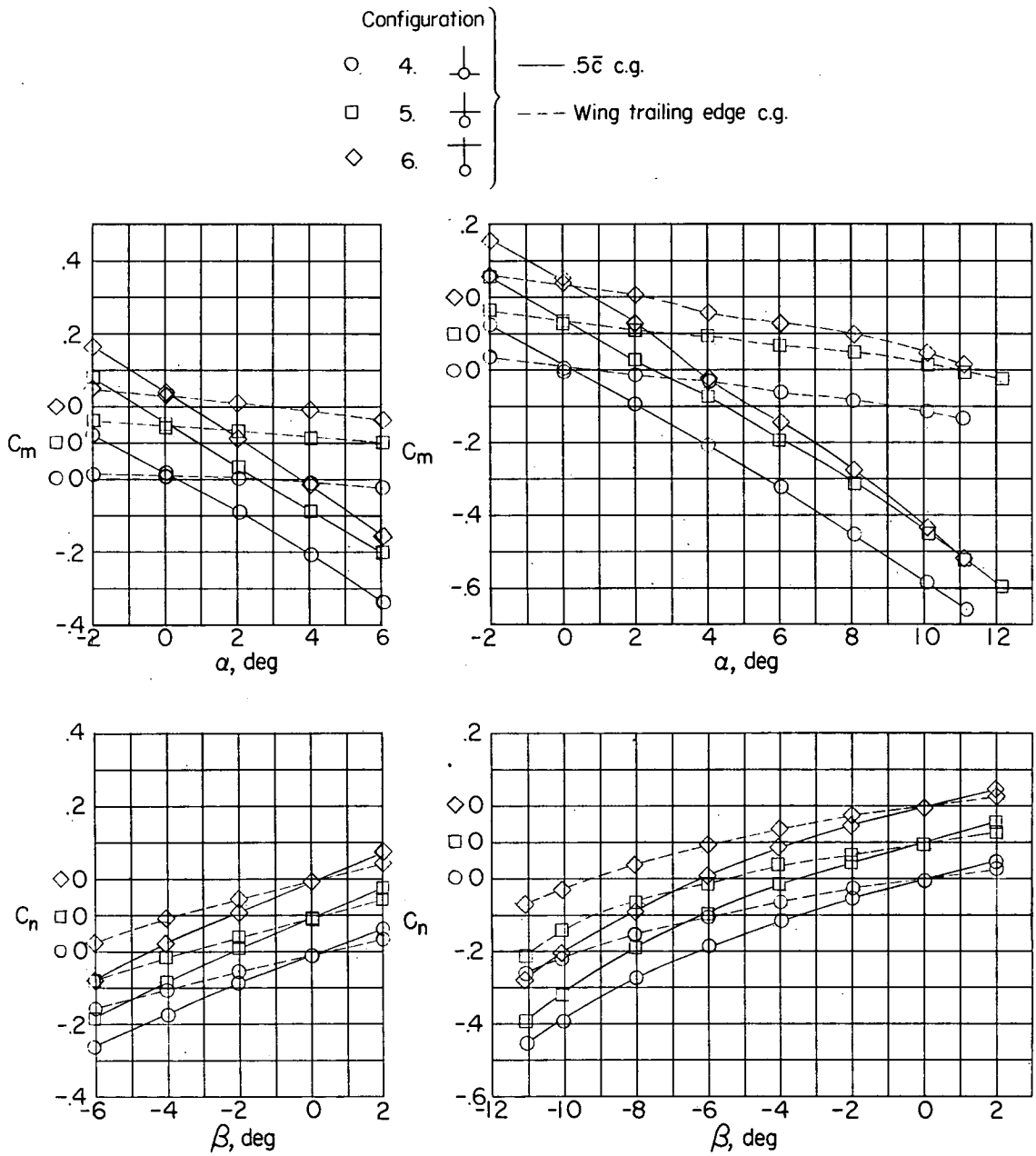

(a) $M_\infty = 1.94$. (b) $M_\infty = 2.41$.

Figure 13.- Effect of transferring center of gravity upon pitching-moment and yawing-moment curves of the no-jet model.

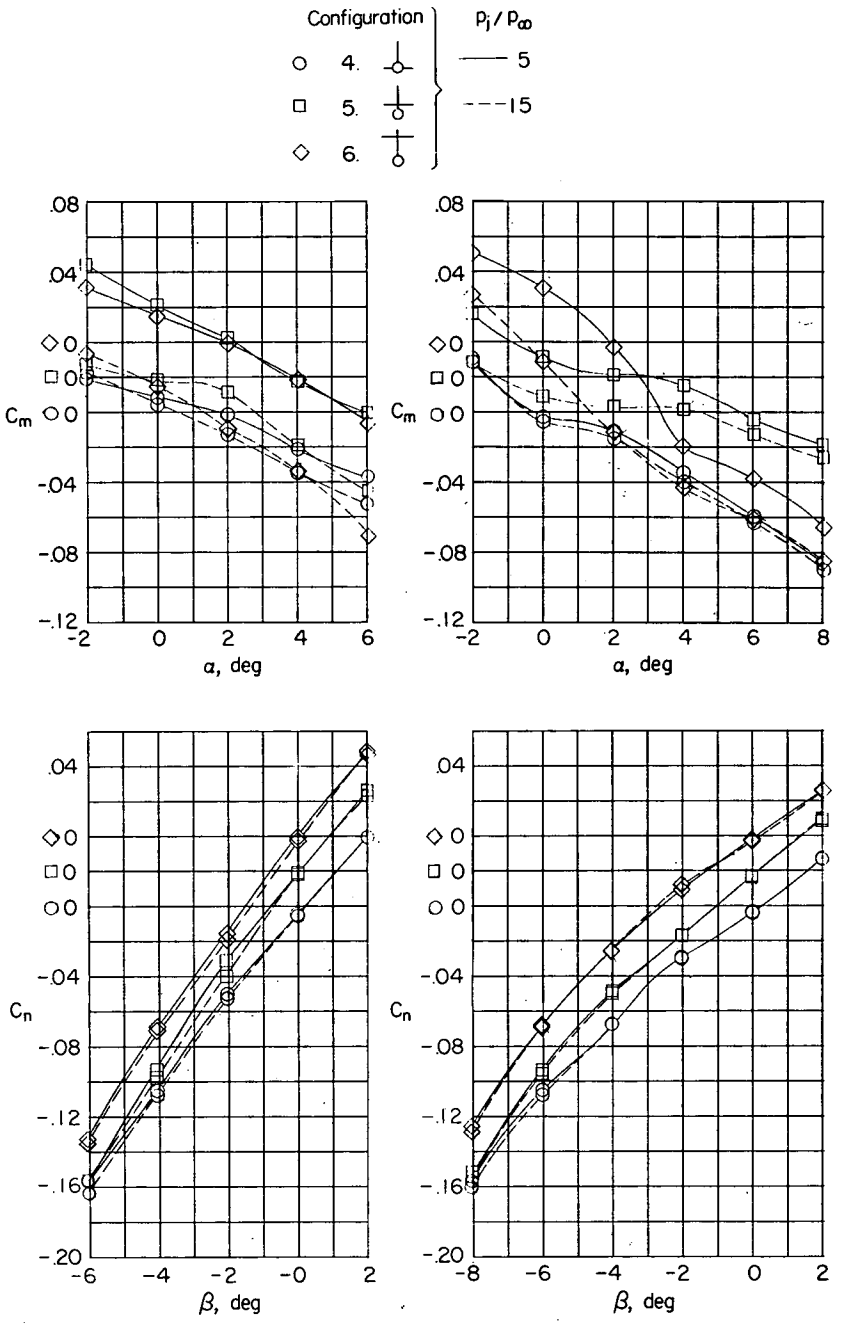

(a) $M_\infty = 1.94$. (b) $M_\infty = 2.41$.

Figure 14.- Variation in the combined pitching moment and yawing moment for the model with its center of gravity located at the wing trailing edge.

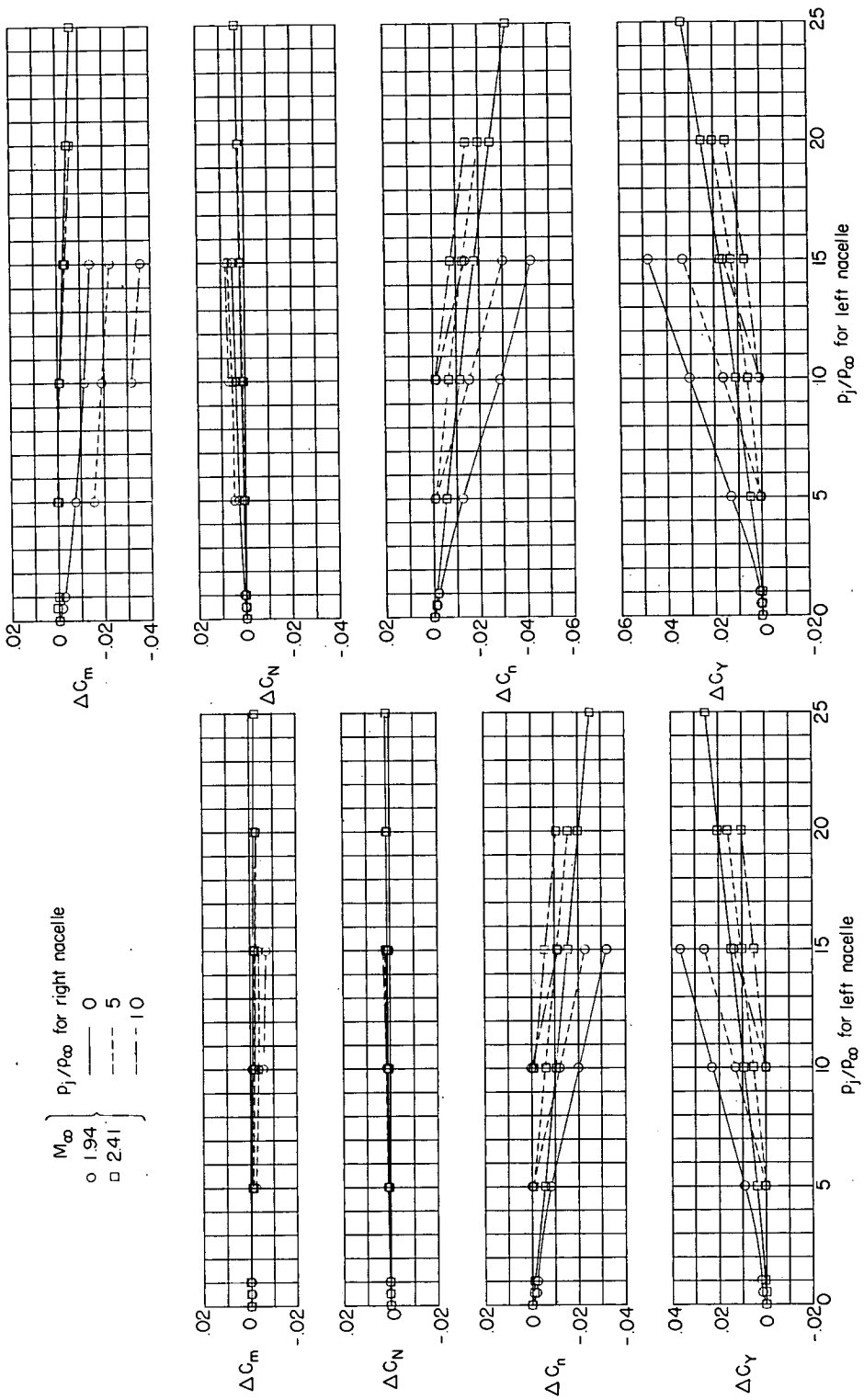

(a) $\alpha = 0^\circ$. (b) $\alpha = 4^\circ$.

Figure 15.- Incremental variations in pitching moment and yawing moment produced by jets operating at unequal jet static-pressure ratios for configuration 4.

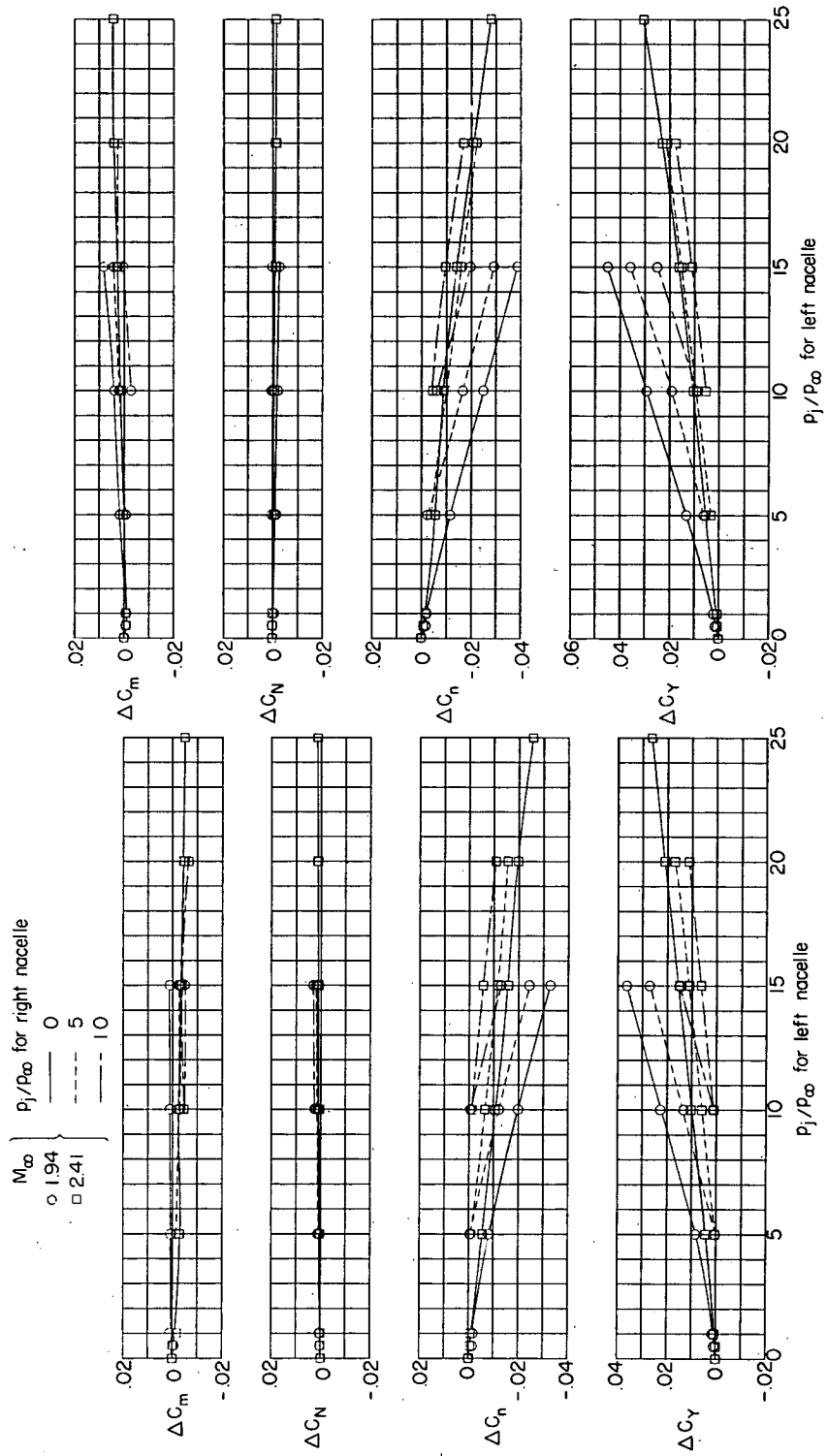

(c) $\beta = 0^\circ$.

(d) $\beta = 4^\circ$.

Figure 15.- Concluded.